Selective oxidation of olefins on molybdate catalysts

SELECTIVE OXIDATION OF OLEFINS ON MOLYBDATE CATALYSTS

D.A.G. VAN OEFFELEN

SELECTIVE OXIDATION OF OLEFINS ON MOLYBDATE CATALYSTS

PROEFSCHRIFT

TER VERKRIJGING VAN DE GRAAD VAN DOCTOR IN DE TECHNISCHE WETENSCHAPPEN AAN DE TECHNISCHE HOGESCHOOL EINDHOVEN, OP GEZAG VAN DE RECTOR MAGNIFICUS, PROF.DR.P.VAN DER LEEDEN, VOOR EEN COMMISSIE AANGEWEZEN DOOR HET COLLEGE VAN DEKANEN IN HET OPENBAAR TE VERDEDIGEN OP DINSDAG 17 OKTOBER 1978 TE 16.00 UUR

DOOR

DOMINICUS ANTONIUS GERARDUS VAN OEFFELEN

GEBOREN TE WINTELRE

DRUK: WIBRO HELMOND

DIT PROEFSCHRIFT IS GOEDGEKEURD DOOR DE PROMOTOREN

PROF. DR. G.C.A. SCHUIT

en

DR. IR. J.H.C. VAN HOOFF

Het onderzoek beschreven in dit proefschrift werd financieel gesteund door de Nederlandse Organisatie voor Zuiver-Wetenschappelijk Onderzoek (ZWO), en werd uitgevoerd onder auspiciën van de Stichting Scheikundig Onderzoek in Nederland (SON).

aan mijn ouders
aan Marlies

CONTENTS

CHAPTER 1

INTRODUCTION

1.1 GENERAL

The selective or partial oxidation is a commercial process for converting relatively cheap feed stocks as hydrocarbons into valuable chemical products for the petrochemical industry.

Olefins and alkylbenzenes are used as hydrocarbon in this respect.

The term "selective" indicates that the oxidation reaction leads to one special product; its rate of production being favoured over others, in particular the total oxidation to CO or CO_2.

The oxidation can be carried out in the gas phase over heterogeneous catalysts (transition metal oxides) or in the liquid phase with the use of homogeneous catalysts (coordination complexes of transition metals). Heterogeneous oxidation has the advantage of simple separation of catalyst and products while for homogeneous oxidation processes this always presents a problem.

Heterogeneous reactions include the oxidation of ethylene to ethylene oxide over silver (1), the oxidation of propylene to acrolein, propylene to acrylic acid, propylene with ammonia to acrylonitrile and the oxidative dehydrogenation of butene to butadiene over mixed molybdates.

A commercially very important process is the ammoxidation of propylene with ammonia to acrylonitrile (ACN).

In the U.S. 772,000 metric tons of ACN were produced in 1975, of which 55% was used in acrylic fibers, and 17% in ABS and SAN resins (2).

The industrial development of oxidation catalysts started by the report of Hearne and Adams (3) in 1948 that acrolein could be produced from propylene by the use of cuprous oxides as catalyst. Around 1960 Veath *et al.* reported the use of bismuth molybdate with a composition 50% $Bi_9PMo_{12}O_{52}$/50% SiO_2 for the oxidation of propene to acrolein (4) and for the reaction of propene together with ammonia and air (ammoxidation) to acrylonitrile (5). This latter process was commercialized by Sohio (Standard Oil Co. of Ohio) and replaced the older process for manufacturing acrylonitrile from ethyn and HCN.

Adams (6) found that on the same catalyst butadiene could be produced from butene.

Later, a uranium-antimony oxide catalyst (7) was used instead of the bismuth molybdates, but these catalysts were critical during operation and gave problems in connection with the storage and transport of the lightly radioactive wastes. Iron-antimony catalysts do not have the latter problem and are still being used in Japan.

Nowadays these catalysts have been replaced by the socalled multicomponent molybdates (8) who are composed of a variety of elements like nickel, cobalt, iron, manganese, potassium, phosphorus, but always contain bismuth and molybdenum. The principal advantages of the multicomponent molybdate catalyst over the earlier bismuth molybdate are a low content of expensive bismuth, somewhat higher conversion and a better use in fluid bed operation, because it is more resistant to small compositional variation of the feed gases.

Besides bismuth molybdates, several phosphorus containing catalysts have been developed for the oxidative dehydrogenation of butene to butadiene, for example, a tin-phosphorus catalyst (9).

1.2 REACTION MECHANISM

It is generally assumed that in the oxidation reactions a reduction-oxidation mechanism is valid. This mechanism was first proposed by Mars and Van Krevelen (10) for the oxidation of naphtalene catalyzed by V_2O_5. The reaction was supposed to occur in two steps: in the first step the hydrocarbon is oxidized and the oxide is reduced, while in the second step there is a reaction between the reduced oxide and the oxygen in the gas phase to arrive at the initial state. This mechanism was later confirmed for the oxidation and ammoxidation on bismuth molybdates and uranium-antimony oxide (11, 12), as well as for the methanol oxidation over iron-molybdenum oxide catalysts (13).

Several reviews have appeared in the last decade about detailed reaction mechanisms of olefin oxidation (14-20).

The most characteristic feature of the oxidation reaction is the formation of an allylic intermediate. This was first proposed by Adams and Jennings (21), later confirmed by Sachtler and De Boer (22) from experiments with isotopically labeled olefins.

In the mechanism of Adams and Jennings (21) the rate limiting step is the dissociative adsorption of the initial olefine. The allylic intermediate is bonded to the surface via a socalled π-allyl complex, in which the plane of the carbon atoms is perpendicular to the axis connecting the metal and the allyl. This model is confirmed by molecular orbital calculations of Haber (23). Matsuura and Schuit (24) arrive at a detailed description of the active site on bismuth molybdates, based on extensive adsorption studies. The active site is believed to consist of one A-site (composed of an oxygen atom on a bismuth atom, O_A, accompanied by two vacancies on bismuth atoms, V_{Bi}) and two B-sites (one vacancy at a molybdenum atom, V_{Mo}, and two oxygens on

molybdenum atoms, O_B).

The oxidative dehydrogenation of 1-butene is then described as follows:

a) dissociative adsorption of butene on B-sites, which is fast

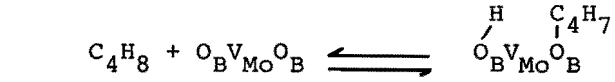

b) transfer of C_4H_7 to a Bi vacancy: rate determining.

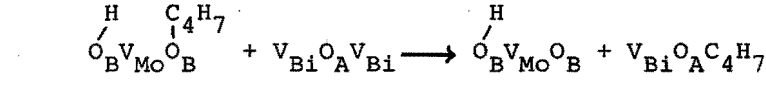

c) transfer of H from C_4H_7 to a B site and formation of C_4H_6: fast

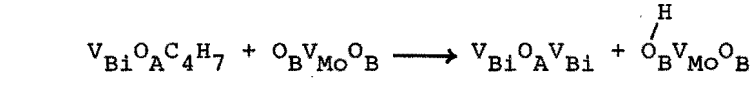

d) migration of H to an A site and formation of a reduced A site and H_2O:

Haber and Grzybowska (25) assume that the formation of the allyl intermediate occurs on bismuth instead of on molybdenum. In this way they can explain that the formation of the allyl intermediate occurs also on Bi_2O_3, leading to dimerization, while acrolein is only formed on bismuth molybdates.

Sleight (26) gives a model for the oxidation of propylene to acrolein. He proposed the formation of an allyl intermediate on a MoO_4^{2-}-group associated with a Bi-cationvacancy, whereby the proton is donated to a neighbouring MoO_4^{2-}-group. The second proton is also donated to this group, while the allyl desorbs as acrolein so that the first MoO_4^{2-} group is converted to MoO_3:

$$C_3H_6 + (MoO_4)^{2-} \longrightarrow (C_3H_5.MoO_4)^{2-} + H^+ + e$$

$$(C_3H_5.MoO_4)^{2-} + (MoO_4)^{2-} \longrightarrow C_3H_4O + (O_3Mo\text{-}O\text{-}MoO_3)^{2-} + H^+ + 3e$$

$$H^+ + \phi(MoO_4)^{2-} \longrightarrow (MoO_3OH)^-$$

The electrons are donated to an overlapping system of an empty Bi 6p conduction band and Mo 4d states. They are used to being donated to an incoming oxygen molecule. By removal of the two oxygen atoms associated with Mo, the Bi-ion coordination is lowered from eight to six. The oxygen molecule takes up the four electrons from the conduction band and gives two O^{2-} ions; they fill up the oxygen vacancies and restore the Mo- and Bi-surroundings.

Although the allyl intermediate is generally accepted, there have appeared in literature some other intermediate complexes. Krylov and Margolis (27) postulate an intermediate positively charged hydrocarbon-oxygen complex, which formation is rate determining.

Alkhazov *et al.* (28) gave a reaction mechanism for the oxidative dehydrogenation of butene with intermediate formation of a surface butene-π-complex; but he also gives the possible formation of an intermediate allyl complex in the formation of products containing the carbonylgroup, like methylvinylketon and crotonaldehyde.

In general, the mechanism for 1-butene oxidative dehydrogenation is assumed to be the same as for propene oxidation. Nevertheless, in some cases this is not valid. For example, with a V_2O_5-MoO_3 catalyst there is a satisfactory oxidation of propene, but only a slight oxidative dehydrogenation; while with zinc-chromium ferrites the reverse situation is occurring: more or less active for butene dehydrogenation, but not for allylic oxidation.

The catalysts we studied are all derived from the

bismuth-molybdenumsystem and for these it is generally recognized that the butene dehydrogenation is operating in the same way as the propene oxidation. For this reason we only used the oxidative dehydrogenation of butene as a test reaction for activity and selectivity, because the reaction requires a much simpler analyzing system.

1.3 ROLE OF OXYGEN

Already in an early stage of the development of the oxidation catalysts it was recognized that lattice oxygen is a reaction partner in this type of selective oxidation. Callahan and Grasselli (29) realized that not all oxygens were active for the oxidation but that there should be a few active oxygens in a sea of inactive oxygens.
Keulks (30) investigated the incorporation of oxygen into the reaction products and into the catalyst by using $^{18}O_2$ in the gas phase during the oxidation of propene to acrolein. He showed that the oxygen in the surface layer at first instance is used for the oxidation and that these layers will be reoxidized by diffusion of oxygen ions from the bulk to the surface. The acrolein product has for a long time a low ^{18}O-content. This was explained by the fact that after adsorption of oxygen there is a fast diffusion through a great number of layers and extensive equilibration with the bulk oxygen ions.

Pendleton and Taylor (31) also studied the reaction between propene and $^{18}O_2$ over bismuth molybdate. They also showed that the lattice is the source for the oxygen incorporated into the acrolein. The oxygen for the CO_2-formation can come from both lattice and gas phase oxygen.

Wragg *et al.* (32) carried out some experiments to

establish the role of gas phase oxygen and oxide ions in the oxidation of propene to acrolein over bismuth molybdate. They used first $^{18}O_2$ as gas phase and a catalyst containing normal oxygen and secondly $^{16}O_2$ in the gas phase and an ^{18}O-enriched catalyst. They came to the conclusion that oxygen in the product acrolein was derived from the lattice and not from the gas phase.

Sancier *et al.* (33) determined the relative contributions of sorbed and lattice oxygen during propene oxidation over silica supported bismuth molybdate using $^{18}O_2$ in the gas phase. They established a temperature dependence; at low temperatures the lattice mobility is low and adsorbed oxygen can play a role in the oxidation, while at higher temperatures (> 350°C) there is a scrambling of oxygen ions from lattice and surface, so that lattice oxygen becomes more important.

Boreskov (34) also indicated that at lower temperatures a different mechanism is valid, i.e. an associative mechanism between O_2 and olefin at the surface.

Otsubo *et al.* (35) prepared bismuth molybdates which were labeled with oxygen-18 either in the bismuth layers or in the molybdenum layers. They showed that the first oxidation with hydrogen is carried out by the Bi_2O_2 layers and that afterwards there is an oxygen migration from the MoO_2 layers to the Bi_2O_2 layers. The anion vacancies produced in the MoO_2 layers act as reoxidation sites.

Keulks and Krenzke (36) studied the oxidation of propene in a flow reactor with the use of ^{18}O over γ- en α-bismuth molybdate. They concluded that the source of oxygen is the lattice oxygen and there is no distinction between the lattice oxygen incorporated into CO_2 and into acrolein: the two reactions therefore appear to occur on the same type of site.

1.4 AIM OF THE INVESTIGATION

The oxidation of olefins on bismuth molybdates has been the subject of numerous investigations and quite detailed reaction mechanisms have been developed. Nevertheless, several details in oxidation mechanism and physicochemical properties of bismuth molybdate based catalysts are not yet clear and deserve further research.

As regards the pure bismuth molybdates there is still the question which of the known bismuth molybdates is the most active and selective oxidation catalyst (chapter 3).

One of the bismuth molybdates is known to be unstable; we tried to stabilize this phase (chapter 5).

Scheelite structured molybdates, like lead molybdate, can be made active for oxidation reactions by simultaneous incorporation of bismuth ions and cation vacancies. Because of their relative simple structure, they were thought to possess unique possibilities for investigating the role of the different components (chapter 4).

The reaction mechanism for the oxidation on multi-component molybdates was investigated by means of the system $Mg_{11-x}Fe_xBiMo_{12}O_n$ (chapter 6).

One of the experimental techniques (chapter 2) used throughout this study was the measurement of electrical conductivity of the catalysts. The dependence of reduction and conductivity was believed to give information on the mechanism of catalytic oxidation over the different bismuth molybdates(chapter 7).

The variety of problems investigated and the variation in catalysts used, may give the impression that this thesis is composed of more or less independent chapters that lack coherence.

In chapter 8 it will be shown that the various catalytic systems studied throughout this thesis have common characteristics and that their comparison gave useful leads for interpretation of the central problem: the reaction mechanism of the selective oxidation of olefins.

REFERENCES

1. P.A. Kilty, W.M.H. Sachtler, Cat. Rev.-Sci. Eng., 10, 1 (1974).
2. Hydrocarbon Proc. 56, May 1977, p 169.
3. G.W. Hearne, M.L. Adams, U.S. Patent 2,451,485 (1948)
4. F. Veath, J.L. Callahan, E.C. Milberger, R.W. Foreman, Proc. 2nd Int. Congr. Catal. (Ed. Technip, Paris, 1960), Vol. 2, p. 2647.
5. F. Veath, J.L. Callahan, E.C. Milberger, Chem. Eng. Process, 5b, 65 (1960).
6. C.R. Adams, Proc. 3rd Int. Congr. Catal., (North Holland Publ. Co., Amsterdam, 1965), Vol I, p. 240.
7. J.L. Callahan, B. Gertisser, U.S. Patent 3,198,750 (1965).
8. R. Krabetz, Chemie-Ing.-Techn., 46, 1029 (1974).
9. E.W. Pitzer, Ind. Eng. Chem., Prod. Res. Developm., 11, 299 (1972).
10. P. Mars, D.W. van Krevelen, Chem. Eng. Sci., Suppl., 3, 41 (1954).
11. K. Aykan, J. Catal., 12, 281 (1968).
12. R.K. Grasselli, D.D. Suresh, J. Catal., 25, 273 (1972).
13. P. Jiru, B. Wichterlova, J. Tichy, Proc. 3rd Int. Congr. Catal., (North Holland Publ. Co., Amsterdam, 1965), Vol. I, p. 199.
14. R.J. Sampson, D. Shooter, in 'Oxidation and Combustion Reviews' (C.F.H. Tripper, ed.). Vol I, p. 223, Elsevier, Amsterdam, 1965.
15. H.H. Voge, C.R. Adams, Adv. Catal., 17, 151 (1967).
16. W.M.H. Sachtler, Catal. Rev., 4, 27 (1970).
17. L.Ya. Margolis, Catal. Rev., 8, 241 (1973).
18. D.J. Hucknall, 'Selective Oxidation of Hydrocarbons', Ac. Pr., London (1974).
19. V.K. Skarchenko, Russ. Chem. Rev., 46, 731 (1977).

20. G.C.A. Schuit, J. Less Common Metals, 36, 329 (1974).
21. C.R. Adams, T. Jennings, J. Catal., 2, 63 (1963).
22. W.M.H. Sachtler, N.H. de Boer, Proc. 3rd Int. Congr. Catal., (North Holland Publ. Co., Amsterdam, 1965), Vol. I, p. 252.
23. J. Haber, M. Sochacka, B. Grzybowska, G. Golzbiewski, J. Mol. Catal., 1, 35 (1975).
24. I. Matsuura, G.C.A. Schuit, J. Catal., 25, 314 (1972).
25. J. Haber, B. Grzybowska, J. Catal., 28, 489 (1973).
26. A.W. Sleight in 'Advanced Materials in Catalysis' (J.J. Burton, R.L. Garten, eds.), Ac. Press, N.Y. 1976.
27. O.V. Krylov, L.Ya. Margolis, Kin. Cat., 11, 358 (1970).
28. T.G. Alkhazov, M.S. Belen'kii, and R.J. Alekseeva, Proc. 4th Int. Congr. Catal., Moscow, 1968, p. 293.
29. J.L. Callahan, R.K. Grasselli, A.J.Ch.E. Journal 9, 755 (1963).
30. G.W. Keulks, J. Catal., 19, 232 (1970).
31. P. Pendleton, D. Taylor, J. Chem. Soc. Faraday I, 72, 1114 (1976).
32. R.D. Wragg, P.G. Ashmore, J.A. Hockey, J. Catal., 22, 49 (1971).
33. K.M. Sancier, P.R. Wentrcek, H. Wise, J. Catal., 39, 141 (1975).
34. G.K. Boreskov, Kin. Cat., 14, 2 (1973).
35. T. Otsubo, H. Miura, Y. Morikawa, F. Shirasaki, J. Catal., 36, 240 (1975).
36. G.W. Keulks, L.D. Krenzke, Proc. 6th Int. Congr. Catal. 2, 806 (1977).

CHAPTER 2

EXPERIMENTAL METHODS

This chapter gives a short description of the different techniques used to characterize the catalysts. Preparational aspects will not be discussed here, but will be reported in the separate chapters.

2.1. CATALYTIC ACTIVITY AND SELECTIVITY

The oxidative dehydrogenation of 1-butene was used as a testreaction for comparing different catalysts regarding their catalytic activity and selectivity. This reaction is a simple selective oxidation reaction in this way that all reaction products (except water) are gaseous and allow a quick gaschromatographic analysis.

Nevertheless, several possible reactions can occur:

$$C_4H_8 + \tfrac{1}{2}O_2 \longrightarrow C_4H_6 + H_2O \text{ (butadiene)}$$

$$C_4H_8 + 3/2\ O_2 \longrightarrow C_4H_4O + 2H_2O \text{ (furan)}$$

$$C_4H_8 + 3O_2 \longrightarrow C_4H_2O_3 + 3H_2O \text{ (maleic anhydride)}$$

$$C_4H_8 + 4O_2 \longrightarrow 4CO + 4H_2O \text{ (carbon monoxide)}$$

$$C_4H_8 + 6O_2 \longrightarrow 4CO_2 + 4H_2O \text{ (carbon dioxide).}$$

The catalysts reported in this thesis yielded mainly butadiene (the more common product) and carbon dioxide (as result of complete combustion). Also isomerization

of 1-butene to cis-2-butene and trans-2-butene is possible.

The butene oxidation was studied in a continuous flow apparatus (1) (fig. 2.1). A constant flow of a mixture of 1-butene and artificial air (80% He - 20% O_2) was passed over the powdered catalyst. The amount of catalyst used was 400 mg (particle size 0.2 - 0.4 mm). The flows were 20 cm^3/min 1-butene and 100 cm^3/min artificial air (ratio C_4H_8:O_2:He = 20:20:80). The catalyst was placed in a microreactor made of quartz glass. The reactor was heated by means of a heating wire, mounted on an aluminum tube. The temperature inside the catalyst bed was measured by a chromel-alumel thermocouple.

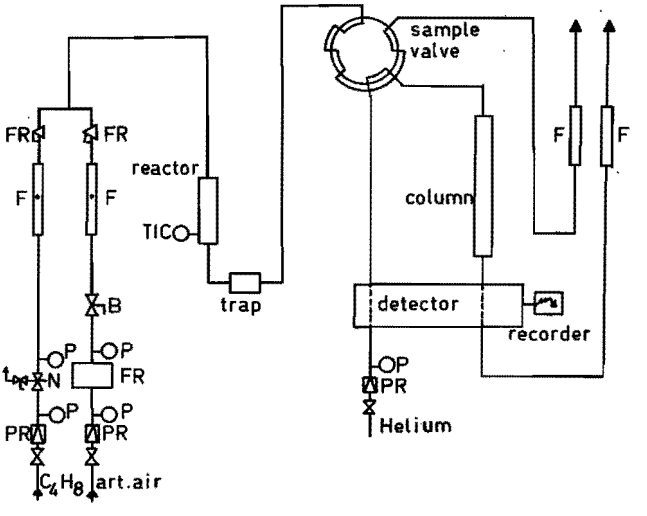

Fig. 2.1 Continuous flow system for 1-butene oxidative dehydrogenation. P = manometer, PR = pressure regulator, F = flow meter, FR = flow regulator, N = Negretti needle valve, B = Brooks needle valve, TIC = temperature indication and control.

Samples of the product stream were led into a gaschromatographic column by means of a sample valve. Helium (40 cm^3/min) was used as carrier gas. The chromatographic column (5m) contained 15% by weight 2,4-dimethylsulfolane on chromosorb (30-50 mesh), by which it was possible to determine quantitatively the relative amounts of carbon dioxide, 1-butene, cis- and trans-2-butene and butadiene. Water and possible oxidation side products were allowed to condense in a cold trap, but were not analyzed further. For converting the recorded signal intensities into concentrations of the gaseous components, we used the following substance specific multiplication factors: CO_2 1.8, 1-butene and 2-butenes 1.00, butadiene 1.03. The total amount of carbon containing compounds was taken as 100, so that the composition could be expressed in percents. We used the following definitions:

$$\text{activity} = \frac{[\text{butenes}]_0 - [\text{butenes}]_T}{[\text{butenes}]_0} \cdot 100\%$$

$$\text{selectivity} = \frac{[\text{diene}]}{[\text{diene}] + \frac{1}{4}[CO_2]} \cdot 100\%$$

in which

$[\text{butenes}]_0$ = concentration of butenes before reaction
$[\text{butenes}]_T$ = concentration of butenes after reaction at temperature T.
$[\text{diene}]$ = concentration of butadiene
$[CO_2]$ = concentration of carbondioxide

2.2 PULSE-EXPERIMENTS

During pulse experiments we used the same apparatus as in continuous flow experiments, but now the reactor is placed between sample valve and gaschromatographic column. The helium carrier gas is passing continuously

over the catalyst; by means of a sample valve it is possible to pulse an amount of 1-butene over the catalyst with subsequent analysis of the reaction products. The volume of the pulse is 0.6 cm^3 (25^0C, 1 atm). By using only 1-butene the oxygen of the oxidic catalyst is used for conversion; so by taking several pulses of 1-butene the catalyst becomes reduced. The degree of reduction can be calculated from the analysis of the reaction products.

2.3 ELECTRICAL CONDUCTIVITY MEASUREMENTS

The electrical conductivity was measured on samples which were pressed to rectangular pellets under a pressure of 1000 kg/cm^2. The dimensions were about 15 x 5 x 5 mm.

A four probe technique was used, in which two of the electrodes served as current leads and the other two as voltage leads. Fig. 2.2 gives a scheme of the

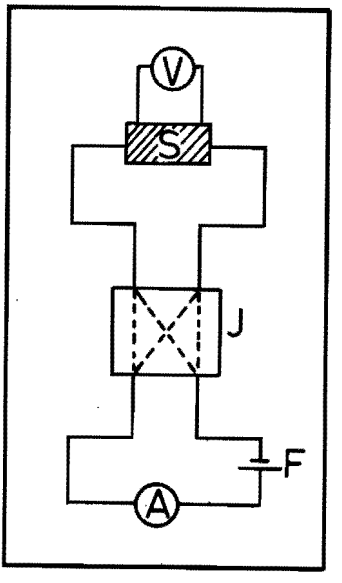

Fig. 2.2 Experimental set up for the electrical conductivity measurements. S = sample, F = constant voltage supply, A = multimeter, V = spotgalvanometer, J = junction box

experimental set up.

A constant voltage supply (Delta Elektronika D 030) delivered a voltage of 6 V. The current developed was measured by means of a spotgalvanometer (Radiometer GVM 22c). The voltage difference across electrodes 3 and 4 was measured by means of a multimeter (Fluke 8600 A).

From current and voltage measurements the resistivity could be calculated. Together with the sample dimensions we can get a specific resistivity and an electrical conductivity:

$$\sigma = \frac{1}{\rho} = \frac{L}{A} \cdot \frac{1}{R}$$

in which

L = distance between electrodes 3 and 4 [cm].

A = cross-sectional area of pellet [cm^2]

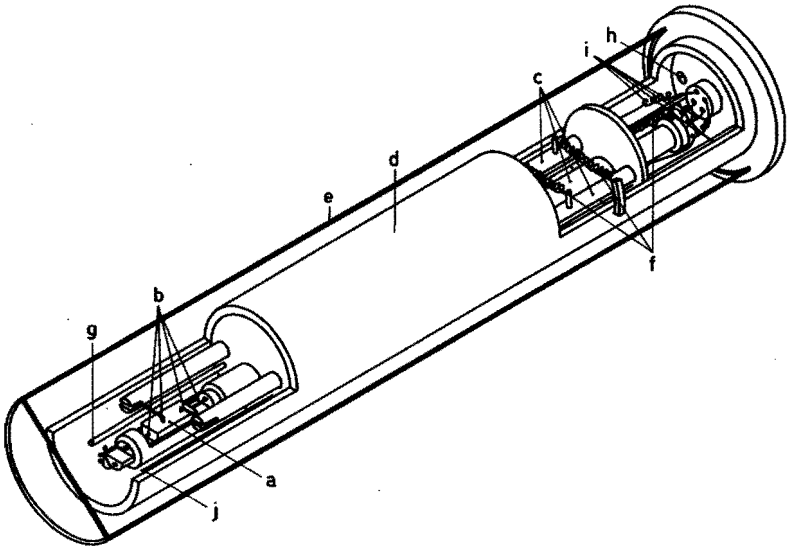

Fig. 2.3 Electrical conductivity cell and sample holder a = sample, b = electrodes, c = alumina ceramic tubes, d = stainless steel holder, e = quartz glass tube, f = springs, g = inlet gases, h = exit gases, i = electrode connections, j = thermocouple

R = resistivity [Ω]
ρ = specific resistivity [Ω.cm]
σ = electrical conductivity [$\Omega^{-1}.cm^{-1}$].

The polarity could be changed to check charging effects.

The sample was spring-loaded between Pt-contacts. Pt was used as electrode material; the Pt-leads were shielded by ceramic tubes. The electrode assembly was placed in a quartz glass tube, which could be supplied with different gases (fig. 2.3). The outlet was connected with a gaschromatographic column; the same as used for the activity measurements. By means of a sample valve it was possible to carry out pulse experiments by pulsing 1-butene in a helium flow. The reactant gases were entering the tube directly below the catalyst pellet. The volume of the pulse was 0.9 cm^3.

Because of the rather large volume of the tube it was not possible to get an ideal plug flow of the gases, preventing a good gaschromatographic analysis of the products. Freezing the reaction products for 15 minutes in a liquid nitrogen trap and subsequent quick heating to room temperature enabled us to get a reproducible analysis of the reaction products.

2.4 X-RAY PHOTO-ELECTRON SPECTROSCOPY

X-ray photo-electron spectroscopy (XPS) or ESCA (electron spectroscopy for chemical analysis) is a technique for measuring electron binding energies.

Photo-electrons are ejected from the sample by mono-energetic X-ray excitation. The kinetic energy of the ejected electrons is analyzed and peaks in the resulting kinetic energy spectrum correspond to electrons of specific binding energies in the sample. These binding energies are dependent on the kind of atom, its valency state, its environment and the penetration depth.

This technique only gives information over the outermost layers of a solid compound, *i.e.* its surface layers (15-20 Å). This makes it a very useful technique for studying catalytic surfaces (2).

From the intensity of the peaks a quantitative composition of the surface layers can be deduced, but first we have to account for different elemental sensitivities. In our XPS measurements we used the sensitivity factors as given by Berthou and Jørgensen (3).

The apparatus used was an AEI ES 200 spectrometer with MgKα-radiation (1253.6 eV). The power supply was run at 12 kV and 15 mA. The spectra were collected using a PDP 8 computer and stored in a 32k disc. The powdered samples were either stuck onto a piece of tape or pressed into a copper gauze.

The instrument was installed at the Physical Chemistry Department of the University of Groningen (the Netherlands).

2.5 MÖSSBAUER SPECTROSCOPY

Mössbauer spectroscopy (4) is a resonant technique, employing a photon source, an absorber and a photon detector. The gamma-ray energy from a radioactive nucleus is modulated by imparting a Doppler velocity to the source. The motion of the source can be achieved in two ways, either constant velocity or constant acceleration. The gamma rays of discrete energies can be resonantly absorbed by absorber nuclei. The number of transmitted photons are plotted versus photon energy and a peak is observed where resonance occurs.

The peak positions in the Mössbauer spectrum are sensitive to the extra nuclear environment, such that different compounds give different spectra. The differences can be attributed to the socalled hyperfine interactions: the interactions between the nuclear charge distribution and the extranuclear electric and magnetic fields. These give rise to the isomer shift

(which reflects the difference in electronic charge density at the nucleus of the source compared to the absorber) and the quadrupole splitting (caused by coupling of nuclear quadrupole moment with the electric field gradient).
Especially the ^{57}Fe-nucleus is a very sensitive probe (besides ^{119}Sn, ^{121}Sb and ^{151}Eu).

Our measurements of ^{57}Fe were carried out at room temperature on a constant accelerator spectrometer with a ^{57}Co-Rh source. The instrument is installed at the IRI (Interuniversity Reactor Institute) (Delft, the Netherlands).

The isomer shift is given relative to the NBS reference material $Na_2Fe(CN)_5.NO.2H_2O$.

2.6 MISCELLANEOUS MEASUREMENTS

X-ray diffraction measurements were performed on a Philips PW 1120 spectrometer with CuKα radiation and Ni filter.

Infrared spectroscopy was carried out with a Grubb-Parsons MK III spectrophotometer for the range 400-4000 cm^{-1} and a Hitachi EP 1-L for the range 200-700 cm^{-1}.
250 mg dried KBr mixed with about 1 mg catalyst was used to make a pellet.

Differential thermal analysis and thermogravimetric analysis was carried out on a Mettler Thermo Analyzer T2-ES with Pt crucibles and α-Al_2O_3 as reference. The sample was heated in an argon atmosphere with a heating rate of 5^{0}C/min.

Surface area measurements were performed on an areameter of Ströhlein, which is based on the BET-method, using nitrogen as adsorbate.

REFERENCES

1. K. Keizer, Ph.A. Batist, G.C.A. Schuit, J. Catal., 15, 256 (1969).
2. W.N. Delgass, T.R. Hugher, C.S. Fadley, Cat. Rev., 4, 179 (1971).
3. H. Berthou, C.K. Jørgensen, Anal. Chem., 47, 482 (1975).
4. H.M. Gager, M.C. Hobson, Catal. Rev., 11, 117 (1975).

CHAPTER 3

BISMUTH MOLYBDATES

3.1 INTRODUCTION

3.1.1 The Bi_2O_3-MoO_3 system

Although several research groups have examined the binary phase system Bi_2O_3-MoO_3, there is no general agreement about the existence of some of the compounds postulated.

Bleyenberg *et al.* (1) identified the following compounds (m.p. = melting point):

$Bi_2O_3.3MoO_3$ m.p. 676°C

$Bi_2O_3.MoO_3$ m.p. 938°C

$3Bi_2O_3.MoO_3$ m.p. 995°C

They did not find the compound $Bi_2O_3.2MoO_3$. At the bismuth rich side of the compounds $Bi_2O_3.3MoO_3$ and $Bi_2O_3.MoO_3$ solid solutions were supposed to occur.

Kohlmuller (2) found only two stoichiometric compounds, $3MoO_3.Bi_2O_3$ (m.p. 666°C) and $MoO_3.10Bi_2O_3$ (m.p. 810°C). Besides these two he found three phases with a variable composition.

Erman (3) found three incongruent compounds, *e.g.* $3MoO_3.Bi_2O_3$, $2MoO_3.Bi_2O_3$ and $MoO_3.Bi_2O_3$. The last compound existed in two forms, the high temperature form being the stable one.

At the present moment there is general agreement about the existence of the compounds Bi_2MoO_6, $Bi_2Mo_3O_{12}$, and Bi_6MoO_{12}, but Bi_4MoO_9, only mentioned by Gattow (4), and $Bi_{20}MoO_{33}$ are still in doubt

From these compounds only Bi_2MoO_6 is occurring in nature as the rare mineral koechlinite (5).

The compounds Bi_2MoO_6, $Bi_2Mo_2O_9$ and $Bi_2Mo_3O_{12}$ fall within the range of compositions which exhibit catalytic activities for selective oxidation reactions.

3.1.2. Structures of the bismuth molybdates

A model for the structure of Bi_2MoO_6 was first proposed by Zemann (6) and later improved by Van den Elzen and Rieck (7).

The compound is a layer structure with alternating sheets of Bi_2O_2 and MoO_2, the sheets being connected by oxygen layers. The Mo^{6+} ions are in a distorted octahedral surrounding with corner sharing of the octahedra in the layers and the octahedral apex ions pointing to Bi^{3+}-cations.

$Bi_2Mo_3O_{12}$ was studied by Cesare *et al.* (8) and later by Van den Elzen and Rieck (9). Its structure can be derived from the scheelite structure ($CaWO_4$) by replacing $3Ca^{2+}$ by $2Bi^{3+}$ and a cation vacancy. The cation vacancies are ordered.

The MoO_4 tetrahedra form Mo_2O_8 pairs, of which there are two forms.

Van den Elzen and Rieck (10) also gave a preliminary model for the structure of $Bi_2Mo_2O_9$ based on X-ray powder diffraction measurements. Its most remarkable feature is the presence of rows of oxygen that are only connected to Bi^{3+}. The structure can be described as $Bi(Bi_3\phi O_2)(Mo_4O_{16})$, where ϕ stands for a cation vacancy.

A more extensive survey of the structural details is given by Gates *et al.* (11).

Going from Bi_2MoO_6 through $Bi_2Mo_2O_9$ to $Bi_2Mo_3O_{12}$ there is a change in Bi coordination; in Bi_2MoO_6 Bi^{3+} is six fold coordinated with 2 oxygens bound only to bismuth, whereas in $Bi_2Mo_3O_{12}$ all oxygens are shared by bismuth in eight-fold surrounding and molybdnum.

Furthermore, there is a decreasing degree of clustering of the Mo-O polyhedra, going from an infinite two-dimensional structure via Mo_4O_{16} to Mo_2O_8.
Finally, there is a trend in the concentration of Bi^{3+}-cation vacancies. The ratio cation vacancies/$2Bi^{3+}$ ranges from zero for Bi_2MoO_6, and ½ for $Bi_2Mo_2O_9$ to 1 for $Bi_2Mo_3O_{12}$.

3.2 PREPARATION OF THE CATALYSTS

The preparations were carried out with the following chemicals:

basic bismuth nitrate $BiONO_3$ (Merck p.a.)
powdered molybdic acid (BDH)
ammonium heptamolybdate $(NH_4)_6Mo_7O_{24}.4H_2O$ (Merck p.a.)
bismuth nitrate $Bi(NO_3)_3.5H_2O$ (Merck).

Bi_2O_3 was prepared by heating basic bismuth nitrate, containing 79.94 wt% Bi_2O_3 at 520°C for 10 h to give α-Bi_2O_3.

MoO_3 was prepared by heating molybdic acid, containing 88.98 wt% MoO_3 at 500°C for 4 h.

Bi_2MoO_6 was prepared according to the slurry method of Batist (12). 16.177 g molybdic acid and 58.289 g basic bismuth nitrate were added to 1 l. boiling water. To the slurry an amount of 4 cm^3 conc. nitric acid was added, after which the reaction was started. The slurry was vigorously stirred. After 12 h of reaction the yellow coloured mass was filtered off, dried at 120°C for 16 h, and calcined at 500°C for 2 h. The reaction could be carried out quantitatively as was shown by examining the obtained weight.

$Bi_2Mo_{1.02}O_{6.06}$. The same method was used as for Bi_2MoO_6, except that we used 16.500 g molybdic acid, resulting in 2 mole% Mo extra. Here again the reaction was quantitatively.

$Bi_{2.04}Mo_1O_{6.06}$. Again a slurry method was used,

starting with 16.177 g molybdic acid and 59.204 g basic bismuth nitrate. The molybdic acid was first dissolved in aqueous ammonia.
After 18 h of stirring and boiling the mass was filtered off, dried at 120°C for 16 h and calcined at 500°C for 2 h .
This preparation also yielded stoichiometric amounts as could be shown by weight analysis.

$Bi_2Mo_2O_9$. To 24.253 g $Bi(NO_3)_3.5H_2O$ was added 13 cm^3 conc. HNO_3 and dissolved in 100 ml water. 8.827 g $(NH_4)_6Mo_7O_{24}.4H_2O$ dissolved in 100 ml water was added to the first solution under stirring. By adding aqueous ammonia the final pH was adjusted at 4. Meanwhile the solutions were cooled in ice baths.
The white precipitate is filtered off, dried at 120°C for 16 h and calcined at 500°C for 2h. This procedure yielded a stoichiometric sample as checked by weight analysis.

$Bi_2Mo_3O_{12}$. 14.577 g basic bismuth nitrate and 75.000 g molybdic acid were brought into 1 l. water. The slurry was heated and stirred for 30 h , during which time the colour remained white. After filtration, drying at 120°C for 16 h and calcining for 2 h at 480°C. The resultant material contained the stoichiometric amounts of bismuth and molybdenum as was checked by weight analysis.

3.3 ACTIVITIES AND SELECTIVITIES

All the catalysts were tested for their activity and selectivity in 1-butene oxidative dehydrogenation as described in chapter 2.
Conditions used were 400 mg catalyst, total gasflow 120 cm^3/min, $C_4H_8:O_2:He = 20:20:80$.

The sample $Bi_{2.04}MoO_{6.06}$ was totally inactive over the complete temperature range investigated (380°C-440°C).

sample	T(°C)	act(%)	select(%)	S(m^2/g)
$Bi_{2.04}MoO_{6.06}$	380-440	0		10.7
$Bi_2Mo_{1.02}O_{6.06}$	380	25.8	92.4	7.3
	400	53.7	94.0	
	420	90.5	95.9	
	440	93.2	95.4	
Bi_2MoO_6	380	78.8	83.2	7.9
	400	78.9	83.6	
	420	79.9	83.9	
	440	83.1	84.6	
$Bi_2Mo_2O_9$	380	9.0	93.4	4.3
	400	30.6	97.2	
	420	60.8	97.1	
	440	70.7	97.0	
$Bi_2Mo_3O_{12}$	440	18.1	96.4	2.3

Table 3.1 Activities and selectivities for the oxidative dhydrogenation of 1-butene and surface areas of the various bismuth molybdates

The sample $Bi_2Mo_{1.02}O_{6.06}$ showed a very high activity and selectivity at temperatures higher than 420°C, whereas the sample Bi_2MoO_6 had already at 380°C a high activity, but this latter catalyst showed a considerable lower selectivity.
The catalyst $Bi_2Mo_2O_9$ showed a fairly high activity and a very high selectivity. The sample $Bi_2Mo_3O_{12}$ prepared had low activity and high selectivity.

At 440°C the order of activity is: $Bi_2Mo_{1.02}O_{6.06}$ > Bi_2MoO_6 > $Bi_2Mo_2O_9$ >> $Bi_2Mo_3O_{12}$ > $Bi_{2.04}MoO_{6.06}$.
The order of selectivity at 440°C is $Bi_2Mo_2O_9$ ≃ $Bi_2Mo_3O_{12}$ ≃ $Bi_2Mo_{1.02}O_{6.06}$ > Bi_2MoO_6.

The inactive $Bi_{2.04}MoO_{6.06}$ becomes reactivated after adding MoO_3. This was accomplished by taking 375 mg

$Bi_{2.04}MoO_{6.06}$ and add physically 25 mg MoO_3, corresponding to about 25 mole% Mo extra. After 30 minutes at T = 440°C in the reactor, this mixture exhibits an activity of 59% and a selectivity of 89.5%. At the end of this reaction time we could observe an appreciable amount of $Bi_2Mo_3O_{12}$ to be present, as shown by the infrared spectrum (bands at 950, 930 and 900 cm^{-1}, which are attributed to the 2/3-compound (12)).

It was also possible to activate the $Bi_{2.04}MoO_{6.06}$ sample by addition of an amount of the $Bi_2Mo_3O_{12}$ sample with low activity.
The result of mixing 300 mg $Bi_{2.04}MoO_{6.06}$ and 100 mg $Bi_2Mo_3O_{12}$ after 30 minutes in the reactor, is a catalyst with an activity of 47% and a selectivity of 89% at 440°C.

3.4 XPS MEASUREMENTS

X-ray photo-electron spectroscopy (XPS or ESCA) provides a means for surface characterization of a solid sample, in particular as regards its composition (see chapter 2).

It offers an opportunity to determine which atoms are present in the surface layers and the valency of these atoms. It is also possible to calculate from the intensities of the photo-electron peaks quantitatively the relative abundancies of the elements. For this, the measured intensities must be corrected for by elemental sensitivities. Sensitivities are given by Berthou and Jørgensen (13), but it must be stressed that they contain a serious source of error as pointed out by them. Nevertheless we want to use these data to get an indication of differences in surface composition of our catalysts. The following sensitivity values were used: Bi 4f: 4.3; Mo 3d: 1.6; O 1s: 0.6. The measured binding energies are standardized against the binding energy value of the C 1s peak. This carbon is always present as a result of oil contamination from the vacuum system.

Cimino (14) points out that this reference method is the most simple and provides results as good as more sophisticated approaches. However, the C 1s line must belong to a single chemical species, which can be checked by observing whether a single line is present. In our samples this was always the case. We choose C 1s = 285.0 eV. Table 3.2 lists the binding energies (standardized) and intensities for the catalysts given before. Table 3.3 compares the calculated bismuth-molybdenum ratios with the observed values from XPS experiments.
The given data are for samples mounted on tape.

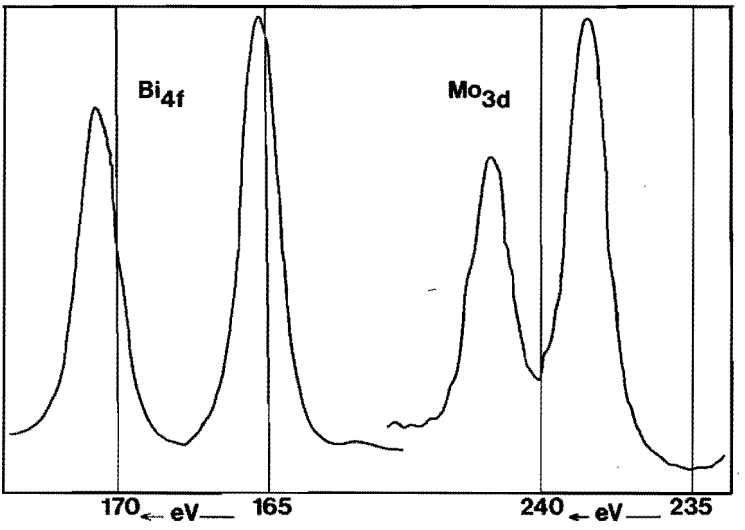

Fig. 3.1 Bi 4f and Mo 3d XPS-signals for Bi_2MoO_6

Fig. 3.1 gives the bismuth and molybdenum signals for one of the samples, *i.e.* Bi_2MoO_6.
Fig. 3.2 shows some oxygen signals. These show a shoulder at higher binding energies. The low binding energy value belongs to O^{2-}, lattice oxygen, while the high binding energy peak is sometimes ascribed to adsorbed oxygen in the form of OH^- or O^-, but there is no agreement in literature (15). With the use of Cu-gauze as sample

mounting material, the high binding energy signal only appears as a broadening at the high binding energy side (fig. 3.3).

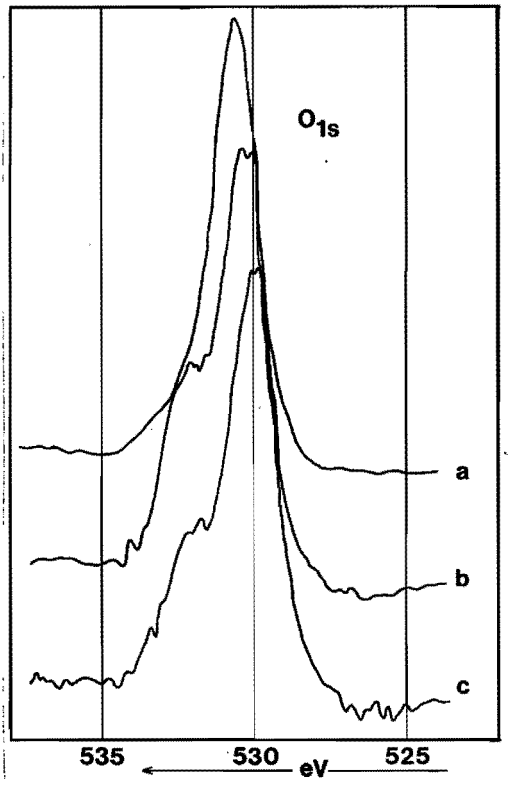

Fig. 3.2 O 1s XPS-signals for Bi_2MoO_6, $Bi_2Mo_{1.02}O_{6.06}$ and $Bi_{2.04}MoO_{6.06}$ (powdered sample mounted on tape)

sample	calc.	XPS
$Bi_2Mo_{1.02}O_{6.06}$	1.96	1.767
$Bi_{2.04}MoO_{6.06}$	2.04	2.245
Bi_2MoO_6	2.00	2.11
$Bi_2Mo_2O_9$	1.00	0.928
$Bi_2Mo_3O_{12}$	0.67	0.695
$Bi_{2.04}MoO_{6.06}$ (after activation)		1.10

Table 3.3 Comparison of the calculated bismuth-molybdenum ratios with the observed values from XPS experiments

sample	Bi 4f		Mo 3d		O 1s	
	b.e. (eV)	int.	b.e. (eV)	int.	b.e. (eV)	int.
$Bi_{2.04}MoO_{6.06}$	159.3 164.6	8.38	232.6 235.7	3.73	530.0 531.7 (sh)	17.41
$Bi_2Mo_{1.02}O_{6.06}$	159.5 164.9	10.65	232.7 235.9	6.03	530.3 532.1 (sh)	25.75
Bi_2MoO_6	159.8 165.1	131.7	233.0 236.2	62.4	530.6	295
$Bi_2Mo_2O_9$	160.0 165.5	28.46	233.0 236.0	30.68	530.8	126.7
$Bi_2Mo_3O_{12}$	159.9 165.4	3.169	233.2 236.1	4.557	530.7	14.96
$Bi_{2.04}MoO_{6.06}$ (after activation)	159.3 164.6	166.76	232.6 235.7	151.3	530	403.4

Table 3.2 XPS data: binding energy values (eV) and intensities of Bi, Mo and O signals for the various catalysts.

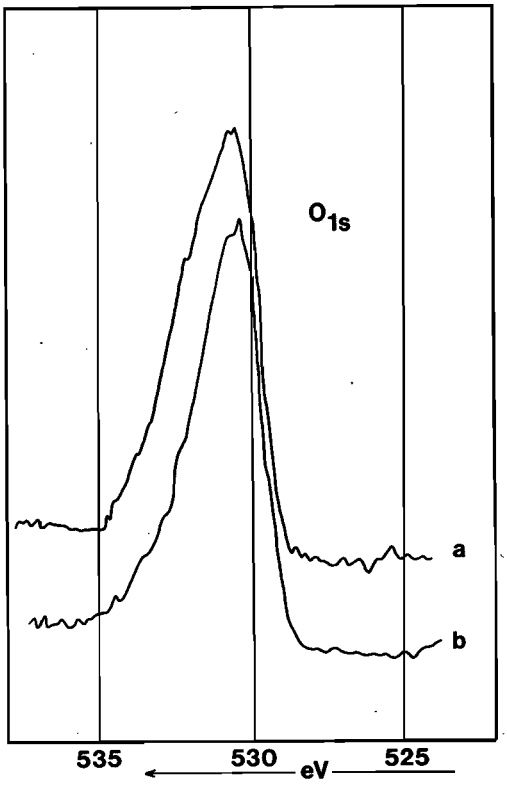

Fig. 3.3 O 1s XPS signals for $Bi_2Mo_{1.02}O_{6.06}$ and $Bi_{2.04}MoO_{6.06}$ (samples pressed in Cu-gauze)

3.5 PULSE EXPERIMENTS

We performed pulse experiments (experimental details: see chapter 2) by pulsing amounts of 1-butene over the powdered sample at different temperatures.
Fig. 3.4 shows the result for the catalyst $Bi_2Mo_{1.02}O_{6.06}$. The conversion of butene per pulse decreases after the first pulse. At 450°C a small increase is observed for the second pulse, but subsequently there is again a decrease in conversion. A completely different behaviour is shown by the catalyst $Bi_{2.04}MoO_{6.06}$ (fig. 3.5). At 400°C there is no conversion during the first three pulses. Afterwards the activity is growing substantially, but after reaching a maximum value it is decreasing again

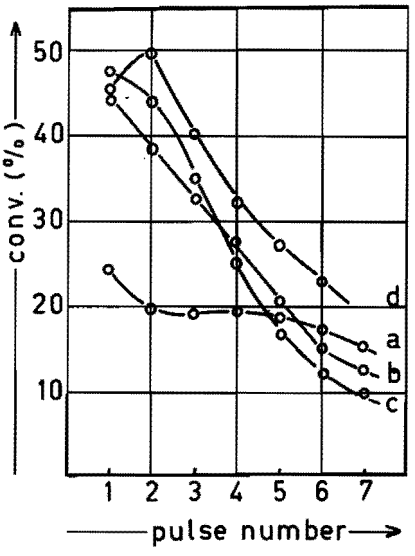

Fig. 3.4 Conversion of 1-butene during pulse experiments on $Bi_2Mo_{1.02}O_{6.06}$ at 350 (a), 400 (b), 425 (c) and 450°C (d)

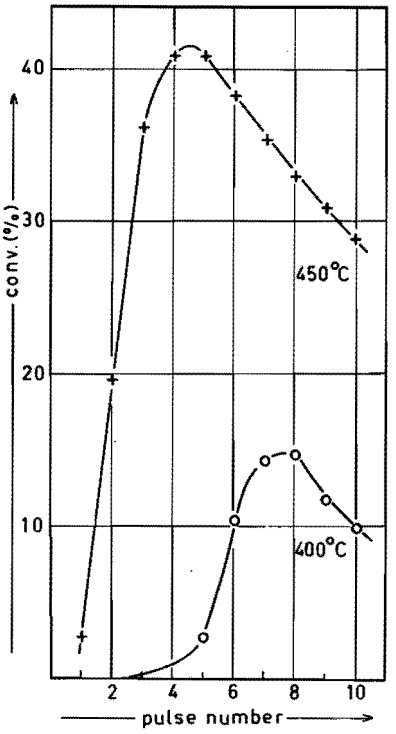

Fig. 3.5 Conversion of 1-butene during pulse experiments on $Bi_{2.04}MoO_{6.06}$ at 400 and 450°C.

as observed with the former catalyst. After an intermediate reoxidation, the conversion at 450°C is starting again at a low level, but is rising very quickly: it reaches its maximum value at the fourth pulse.
During this activation process not only the conversion is rising, but also the selectivity.
After activation by reduction at 450°C, the sample $Bi_{2.04}MoO_{6.06}$ was measured in XPS (table 3.2 and 3.3). The calculated Bi/Mo ratio is now 1.10; compared to the former value of 2.245 this is a strong decrease, indicating a considerable cation migration during the activation process.

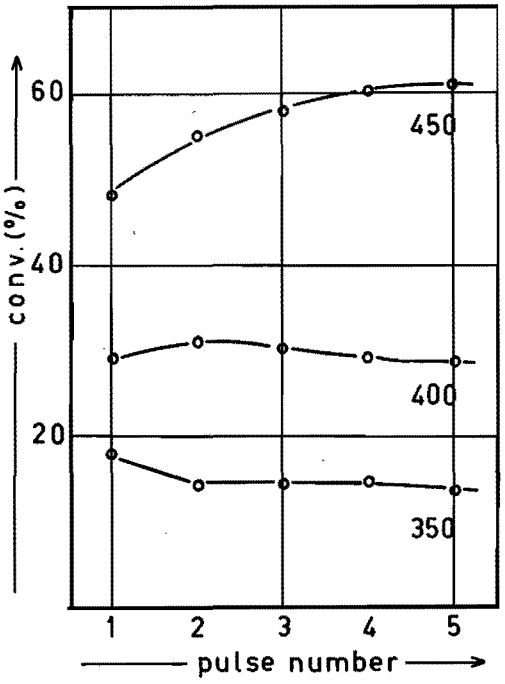

Fig. 3.6 Conversion of 1-butene during pulse experiments on $Bi_2Mo_2O_9$ at 350, 400 and 450°C

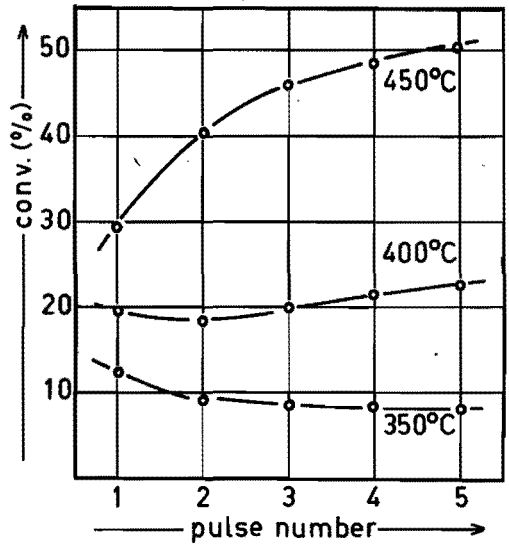

Fig. 3.7 Conversion of 1-butene during pulse experiments on $Bi_2Mo_3O_{12}$ at 350, 400 and 450°C

The catalysts $Bi_2Mo_2O_9$ and $Bi_2Mo_3O_{12}$ show other characteristics (fig. 3.6, 3.7 and 3.8). At 350°C and 400°C a more or less constant level of conversion is observed, while at 450°C the conversion is even increasing during the first pulses. Fig. 3.8 shows that the catalyst $Bi_2Mo_2O_9$ reaches a maximum value after 10 pulses.

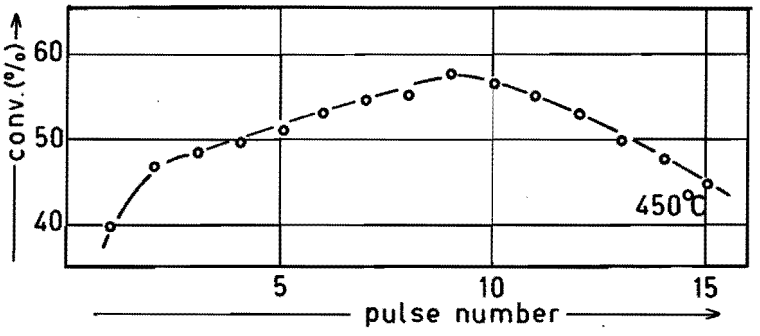

Fig. 3.8 Conversion of 1-butene during pulse experiments on $Bi_2Mo_2O_9$ at 450°C

It could be shown that during this reduction process the catalyst decomposed; an X-ray diagram taken after the reduction indicated an appreciable amount of Bi_2MoO_6 to be present.

3.6 ELECTRICAL CONDUCTIVITY MEASUREMENTS

Preliminary measurements showed that reduction of the catalyst sample caused the electrical conductivity, as measured with the method of chapter 2, to increase substantially.
Also it was clear that the original conductivity could be restored by reoxidation of the reduced material. This behaviour shows that much could be learned from monitoring the electrical conductivity changes during reduction and/or reoxidation.

The measurements performed can be divided into several groups:

a) measurement of the temperature dependence of the conductivity in the oxidized state. From these measurements an activation energy for conduction can be calculated.
b) measurement of conduction after admission of pulses of 1-butene (reduction) at different temperatures, together with the conversion of the butene at the same temperature (simultaneous measurement of conduction and conversion).
c) measurement of conduction and conversion after a reoxidation.

3.6.1 Temperature dependence of the conductivity

For this purpose we examined two of our samples, *i.e.* $Bi_2Mo_{1.02}O_{6.06}$ and $Bi_{2.04}MoO_{6.06}$, so the active and the inactive sample. The temperature range of investigation was 350°C-500°C. The measurements were carried out in air. The measured values of conductivity can be analyzed using the formula $\sigma(T) = \sigma_o.e^{-E/kT}$.
By plotting log σ *vs.* $\frac{1}{T}$ we get a curve whose slope is a measure for the activation energy of conduction.

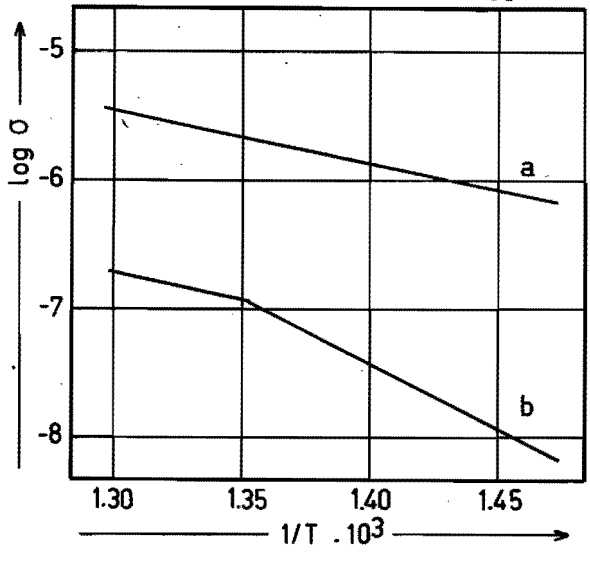

Fig. 3.9 Temperature dependence of the electrical conductivity of $Bi_2Mo_{1.02}O_{6.06}$ (a) and $Bi_{2.04}MoO_{6.06}$ (b) in air

Fig. 3.9 gives the plot for the active and the inactive sample. The active sample has a much lower activation energy (0.8 eV) than the inactive sample (1.97 eV). The conductivity is higher for the active sample.
After reduction of $Bi_2Mo_{1.02}O_{6.06}$ with propene at 400°C for 5 min. we can again measure the temperature dependency. The calculated activation energy is now 0.87 eV for the low temperature range (T < 420°C) and 0.59 eV for the higher temperatures (T > 420°C). Reoxidation with O_2 for 5 min. restores the original value of 0.8 eV.

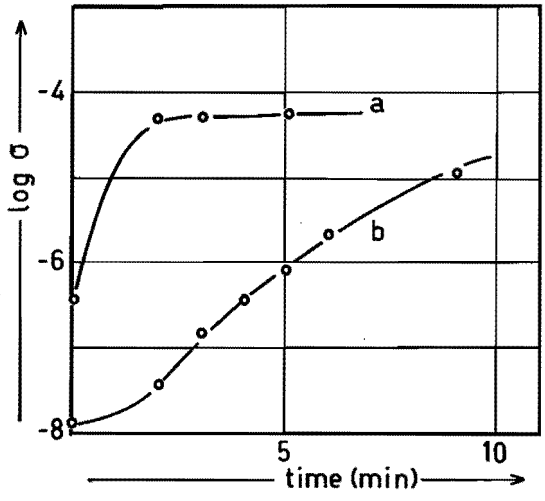

Fig. 3.10 Electrical conductivity as a function of the time of reduction with propene of $Bi_2Mo_{1.02}O_{6.06}$ (a) and $Bi_{2.04}MoO_{6.06}$ (b) at 400°C

The time dependence of the conductivity under reducing conditions (propene 5 cm^3/min) at T = 400°C demonstrates a marked difference between the two samples (fig. 3.10). The active sample gives an immediate rise in conductivity, while the inactive sample has a much slower increase. After several minutes of reduction with propene the conductivity appears to approach the conductivity of the active sample. We will return to this phenomenon later on.

When we carry out the temperature dependence measurements in a helium atmosphere instead of air, we get different results. The initial activation energy for the active sample is much lower than under air, 0.45 eV. After several heating-cooling periods the activation

energies for active and inactive sample appear to reach the same value (table 3.4).

	heating-cooling cycle			
	1	2	3	4
$Bi_2Mo_{1.02}O_{6.06}$	0.45	0.46	0.67	0.81
$Bi_{2.04}MoO_{6.06}$	1.02	1.10	0.87	0.79

3.6.2 Admission of 1-butene

1-Butene was used instead of propene, because of the relatively simpler analysis of the products of oxidation. Conductivity and conversion were measured simultaneously. The time between the successive pulses of butene was fixed at 25 minutes, because of time requirements for analyzing the reaction products.

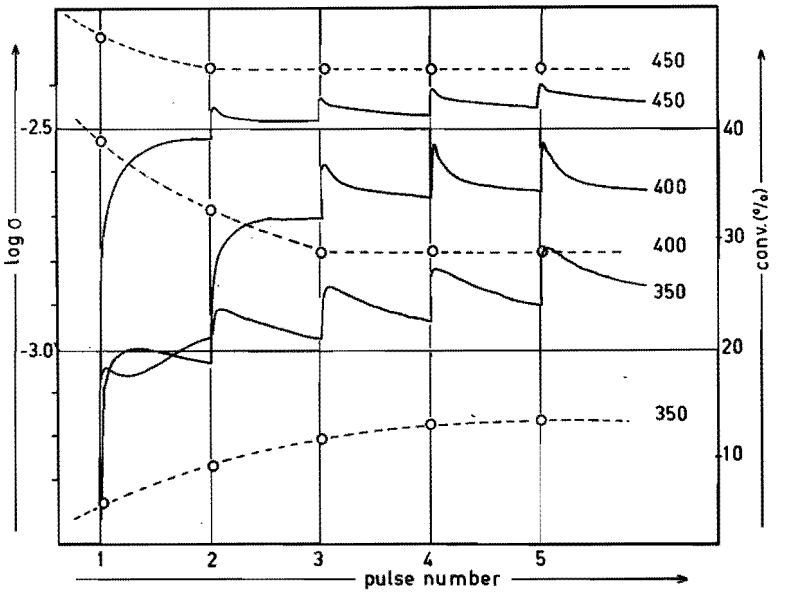

Fig. 3.11a Conversion of 1-butene and electrical conductivity during pulse reduction of Bi_2MoO_6 at 350, 400 and 450°C (detailed picture)

Fig. 3.11a gives an example (Bi_2MoO_6) of the changes in conductivity with increasing number of butene pulses for three different temperatures.
In general the conductivity is rising with the number of pulses of 1-butene. It is noteworthy however, that between pulses a decrease of the conductivity can be observed. This decrease is generally noticeable in all measurements.

In order to avoid complicated drawings, the following figures will show only the maxima in conductivity after each pulse (compare fig. 3.11a with fig. 3.11b).

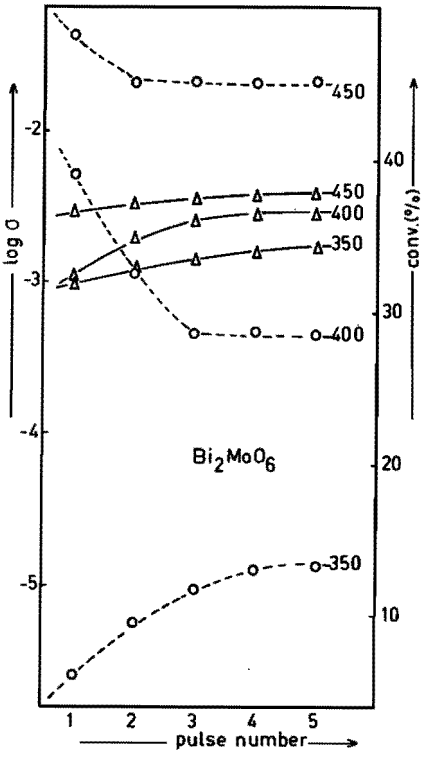

Fig. 3.11b Conversion of 1-butene and electrical conductivity during pulse reduction of Bi_2MoO_6 at 350, 400 and 450°C (only maxima of conductivities are indicated).

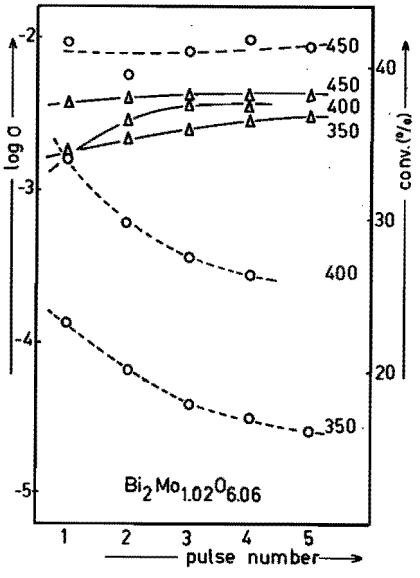

Fig. 3.12 Conversion of 1-butene and electrical conductivity during pulse reduction of $Bi_2Mo_{1.02}O_{6.06}$ at 350, 400 and 450°C

Fig. 3.12-3.16 show the measured conductivity and conversion values at 350°C, 400°C and 450°C for resp. $Bi_2Mo_{1.02}O_{6.06}$, $Bi_{2.04}MoO_{6.06}$, $Bi_2Mo_2O_9$, $Bi_2Mo_3O_{12}$ and MoO_3.

Fig. 3.12 shows that $Bi_2Mo_{1.02}O_{6.06}$ has already at 350°C a fairly high conductivity and a high conversion value (log σ = -2.8 resp. η = 0.23 at the first pulse). During further reduction the conductivity is increasing somewhat, but already after a few pulses a maximum value is reached. At 450°C there is hardly any change both in conductivity and conversion.
This sample $Bi_2Mo_{1.02}O_{6.06}$ shows the highest level of conduction of all our catalysts (highest value log σ = -2.4). The conversion of butene is decreasing from the first pulse on, but at 450°C this is nearly constant (η = 0.42).

Fig. 3.11b indicates that Bi_2MoO_6 shows nearly the same behaviour as the former sample. The conductivity values are at a slightly lower level (maximum log σ = -2.45 at 450°C), but the conversion values are here even a little higher than with the $Bi_2Mo_{1.02}O_{6.06}$ sample.

Fig. 3.13 shows some remarkable features. The sample $Bi_{2.04}MoO_{6.06}$ has a very low level of conversion at 350°C; also the conductivity is at a low level compared to the former samples (log σ = -4). At 400°C after two pulses of butene the conversion is increasing very much and at the same time the conductivity arrives at a much higher level. At 450°C the conversion reaches almost the same level as the active catalysts; again the conductivity follows this trend and becomes as high as the value of the conductivity of the sample $Bi_2Mo_{1.02}O_{6.06}$. After having measured at 450°C, the temperature was lowered to 400°C and again butene pulses were given; there was no initial period and from the first pulse it showed a high conversion.

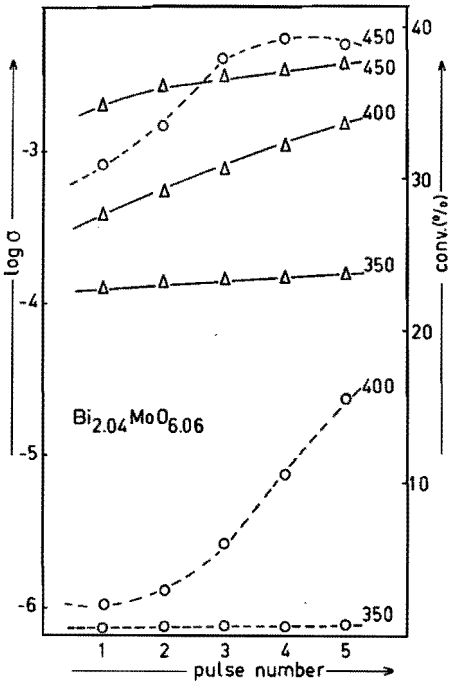

Fig. 3.13 Conversion of 1-butene and electrical conductivity during pulse reduction of $Bi_{2.04}MoO_{6.06}$ at 350, 400 and 450 °C

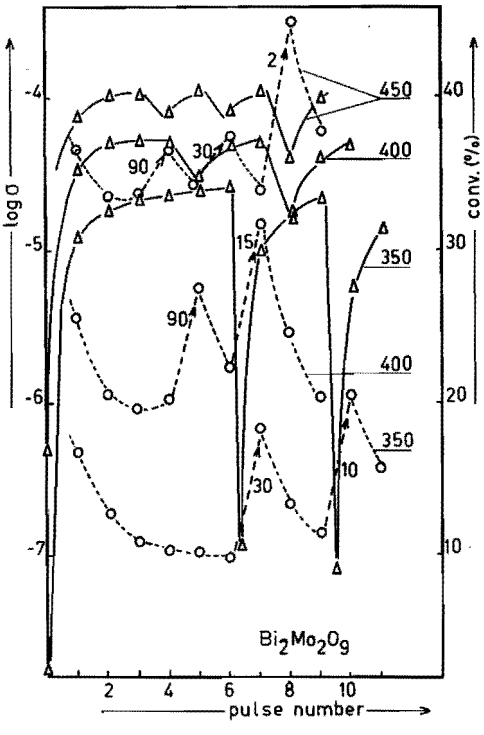

Fig. 3.14 Conversion of 1-butene and electrical conductivity during pulse reduction and oxidation of $Bi_2Mo_2O_9$ at 350, 400 and 450 °C. The numbers indicate the time intervals (in minutes) between an oxygen pulse and the next butene pulse.

The samples $Bi_2Mo_2O_9$ and $Bi_2Mo_3O_{12}$ show in principle the same behaviour as the $Bi_2Mo_{1.02}O_{6.06}$ sample, although the conductivity level is lower (maximum log σ = -4 for $Bi_2Mo_2O_9$ and log σ = -4.5 for $Bi_2Mo_3O_{12}$) (fig. 3.14 and 3.15).

Fig. 3.16 shows the situation for MoO_3 which has a very low conversion and a low conductivity level (log σ = -6).

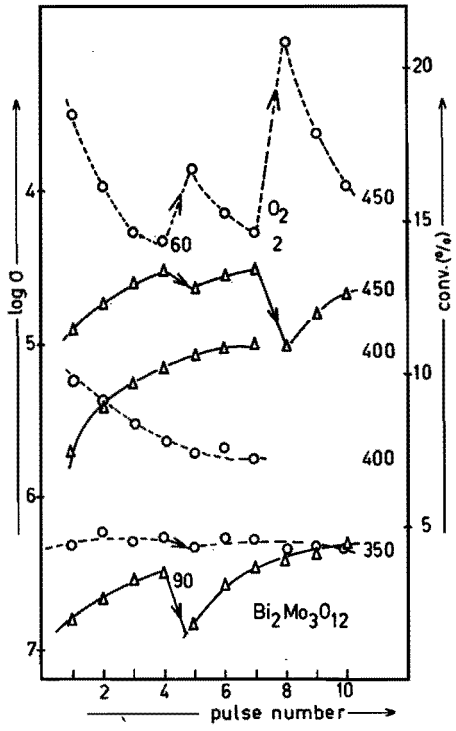

Fig. 3.15 Conversion of 1-butene and electrical conductivity during pulse reduction of $Bi_2Mo_3O_{12}$ at 350, 400 and 450°C

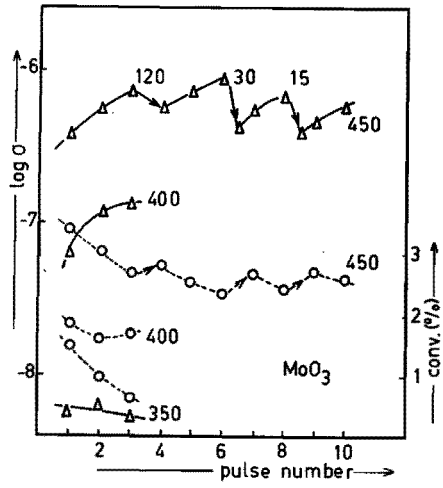

Fig. 3.16 Conversion of 1-butene and electrical conductivity during pulse reduction and oxidation of MoO_3 at 350, 400 and 450°C. The numbers indicate the time intervals (in minutes) between an oxygen pulse and the next butene pulse.

3.6.3 Reoxidation

The foregoing experiments show that the conductivity is increasing by reduction while simultaneously the fractional conversion is decreasing. The question is now what is the behaviour of conductivity and conversion after an intermediate oxidation pulse. The method chosen was to dose an oxygen pulse at a certain moment after passage of a butene pulse and subsequently apply a new butene pulse. The time between oxygen pulse and second butene pulse was varied. During the whole series of pulses there always remains a helium flow over the catalyst.

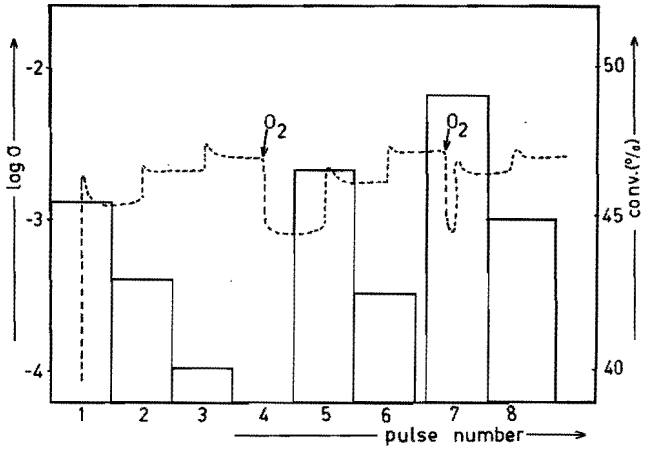

Fig. 3.17 Conversion of 1-butene and electrical conductivity during pulse reduction and oxidation of $Bi_2Mo_{1.02}O_{6.06}$ at 400°C with different time intervals between an oxygen pulse and the next butene pulse

The scenario of the experiments was as follows:

a) a series of butene pulses is fed to the reactor similarly as before (time intervals of 25 minutes)
b) an oxygen pulse is given
c) after $t = t_1$ a new butene pulse follows
d) a new series of butene pulses is added to arrive at the same situation as after the first series.
e) again an oxygen pulse is added and
f) after $t = t_2$ a new butene pulse follows.

Fig. 3.17 shows the conductivity and conversion values during these experiments for the $Bi_2Mo_{1.02}O_{6.06}$ sample. After reoxidation the conductivity is lowered. Most remarkable is the fact that the conversion after reoxidation is dependent on the time between the oxygen pulse and the next butene pulse, *i.e.* the time during which the oxygen can do its reoxidizing work.
A short time results in a high conversion, while a long time gives a lower conversion, although this is still higher than the conversion with the first butene pulse.

Reoxidation experiments were also carried out with the $Bi_2Mo_2O_9$ (fig. 3.14) and $Bi_2Mo_3O_{12}$ (fig. 3.15) with similar results as given above.

Another type of experiment was performed with $Bi_2Mo_3O_{12}$. We examined the influence of the reoxidation during longer periods under helium. At 450°C after the fourth butene pulse we kept the catalyst for 1 hour in a helium atmosphere. The next butene pulse showed a higher conversion, while the conductivity during the intermediate period had decreased somewhat.
With MoO_3 (fig. 3.16) little changes during reoxidation were observed apart from a considerable decline in selectivity.
This decrease in selectivity after a reoxidation pulse was also observed for the samples $Bi_2Mo_{1.02}O_{6.01}$ and $Bi_2Mo_3O_{12}$ although to a lesser degree.
Table 3.5 gives the selectivities for $Bi_2Mo_{1.02}O_{6.06}$, $Bi_2Mo_3O_{12}$ and MoO_3 after different time intervals between the reoxidation and the next butene pulse.

The greatest changes are observed with the catalysts that have the lowest activity values, *i.e.* $Bi_2Mo_3O_{12}$ and MoO_3.

The catalyst $Bi_2Mo_{1.02}O_{6.06}$ was used to study the conductivity under reaction conditions by giving pulses of mixtures of oxygen and butene at T = 400°C.
Fig. 3.18 gives the influence of the ratio $r = \frac{\text{butene}}{\text{butene + oxygen}}$ on conductivity and conversion.

$Bi_2Mo_{1.02}O_{6.06}$		$Bi_2Mo_3O_{12}$		MoO_3	
t(min)	select(%)	t(min)	select(%)	t(min)	select(%)
initial	98.8	initial	97.8	initial	89.0
	99.2				
		90	98.1	120	93.5
25	97.8				
	99.0	15	97.2	30	89.6
	99.2				
		2	96.5	10	81.3
5	97.9				
	99.0				
	99.2				

Table 3.5 Selectivities(%) of various catalysts after different time intervals (min.) between reoxidation and next butene pulses

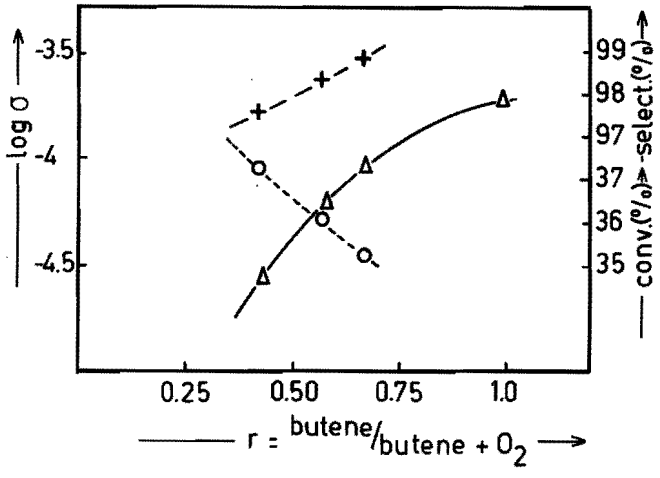

Fig. 3.18 Electrical conductivity, conversion of 1-butene and selectivity during pulses of butene-oxygen mixtures with variable composition on $Bi_2Mo_{1.02}O_{6.06}$ at 400°C.

It shows that the conductivity is lower, the more oxygen is present in the pulse while the fractional conversion is higher for greater oxygen contents. The selectivity of the

reaction increases with higher butene ratios.

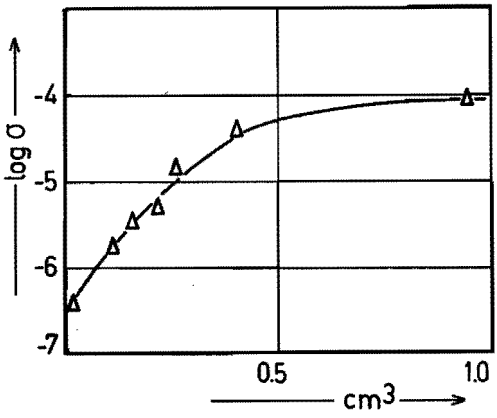

Fig. 3.19 Relation between the electrical conductivity after the first pulse of butene and the volume of the pulse (in cm^3) at T = 450°C for $Bi_2Mo_2O_9$

The variation of the amount of butene added for one single pulse was studied for $Bi_2Mo_2O_9$ at 450°C (fig. 3.19) *i.e.* a situation in which the use of one pulse of the habitually applied size *i.e.* 0.9 cm^3 immediately gave a maximum conductivity that did not vary anymore with additional pulses. By varying the amount of butene added in the first pulse after complete reoxidation of the catalyst it was tried to determine how much butene was necessary to arrive at the maximum level. Two loops were used for this purpose while moreover the butene content could be varied still further by dilution with helium. It is seen that amounts in the order of half those normally added suffice to obtain maximal conductivity. It should be stressed that this is not due to complete reduction of the catalyst as seen by the amount of butene converted that is still rising.

Some remarks have to be made regarding the conductivity of bismuth oxide. No conductivity could be measured below 500°C. By reduction at 500°C the conductivity was lowered, by reoxidation it was increased again. This is completely opposite to the behaviour of the bismuth molybdates. This phenomenon can be ascribed to the p-type behaviour of Bi_2O_3 compared to the n-type semiconductivity of the bismuth molybdates and MoO_3 (fig. 3.20).

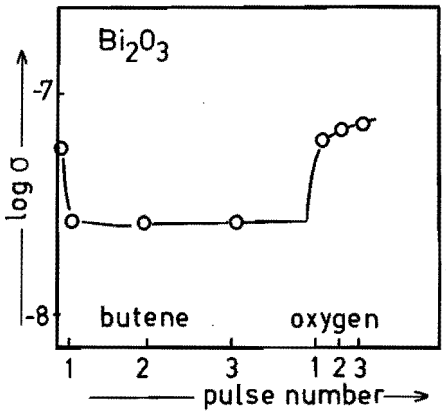

Fig. 3.20 Electrical conductivity of Bi_2O_3 at 500°C during 1-butene and oxygen pulses.

3.7 SUMMARY OF RESULTS

The rate of incipient reduction of a catalyst appears not so much dependent on its bulk structure or composition then on the composition of the surface layers. These can differ appreciably from that in the bulk. Maximum activity appears to be located between 1 < (Bi/Mo)surface < 2.

The inactive catalysts with a (Bi/Mo)surf. > 2 can be made to become active by reduction, a conversion that can be reversed by reoxidation. This points to a cation migration in the surface layers. The process appears to be autocatalytic (or concerted): once it starts it accelerates. Although slower than the actual reduction it appears nevertheless fast enough to become easily observable.

Combinations of two catalysts with low and high Bi/Mo ratios can be reasonably active. Therefore, there appears to be cation migration (for instance as MoO_3) from the particles of one of the catalysts to that of the other. An alternative explanation may be that the two basic subreactions in the oxidative dehydrogenation

viz. reduction by the hydrocarbon and reoxidation by oxygen can take place on the different surfaces of the two catalysts. This requires transport of intermediates, protons and electrons from one surface to the other.

Diffusion of oxygen from the bulk of the catalyst to its surface depleted by reduction is generally acknowledged as of similar rate as the reduction and sometimes even as rate determining. The process could be readily observed in our experiments: it was usually found to be lower in rate than the reduction below 450°C, but might become faster than that at higher temperatures. Diffusion appears to be slower for high (2/1) and low 2/3) ratios of Bi/Mo and to be somewhat faster in the middle ranges.

Reduction causes the catalyst to become electrically conductive, a process that is reversed by reoxidation. The conductivity seems to reside in the surface layers: deep reduction does not lead to increased conductivity. There seems to be a connection between the increase in conductivity and the oxygen diffusion: the faster the latter, the more restricted the increase in conductivity. The conductivity is certainly of the semiconductive type and it would be of great interest to determine its activation energy for various catalysts. No theoretical model seems to exist however that enables this calculation and a comparison of the activation energies with catalytic activity. Even so monitoring of the electrical conductivity appears to be of considerable importance in elucidating the oxidation mechanism.

Apart from activities, also selectivities of catalysts have to be considered. As a general rule selectivities become lower at the fringes of the high activity range. If a catalyst can be brought to change from the inactive to the active range, as the $Bi_{2.04}MoO_{6.06}$ catalyst, it

passes through an intermediate situation with relatively low activity and selectivety.

If a series of alternating pulses of butene and oxygen are led over a catalyst the outcome depends on the time interval between oxygen and butene pulses. If this is short, conversion of the butene pulse is relatively high but selectivity is not maximal, while at longer time intervals the conversion is lower but selectivity is higher. This might indicate the formation of an intermediate oxygen surface species of sufficient life time to make itself observable by higher oxidation activity but lower selectivity.

REFERENCES

1. A.C.A.M. Bleyenberg, B.C. Lippens, G.C.A. Schuit, J. Catal., 4, 581 (1965).
2. R. Kohlmuller, J.-P. Badaud, Bull. Soc. Chim. France, 3434 (1969).
3. L.Ya. Erman, E.L. Gal'perin, B.P. Sobolev, Russ. J. Inorg. Chem., 16, 258 (1971).
4. G. Gattow, Z. Anorg. Allgem. Chem., 298, 64 (1958).
5. W.T. Schaller, U.S. Geol. Survey, Bull. 610, 9 (1916).
6. J. Zemann, Heidelberger Beitr. Mineral. Petrog., 5, 139 (1956).
7. A.F. van den Elzen, G.D. Rieck, Acta Cryst., B 29, 2436 (1973).
8. M. Cesare, G. Perego, A. Zazetta, G. Manare, B. Notari, J. Inorg. Nucl. Chem., 33, 3595 (1971).
9. A.F. van den Elzen, G.D. Rieck, Acta Cryst., B 29, 2433 (1973).
10. A.F. van den Elzen, G.D. Rieck, Mat. Res. Bull., 10, 1163 (1975).
11. B.C. Gates, G.C.A. Schuit, "Chemistry of catalytic processes", p. 373 (to be published).
12. Ph.A. Batist, J.F.H. Bouwens, G.C.A. Schuit, J. Catal., 25, 1 (1972).
13. H. Berthou, C.K. Jørgensen, Anal. Chem., 47, 482 (1975).
14. A. Cimino, B.A. de Angelis, J. Catal., 36, 11 (1975).

CHAPTER 4

BISMUTH DOPED LEAD MOLYBDATE

4.1 INTRODUCTION

Scheelite structured molybdates, tungstates and vanadates were reported by Aykan (1, 2) and Sleight (3, 4). They introduced point defects as cation vacancies and obtained phases like $A^{1+}_{0.5-3x}Bi^{3+}_{0.5+x}\phi_{2x}MoO_4$ (A^{1+} = Li, Na, Ag) or $A^{2+}_{1-3x}Bi^{3+}_{2x}\phi_xMoO_4$ (A^{2+} = Pb, Cd, Ca), where ϕ represents a vacant lattice site.

Both systems showed a very low activity for propene oxidation, at x = 0, but a very sharp increase with increasing x. This indicates that both defects and bismuth ions have to be present for high activity and selectivity.

Similar combinations of defects and bismuth ions occur in some common bismuth molybdates, so the model catalyst $Pb_{1-3x}Bi_{2x}\phi_xMoO_4$ can be helpful in understanding the mode of action of the bismuth molybdates. In this chapter we report some experiments in this field.

4.2 THE PbO-Bi_2O_3-MoO_3 SYSTEM

The ternary system PbO-Bi_2O_3-MoO_3 was first investigated by Belyaev and Smolyaninov (5).
In the binary system Bi_2O_3-PbO only one distinct phase was detected: $3Bi_2O_3.2PbO$ with melting point 704°C.
The system Bi_2O_3-MoO_3 contained several compounds: $Bi_2(MoO_4)_3$, m.p. 648°C; Bi_2MoO_6, m.p. 970°C and

$3Bi_2O_3.MoO_3$, m.p. 990°C. Solid solutions with Bi_2MoO_6 were formed.

In the $PbO-MoO_3$ system two compounds were found: Pb_2MoO_5, m.p. 952°C and $PbMoO_4$, m.p. 1065°C. The ternary system $PbO-Bi_2O_3-MoO_3$ was characterized by six ternary points, of which five were eutectics and one peritectic.

Viskov *et al.* (6) in their search for new ferroelectric compounds found a ternary polycrystalline compound with the composition $Pb_3Bi_2MoO_9$ having the pyrochlore structure.

Some data are given in literature regarding the system lead molybdate-bismuth molybdate (α-phase). Zambonini (7) reports an eutecticum at 71.5 mole% $Bi_2(MoO_4)_3$ at about 613°C but could not find evidence for mutual solubility. Later, Howard *et al.* (8) investigated the lead molybdate-α-bismuth molybdate phase diagram. They concluded that the system is a simple eutectic system. A maximum solid solubility of 6 mole% was found at the lead molybdate end of the diagram. On the other hand, lead molybdate appears to be insoluble in bismuth molybdate. The eutectic point was found to be at 11 mole% $PbMoO_4$ and 634°C.

The earlier literature contains, as far as catalysis is concerned, only one patent (9), describing an ammoxidation reaction of olefins over silica supported molybdates with the general composition $Pb_aBi_bMoO_c$ where a = 0.08 - 0.75, b = 0.1 - 0.8 and c = 3.1 - 4.5, while a + b = 0.55 - 1.1.

During the preceding six years, Aykan (1, 2) and Sleight (3, 4) investigated the system as part of a more elaborate structural and catalytic study on scheelite type molybdates, tungstates and vanadates. Some of the samples of interest for catalysis are described in a patent (10). For instance, they prepared phases of the formula $Pb_{1-3x}Bi_{2x}\phi_xMoO_4$ by heating mixtures of the individual oxides, where ϕ represents a cation vacancy. These phases are described as defect scheelites. They were used to examine the relationship between cation

defects and catalytic properties. As test reaction, the oxidation and ammoxidation of propene and the oxidative dehydrogenation of butene were used. Both defects and bismuth ions have a considerable effect on activity and selectivity of olefin oxidation. The defects were assumed to promote the formation of the allyl radical, while bismuth has a role in the reoxidation of the active site.

4.3 RESULTS

We started our experiments from the compound $PbMoO_4$. Lead molybdate is a compound which has a well defined crystal structure, referred to as a scheelite ($CaWO_4$)-type compound (11) (fig. 4.1). In the same way as Sleight *et al.* (3) we replaced part of the lead ions by bismuth ions, so that vacancies are introduced: $3Pb^{2+} \longleftrightarrow 2Bi^{3+} + \phi$. However, our method to effect this was by coprecipitation from mixed solutions of Pb- and Bi-nitrate instead of by the interaction of solid oxides at higher temperatures as applied by Sleight (6). Precipitation might lead to larger surface areas and therefore greater activity of the catalyst.

We prepared a series of samples with the overall composition $Pb_{1-3x}Bi_{2x}\phi_xMoO_4$ ($0 < x < 0.2$). Sleight (6) prepared these with $0 < x < 0.15$ by heating mixtures of the component oxides at a temperature of at least 700°C. Even their sample with $x = 0.01$ showed considerable activity and selectivity for the ammoxidation of propylene, while lead molybdate itself was inactive. Because of the low surface area of the samples ($< 1\ m^2/g$), the activities were usually lower than for the bismuth molybdates. Our method of preparation was chosen differently because we wanted to prepare samples with surface areas comparable to the bismuth molybdates. Therefore we used coprecipitation from solutions similar to that used for the β-bismuth

molybdate compound.

Bismuth nitrate solution, lead nitrate solution and an ammonium heptamolybdate solution were brought together; the resulting precipitate was filtered off, dried at 120°C for 12 hours and calcined at 400°C for 2 hours. The solutions were previously cooled in ice baths at 0°C. Subsequent to bringing together the solutions, the pH was adjusted at pH = 5 by adding ammonia. No residence was left in the filtrate water after filtration.
We prepared samples of the composition $Pb_{1-3x}Bi_{2x}\phi_xMoO_4$ with x = 0.01, 0.02, 0.04, 0.06, 0.10 and 0.20.
Fig. 4.2a-c gives the activity and selectivity for butene oxidative dehydrogenation.
Fig. 4.3 gives the activity and selectivity for one temperature (T = 475°C) as function of x.

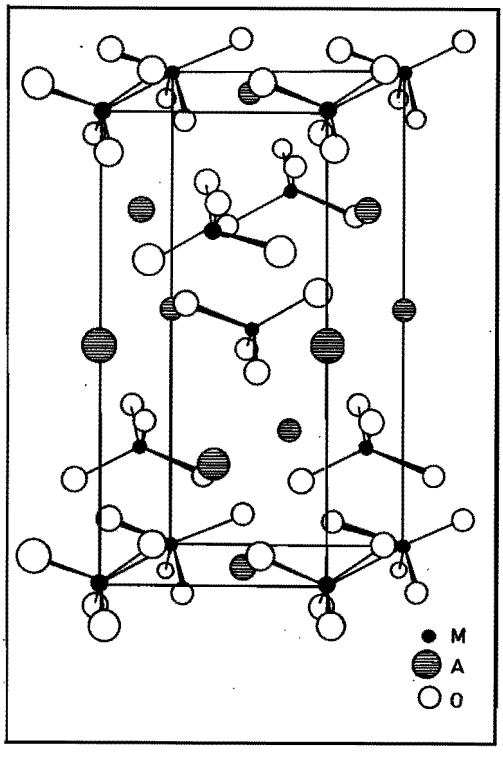

Fig. 4.1 Scheelite structure of $AMoO_4$ with unit cell outlined (from Sleight (4))

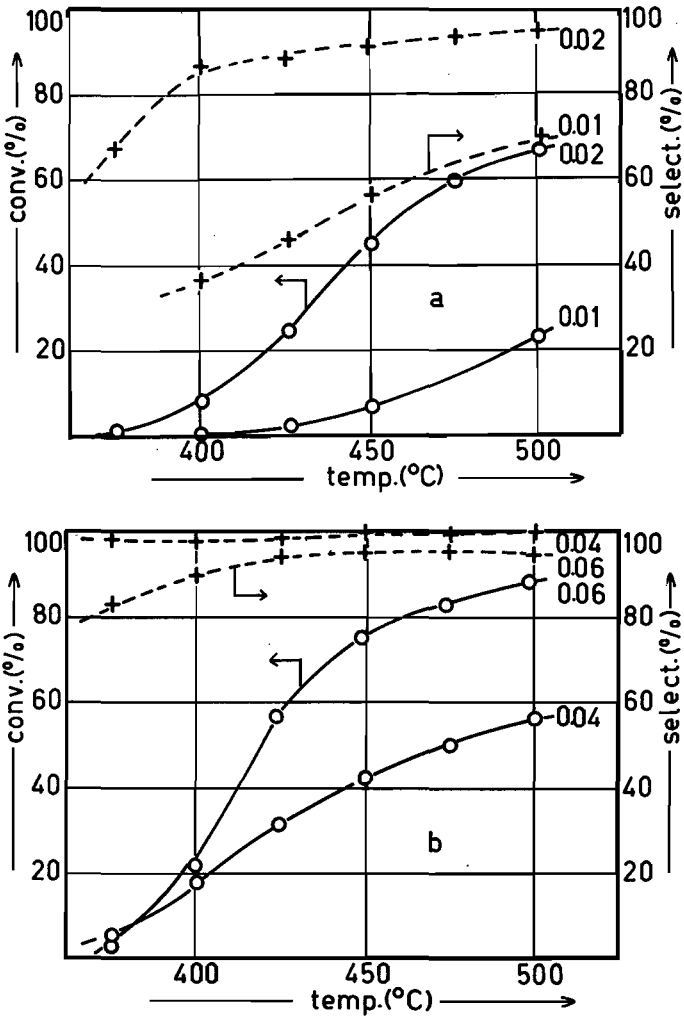

Fig. 4.2 Activities and selectivities in 1-butene oxidative dehydrogenation for $Pb_{1-3x}Bi_{2x}MoO_4$ *as function of temperature.*

(a) $x = 0.01$ *and* $x = 0.02$

(b) $x = 0.04$ *and* $x = 0.06$

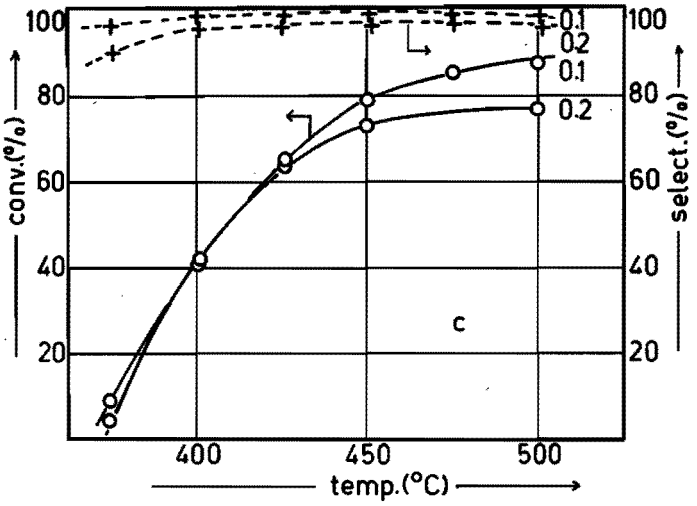

Fig. 4.2 Activities and selectivities in 1-butene oxidative dehydrogenation for $Pb_{1-3x}Bi_{2x}MoO_4$ as function of temperature.
(c) x = 0.1 and x = 0.2

As can be seen, there is a sharp increase in activity already at a small value of x. This is accompanied by a simultaneous increase in selectivity. Maximum activity and selectivity is reached at x = 0.06.

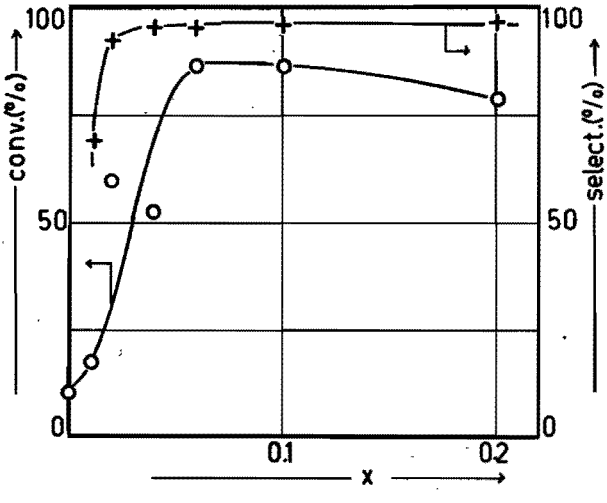

Fig. 4.3 Activities and selectivities in 1-butene oxidative dehydrogenation for $Pb_{1-3x}Bi_{2x}MoO_4$ as function of x at 475°C.

Fig. 4.4 gives the X-ray diagrams (line drawings) of two of the phases. Up to x = 0.10 we can only see reflections belonging to the scheelite phase of $PbMoO_4$. At x = 0.20 the system consists of a mixture of Bi-doped lead molybdate and α-bismuth molybdate. The indexing of the reflections is well known from earlier work (Sleight, (4)).
It is shown once more in fig. 4.5.

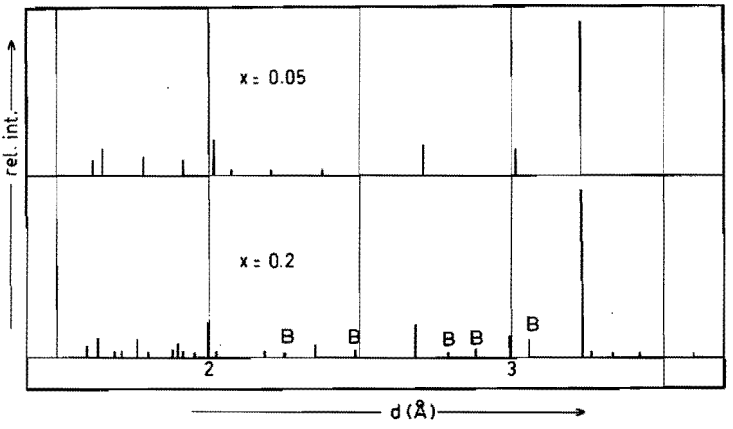

Fig. 4.4 X-ray line diagrams of $Pb_{1-3x}Bi_{2x}MoO_4$ with x = 0.05 and x = 0.2 (B = α-bismuth molybdate line)

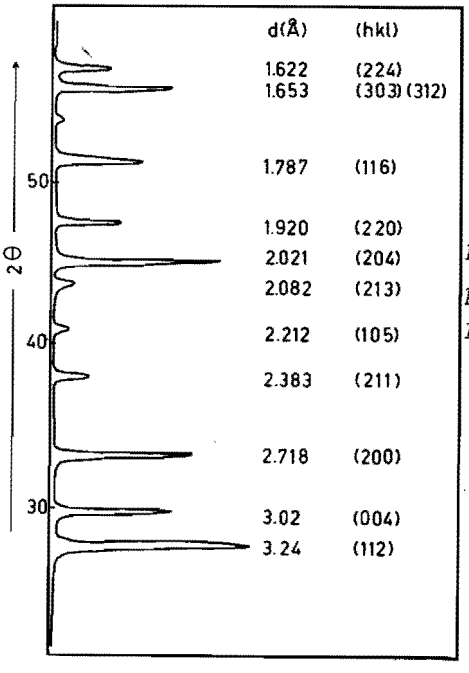

Fig. 4.5 X-ray diffraction pattern and indexing of $PbMoO_4$

Since the structure is tetragonal the following formula is valid:

$$\frac{h^2 + k^2}{a_0^2} + \frac{l^2}{c_0^2} = \frac{1}{d_{hkl}^2}$$

in which h, k and l are Miller indices of the reflection planes and a_0 and c_0 are lattice parameters.
By choosing two appropriate diffraction lines, *e.g.* (hkl) = (004) and (hkl) = (200), we can calculate the cell-parameters a_0 and c_0, for $c_0 = 4\ d_{004}$ and $a_0 = 2\ d_{200}$.

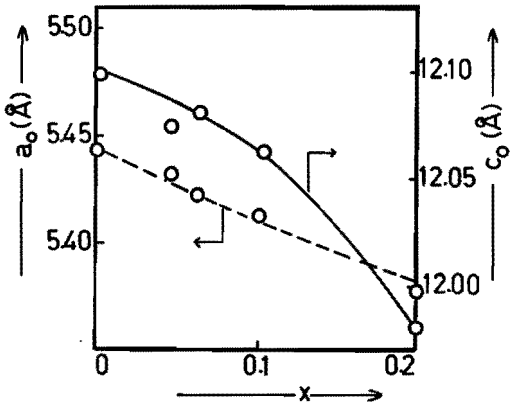

Fig. 4.6 Cell parameters a_0 and c_0 as function of x for $Pb_{1-3x}Bi_{2x}MoO_4$

The calculated parameters are listed in table 4.1 and represented in fig. 4.6 as a function of x.

$Pb_{1-3x}Bi_{2x}MoO_4$	2θ	d_{004}	2θ	d_{200}	c_0	a_0
x = 0	29.5	3.0253	32.0	2.7200	12.1012	5.440
x = 0.04	29.6	3.0153	33.03	2.7095	12.0612	5.4190
x = 0.06	29.55	3.0203	33.00	2.7120	12.0812	5.4240
x = 0.1	29.60	3.0153	33.08	2.7056	12.0612	5.4112
x = 0.2	29.82	2.995	33.32	2.688	11.980	5.376

Table 4.1 Lattice parameters of $Pb_{1-3x}Bi_{2x}MoO_4$

The lattice constants a_0 and c_0 decrease continuously with increasing x, indicating that the lattice is influenced by the incorporation of bismuth ions and cation vacancies. When we consider this system as a

solid solution, then it is obeying Vegards law in this way that the parameter (a_0) of the solution is directly proportional to the atomic percent of solute (x).

One of the samples with composition $Pb_{0.7}Bi_{0.2}MoO_4$ was investigated in more detail.
First, we compared different procedures of preparation as to their influence on structure and catalytic activity. The variations investigated were temperature (0^0C against 80^0C) use of ammonium heptamolybdate or molybdic acid, time of ageing of the precipitate (few minutes *vs.* two hours), pH of the solutions (pH = 4 *vs.* pH = 10), filtration *vs.* evaporation. The results showed that the way of preparation is not very critical as regards activity and selectivity. For most of the samples the activity for oxidative butene dehydrogenation starts at about 350^0C and reaches an optimum at about 450^0C, between 85 and 90% conversion, the selectivities being higher than 90%.

The X-ray diffraction patterns give the general pattern for the scheelite structure. In a few cases we did observe some lines with very low intensity, which can be ascribed to bismuth molybdate 2/1 indicating that there was no complete solid solution. However, even these samples did not give a lower catalytic activity.

Comparison precipitation and solid state synthesis

A sample with composition $Pb_{0.7}Bi_{0.2}MoO_4$ was prepared according to the method used by Sleight (3) and compared with a similar sample, made by the precipitation technique. The solid state preparation consisted of mixing the component oxides thoroughly and heating them for 2 hours at 700^0C. Under our reaction conditions the activity of the first sample was found to be much lower than that of the precipitation sample (fig. 4.7). The surface area of this sample was also much lower than for the precipitation sample.

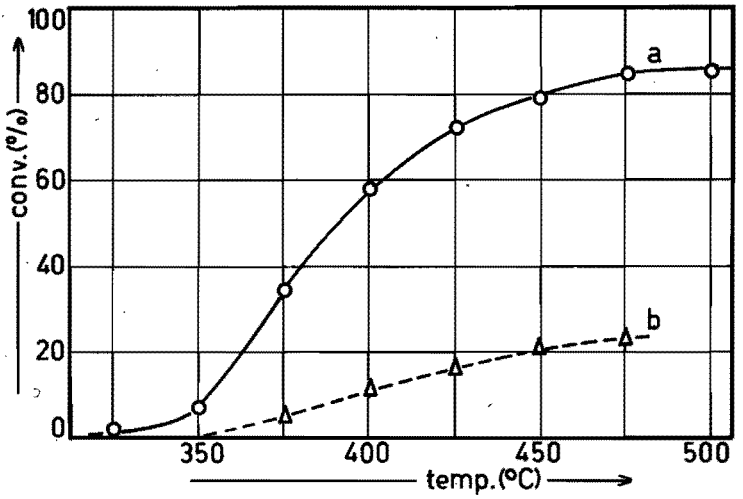

Fig. 4.7 Activities for 1-butene oxidative dehydrogenation as function of temperature on $Pb_{0.7}Bi_{0.2}MoO_4$ (a) prepared according to a precipitation procedure (b) prepared from oxides at 700°C

If we assume that the oxidation of 1-butene is of first order in the C_4-concentration, the activity per unit of surface area can be calculated. Table 4.2 gives the pertinent data for T = 475°C.

$Pb_{0.7}Bi_{0.2}MoO_4$	η_{475}	SA(m^2/g)	k/s
precipitation	0.84	6.4	0.84
from oxides	0.22	0.5	1.33

Table 4.2 Comparison of activity, surface area and reaction rate per unit of surface area of the differently prepared samples of $Pb_{0.7}Bi_{0.2}MoO_4$

The X-ray diagrams of both samples agree with an essentially pure scheelite structure, the precipitation sample showing a very samll amount of γ-bismuth molybdate (fig. 4.8)

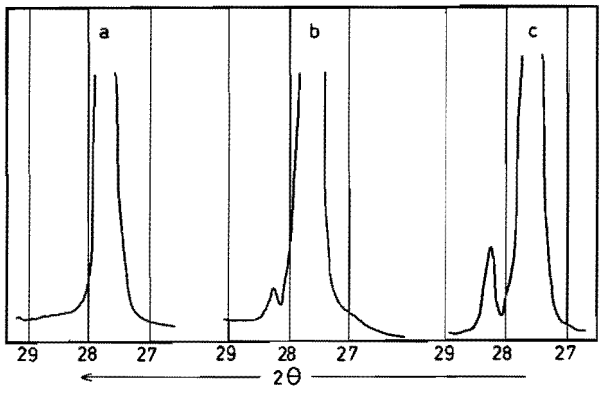

Fig. 4.8 Part of the X-ray diffraction pattern of $Pb_{0.7}Bi_{0.2}MoO_4$.
(a) prepared from oxides at 700°C
(b) prepared by precipitation
(c) after 20 h under reaction conditions at 475°C

After prolonged heating of this latter catalyst under reaction conditions (butene/O_2 mixture at T = 475°C) for 20 hours the decomposition was more extensive as shown by the growth in intensity of the γ-phase peak at d = 3.15 Å.

X-ray photo-electron spectroscopy was performed on these two samples (fig. 4.9).

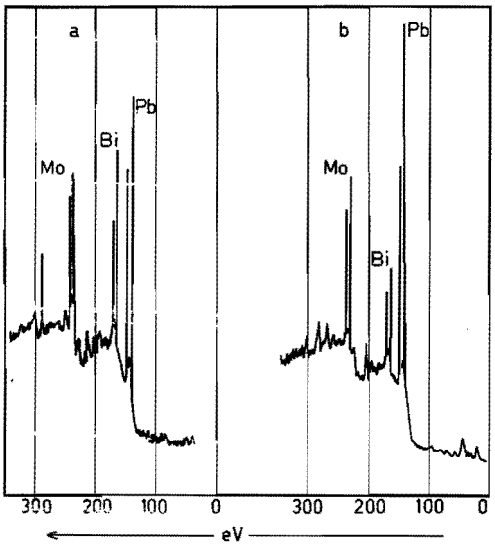

Fig. 4.9 XPS-spectra of $Pb_{0.7}Bi_{0.2}MoO_4$
(a) precipitation sample
(b) sample from oxides

The method gives information about the outermost 15-20 Å of the particles. From the intensities we can calculate the relative ratios of lead, bismuth and molybdenum ions at the surface layers. Putting the molybdenum content at 1.00, the lead and bismuth contents found were those tabulated in table 4.3.

	Mo	Pb	Bi
bulk composition	1.00	0.70	0.20
surface { precipitation	1.00	0.57	0.41
surface { from oxides	1.00	0.67	0.21
after reaction	1.00	0.57	0.32

Table 4.3 Surface concentrations of Mo, Pb and Bi in $Pb_{0.7}Bi_{0.2}MoO_4$ *as measured by XPS*

When compared with the bulk composition $Pb_{0.7}Bi_{0.2}MoO_4$ the sample, prepared from the oxides at high temperature, turns out to have a surface composition nearly equal to that of the bulk, while the precipitation sample has its surface enriched in bismuth.

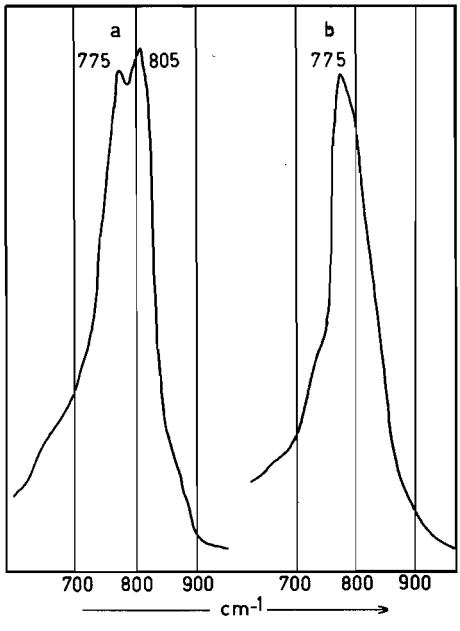

Fig. 4.10 Part of the infrared spectrum of $Pb_{0.7}Bi_{0.2}MoO_4$ *(a) and* $PbMoO_4$ *(b)*

Infrared spectra were recorded for the doped lead molybdate and compared with pure lead molybdate (fig. 4.10). The bismuth doped sample has a second band at 805 cm^{-1} which is not present in the pure lead molybdate.
There is no difference in the infrared spectra between the precipitation and the solid state synthesis sample, except for an intensity difference which can be attributed to a particle size effect.
The new band represents the stretching of a MoO_4-group different in symmetry from that present in $PbMoO_4$ as is to be expected because of the absence of a cation near to it. It may be remarked that the spectrum is similar to that of Bi_2MoO_9.

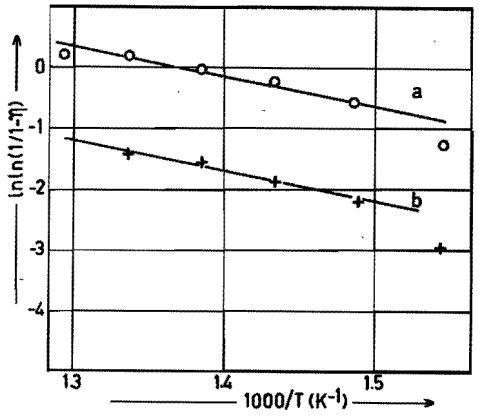

Fig. 4.11 Activation energies for $Pb_{0.7}Bi_{0.2}MoO_4$ in case of a first order reaction in butene
(a) precipitation sample
(b) from oxides

The kinetics of the butene oxidation were not studied for these samples. For pure bismuth molybdates it is known that the butene oxidative dehydrogenation is of first order in 1-butene above 400°C. If we assume this to be the case also for these samples and $\ln k - \frac{1}{T}$ Arrhenius plots are made, we obtain the results shown in fig. 4.11. At the higher temperatures, a low activation energy is found (~ 10 kcal/mole) with hardly any difference between the two samples and about equal to that found for bismuth molybdates.

The activity of the precipitated catalyst was found to decay slowly with time spent under reaction conditions

(at 475°C) as shown in fig. 4.12.

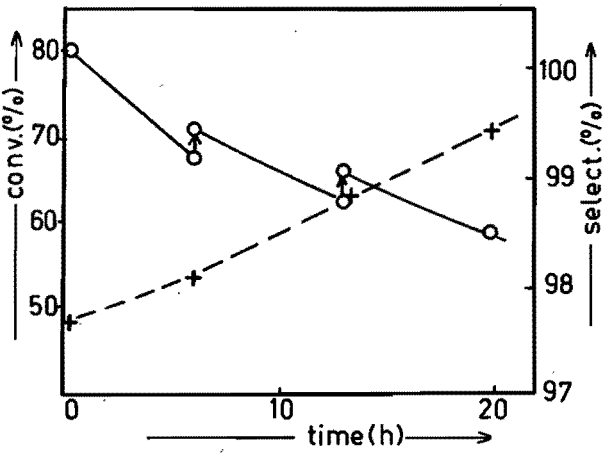

Fig. 4.12 Stability test for $Pb_{0.7}Bi_{0.2}MoO_4$ (normal reaction conditions at 475°C).

At certain periods during the experiment the run was discontinued with the catalyst staying under helium at room temperature. It is noteworthy that this led to a slight restoration of the activity as indicated by the breakpoints in the curve.

The surface composition of the used catalyst was measured in X-ray photo-electron spectroscopy (table 4.3). The bismuth concentration at the surface is lowered with respect to that of the fresh catalyst.

Pulse experiments, where the catalyst is reduced by pulses of a known amount of butene and the reaction products are subsequently analyzed, were performed on the two samples. Fig. 4.13 gives the conversion of the butene pulse as a function of the number of pulses passed and this for different temperatures. It is clear that the higher the temperature, the higher the conversion. It is seen that during the first three pulses of 1-butene, there is an increase in conversion, *i.e.* activity. It appears that for this catalyst system the activity is optimal when it is slightly reduced. There is no principal difference between the results for the two types of lead bismuth molybdate.

The same samples were also studied as to their electrical conductivity. First, we measured the temperature

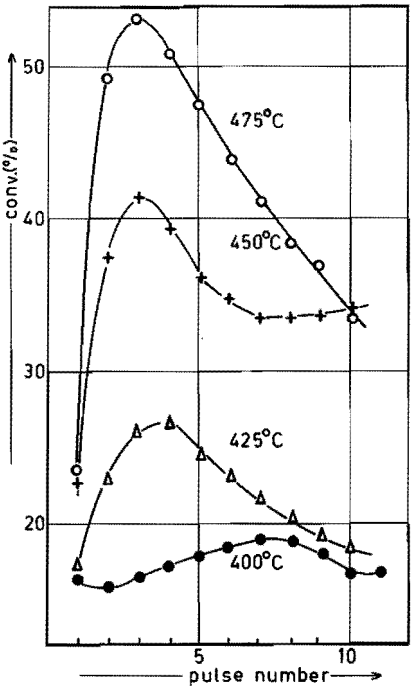

Fig. 13a Conversion of 1-butene during pulse reduction of $Pb_{0.7}Bi_{0.2}MoO_4$ (precipitation sample) at different temperatures

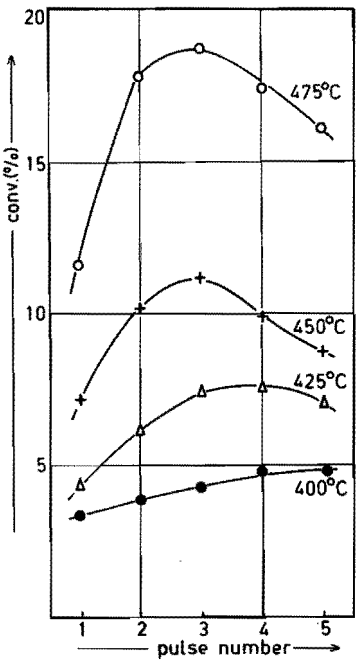

Fig. 13b Conversion of 1-butene during pulse reduction of $Pb_{0.7}Bi_{0.2}MoO_4$ (prepared from oxides at 700°C) at different temperatures)

dependence of electrical conductivity under helium. Fig. 4.14 shows that this dependency is split up into two parts. At low temperatures we get a high "activation energy", while at higher temperatures a lower value is found.

In our conductivity apparatus, it was possible to measure simultaneously the electrical conductivity and the conversion of butene. The fig. 4.15,4.16 and 4.17 give the results for precipitation catalyst, solid state catalyst (both $Pb_{0.7}Bi_{0.2}MoO_4$) and lead molybdate as function of the number of pulses of 1-butene at three different temperatures. The conductivity is rising with

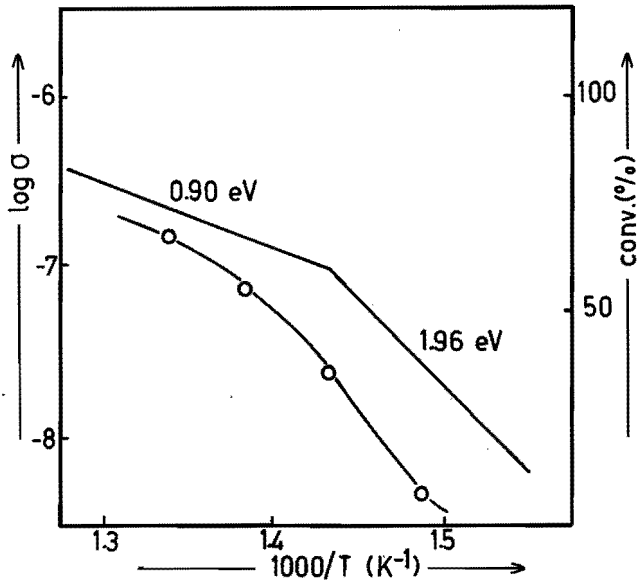

Fig. 4.14 Temperature dependence of the electrical conductivity of $Pb_{0.7}Bi_{0.2}MoO_4$ (precipitation sample) in helium. Also indicated is the activity pattern for the same catalyst for 1-butene oxidative dehydrogenation

the number of pulses, while the conversion per pulse is decreasing. At the highest temperature (T = 450°C) there is hardly any increase in conductivity after the passage of a subsequent butene pulse, but also the conversion per pulse is not changing very much. At this point there is still a certain conversion (for example, 20% in the case of precipitation sample) and the conductivity is nearly staying constant. The reduction of the catalyst is continuing, without having a further effect on the conductivity. The same is valid for both precipitation and solid state sample, even for the pure lead molybdate, be it at higher temperatures.

Note that these experiments do not show the incipient increase in activity as apparent in fig. 4.13, presumably due to a greater volume of the pulse.

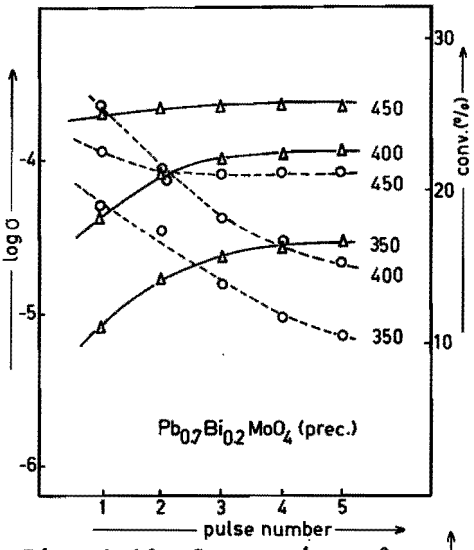

Fig. 4.15 Conversion of 1-butene and electrical conductivity during pulse reduction of $Pb_{0.7}Bi_{0.2}MoO_4$ (precipitation sample) at 350, 400 and 450°C

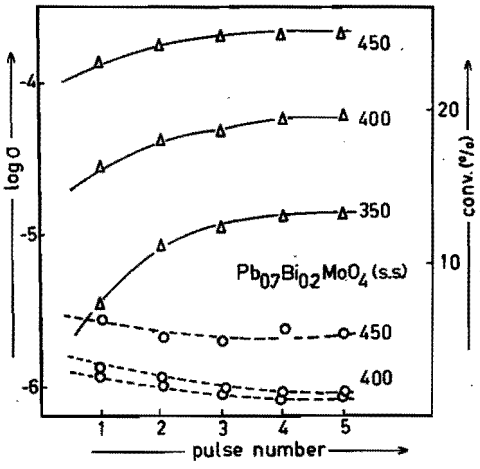

Fig. 4.16 Conversion of 1-butene and electrical conductivity during pulse reduction of $Pb_{0.7}Bi_{0.2}MoO_4$ (prepared from oxides at 700°C) at 350, 400 and 450°C)

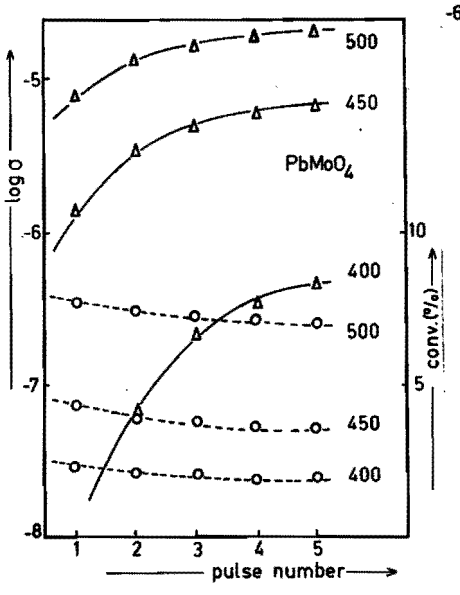

Fig. 4.17 Conversion of 1-butene and electrical conductivity during pulse reduction of $PbMoO_4$ at 400, 450 and 500°C

The level of electrical conductivity is low for pure lead molybdate (log σ = -5.3 at 450°C), but much higher for the other two samples (log σ = -3.8 at 450°C). It is remarkable that both samples of $Pb_{0.7}Bi_{0.2}MoO_4$ show the same conductivity level, although the conversion level is very much lower for the solid state catalyst. This seems to suggest that the conductivity is localized in the surface layers.

4.4 CONCLUSIONS

Our experiments have confirmed those of Sleight *et al.* who showed that "doping" of $PbMoO_4$ by Bi, thus forming a solid solution of composition $Pb_{1-3x}Bi_{2x}\phi_xMoO_4$, produced catalysts active for the selective oxidation of olefins. The method of Sleight to prepare the catalyst, *i.e.* heating of the oxides at 700°C produces low surface area samples that as a consequence have relatively low activity. It is shown here however that catalysts made by co-precipitation, which have generally surface areas a factor 10 higher, are very similar in properties but also considerably more active.

However, their activities per unit of surface area were lower than those prepared according to Sleight. XPS measurements showed that our samples had a considerable surface enrichment of Bi at the cost of Pb. It proved moreover difficult to prepare homogeneous products, some of our samples showing X-ray diffraction lines common to γ-bismuth molybdate. Prolonged testing of the precipitation catalysts showed a considerable decay in activity as a function of run time with a concomitant increase in intensity of X-ray lines not pertaining to the $PbMoO_4$ pattern. The general impression is that at temperatures around 400-450°C the solid solutions tend to decompose in $PbMoO_4$ and Bi_2MoO_6.

Sample of $Pb_{1-3x}Bi_{2x}\phi_xMoO_4$ become reduced by passing

pulses of butene over the samples in the absence of oxygen in the gasphase. Simultaneously herewith their electrical conductivity increases from values as low as log σ = -7 to log σ = -3.5.

REFERENCES

1. K. Aykan, D. Halvorson, A.W. Sleight, D.B. Rogers, J. Catal., 35, 401 (1974).
2. K. Aykan, A.W. Sleight, D.B. Rogers, J. Catal., 29, 185 (1973).
3. A.W. Sleight, K. Aykan, D.B. Rogers, J. Solid State Chem., 13, 231 (1975).
4. A.W. Sleight in "Advanced Materials in Catalysis" (J.J. Burton, R.L. Garten, eds.), Ac. Press, N.Y. 1976.
5. I.N. Belyaev, N.P. Smolyaninov, Zh. Neorg. Khim., 7, 1126 (1962).
6. A.S. Viskov, Yu.N. Venevtsev, G.S. Zhdanov, Dokl. Akad. Nauk SSSR, 162, 323 (1965).
7. F. Zambonini, Gazz. Chim. Ital., 50, 128 (1920).
8. D.F. Howard, G.P. Bowman, R.K. Saxer, J.R. Myers, Transact. Metall. Soc. AIME, 230, 850 (1964).
9. Austrian Patent 247.304 (1966).
10. U.S. Patent 3.806.470 (1974).
11. J. Leciejewicz, Z. Krist., 121, 158 (1965).

CHAPTER 5

STABILIZED β-BISMUTH MOLYBDATE

$Bi_2Mo_2O_9$, β-bismuth molybdate, is not stable at ordinary temperatures. Its stability is confined to the temperature range between 550°C and 670°C. The compound was first mentioned by Erman *et al.* (1), later its existence was confirmed by Batist *et al.* (2).

Its structure is not known with certainty, because so far it was not possible to prepare single-crystals that were not extensively twinned. Nevertheless, Van den Elzen and Rieck (3) proposed a preliminary structure from the X-ray powder diffraction diagram. They came to the conclusion that the structure is best described by the formula: $Bi(Bi_3\phi O_2)Mo_4O_{16}$, where ϕ is a cation vacancy. A most important structural characteristic is the row of oxygens in the y-direction that is only connected to Bi^{3+}. Furthermore, cation vacancies on sites that belong typically to those normally occupied by Bi^{3+}, form an essential part of the structure.

The compound can be prepared by precipitation from solutions. Grzybowska (4) mixed appropriate amounts of $Bi(NO_3)_3.5H_2O$ in 1 N HNO_3 and ammonium heptamolybdate in aqueous solutions at room temperature, while maintaining a constant pH of 2 during the precipitation by adding simultaneously aqueous ammonia.

Trifirð (5) prepared the β-bismuth molybdate by mixing solutions of $Bi(NO_3)_3.5H_2O$ and H_2MoO_4 in distilled water (400-1500 ml) acidified with HNO_3. He worked at a temperature of 80°C and a pH of 2.2.

In all these preparations the formation of small amounts of γ-bismuth molybdate could not be avoided. Because of its intrinsic instability, it is very difficult to prepare $Bi_2Mo_2O_9$ in a very pure form. The relatively most adequate procedure is precipitation from cooled (0°C) solutions of $Bi(NO_3)_3.5H_2O$ in HNO_3 and water and ammonium heptamolybdate in water. After filtration, drying of the precipitate and heating at 500°C for 2 hours, we obtain a slightly yellowish compound, whose X-ray diffraction diagram always indicates that it contains some γ-bismuth molybdate, because of the presence of the principal diffraction lines for γ-bismuth molybdate, *i.e.* d = 3.15 Å and d = 2.74 Å. It was found that all bismuth and molybdenum were retained in the precipitate, because the filtrate water after evaporation contained no residue. Similar checks were used when preparing samples as mentioned further in this chapter.

By replacing part of the bismuth ions in the solutions by two-valent ions like Pb^{2+}, Ca^{2+} and Cd^{2+} we hoped to stabilize the β-phase. Starting with $Bi_2\phi_{0.5}Mo_2O_9$ we prepared samples with the general formula $Bi_{2-2x}A_{3x}\phi_{0.5-3x}Mo_2O_9$ with A = Pb, Ca or Cd and x = 0.0625 - 0.5 (table 5.1). The oxidative dehydrogenation of 1-butene was used to test their catalytic activity and selectivity. Their phase composition was checked by X-ray diffraction.

$Bi_2\phi_{0.5}Mo_2O_9$	
$Bi_{1.8}Pb_{0.3}\phi_{0.4}Mo_2O_9$ $Bi_{1.5}Pb_{0.75}\phi_{0.25}Mo_2O_9$ $Bi_{1.0}Pb_{1.5}Mo_2O_9$	$Bi_{1.875}Ca_{0.1875}\phi_{0.4375}Mo_2O_9$ $Bi_{1.5}Ca_{0.75}\phi_{0.25}Mo_2O_9$ $Bi_{1.0}Ca_{1.5}Mo_2O_9$
$Bi_{1.875}Cd_{0.1875}\phi_{0.4375}Mo_2O_9$ $Bi_{1.5}Cd_{0.75}\phi_{0.25}Mo_2O_9$ $Bi_{1.0}Cd_{1.5}Mo_2O_9$	

Table 5.1 List of samples prepared with general formula $Bi_{2-2x}Pb_{3x}\phi_{0.5-3x}Mo_2O_9$

The X-ray diffraction diagram of β-bismuth molybdate is very complex. As a reference we use the data of Van den Elzen and Rieck (3). The positions of the diffraction lines and the relative intensities are given in a line diagram in fig. 5.1. Indicated are the lines that belong to the γ-phase.

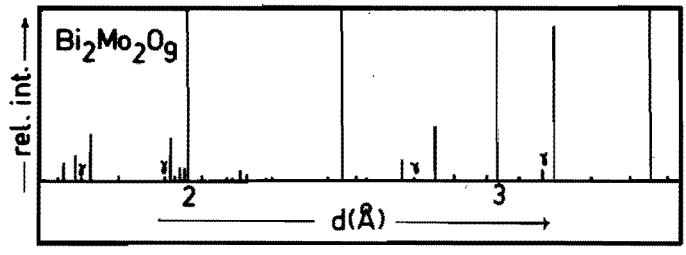

Fig. 5.1 X-ray diffraction line diagram of $Bi_2Mo_2O_9$ (after Van den Elzen and Rieck (3))

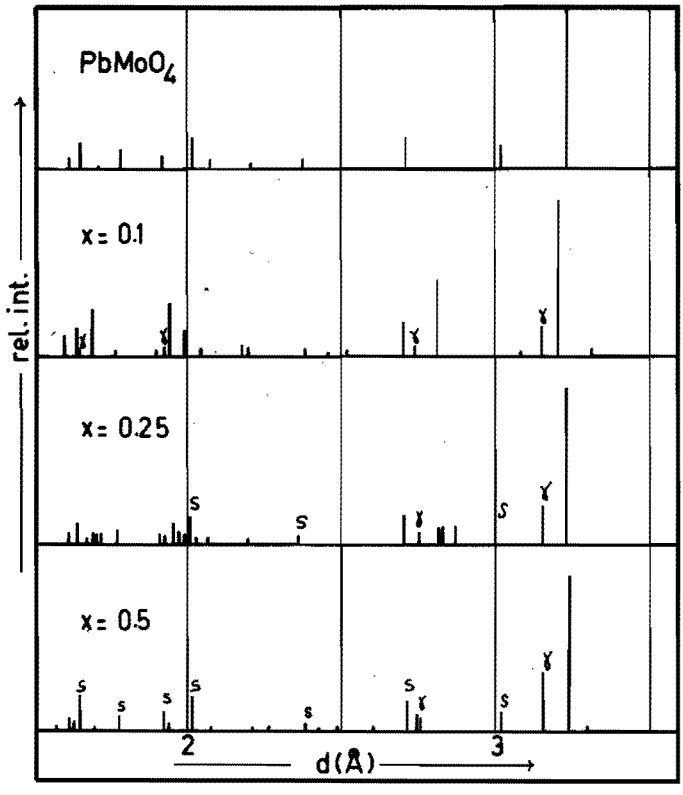

Fig. 5.2a X-ray diffraction line diagrams of $PbMoO_4$ and $Bi_{2-2x}Pb_{3x}Mo_2O_9$. γ = Bi_2MoO_6, S = Scheelite

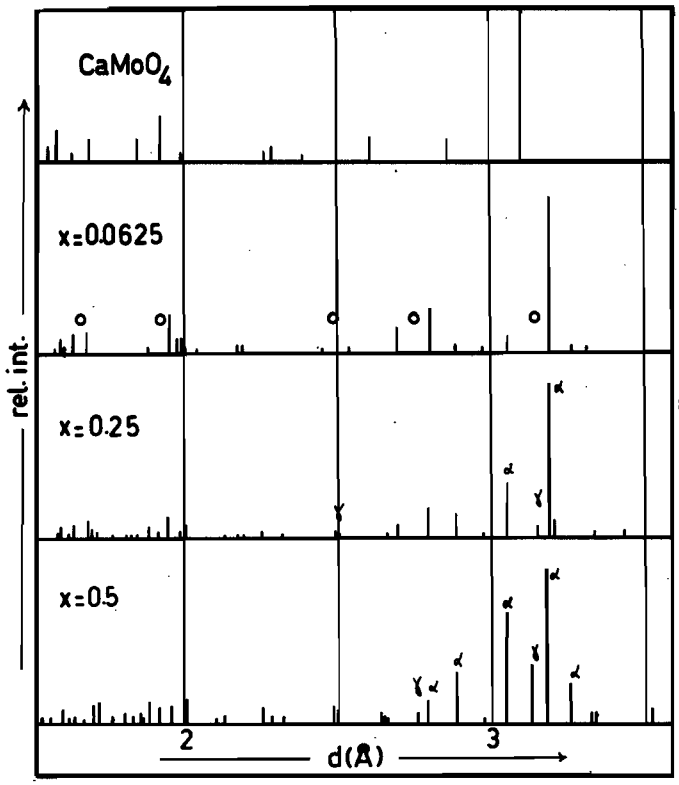

Fig. 5.2b X-ray diffraction line diagrams of $CaMoO_4$ *and* $Bi_{2-2x}Ca_{3x}Mo_2O_9$.
o = *absent* γ,
γ = Bi_2MoO_6,
α = $Bi_2Mo_3O_{12}$,
S = *scheelite*

Fig. 5.2a contains the line diagrams for $PbMoO_4$ and the Pb^{2+}-doped samples. It is seen that we get a formation of new phases when we replace part of the bismuth, thus filling up the vacancies. There is a regular increase in the intensity of the γ-bismuth molybdate diffraction lines (at d = 3.15 Å and d = 2.74 Å) together with a shift of other lines to a scheelite pattern. The sample with x = 0.5 is clearly a mixture of lead molybdate and γ-bismuth molybdate. This decomposition is in accordance with the following reaction:

$$Bi_{1.0}Pb_{1.5}Mo_2O_9 \longrightarrow 0.5\ Bi_2MoO_6 + 1.5\ PbMoO_4$$

The Ca^{2+}- and Cd^{2+}-doped samples show similar characteristics, although there are some differences (fig. 5.2b and fig. 5.2c). The diagrams of the samples with x = 0.0625 do not show the minor lines ascribed to γ-bismuth molybdate. This means that with small amounts

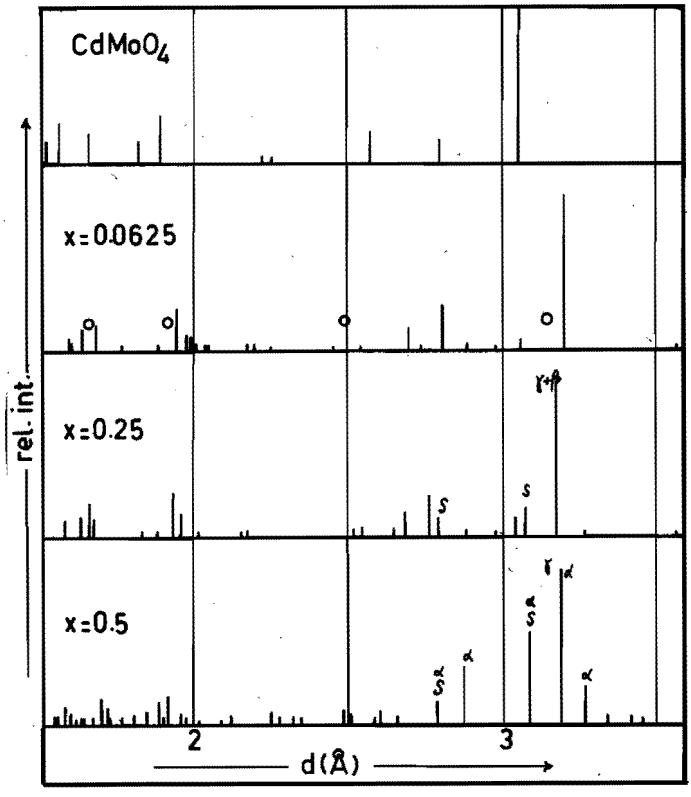

Fig. 5.2c X-ray diffraction line diagrams of $CdMoO_4$ *and* $Bi_{2-2x}Cd_{3x}Mo_2O_9$.
o = *absent* γ,
γ = Bi_2MoO_6,
α = $Bi_2Mo_3O_{12}$,
S = *Scheelite*

of foreign ions there is indeed a stabilization of the β-phase. However, higher amounts of Ca^{2+} or Cd^{2+} lead again to a decomposition into the binary molybdates. The diagrams of the Ca^{2+}- and Cd^{2+}-doped samples show besides γ-phase and scheelite lines also α-phase lines.

Fig. 5.3 gives DTA measurements on some of the samples. It shows again that the β-phase is not stable above 670°C, because the observed peaks can be ascribed to respectively the decomposition into α- and γ-phase (at 670°C) and to the melting of the α-phase (at 710°C). The diagram for the Cd^{2+}-doped β-phase does not show these peaks confirming the stabilization of the β-phase by Cd^{2+} (x = 0.0625). However, doping with Ca^{2+} (x = 0.0625) does not improve the stability, because the two peaks are present. This is not in agreement with the observed X-ray diagram that points to a stabilization.

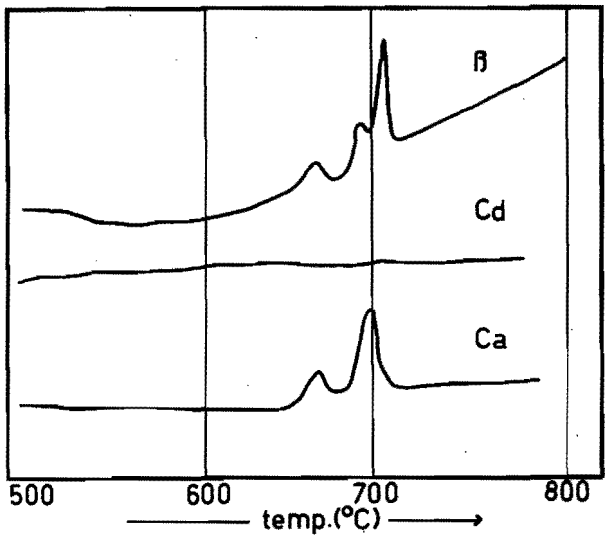

Fig. 5.3 DTA experiments on $Bi_2Mo_2O_9$, $Bi_{2-2x}A_{3x}Mo_2O_9$ *with* $A = Cd^{2+}$, Ca^{2+} *and* $x = 0.0625$

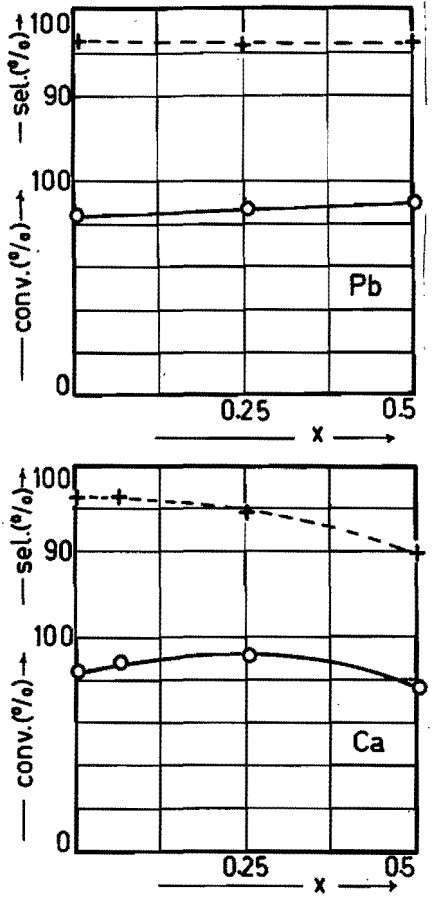

Fig. 5.4 Conversion of 1-butene and selectivities of $Bi_{2-2x}A_{3x}Mo_2O_9$ *as function of x at 450°C for A = Pb, Ca and Cd*

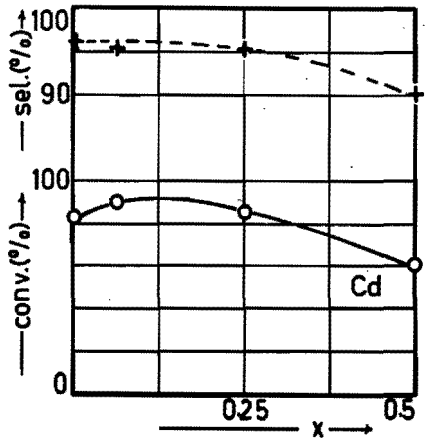

The simultaneously recorded TGA curves showed no evidence for weight losses.

All samples were tested for the activity and selectivity in 1-butene oxidative dehydrogenation. Fig. 5.4 gives the observed values at 450°C. In none of the three cases was there an appreciable influence of the doping on either activity or selectivity of the catalyst as compared to the β-phase. There seems to be only a slight increase in activity by adding small amounts of Cd^{2+} and Ca^{2+} (x = 0.0625).

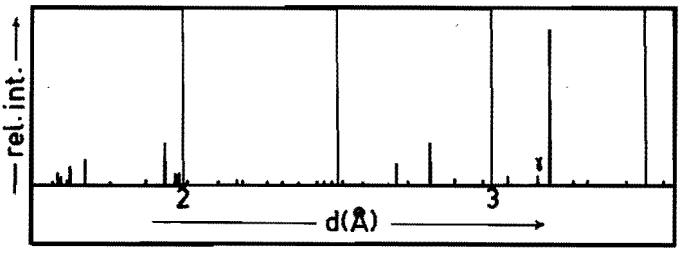

Fig. 5.5 X-ray diffraction line diagram of $Bi_{2-2x}Cd_{3x}Mo_2O_9$ *with x = 0.0625 after use in reaction conditions*

The Cd^{2+}-doped sample with x = 0.0625 was tested for a period of 5 hours at 475°C after which again an X-ray diagram was made (fig. 5.5). It indicated a decomposition after prolonged use of the catalyst, because the principal γ-phase line at d = 3.15 Å is present now. During this time no decline in activity was observed.

CONCLUSION

The structure of $Bi_2Mo_2O_9$, as proposed by Van den Elzen and Rieck (3), contains a considerable amount of vacancies. By replacing part of the Bi^{3+}-ions by two-valent ions (Pb^{2+}, Ca^{2+} and Cd^{2+}), thus filling up the vacancies, it was tried to stabilize this unstable phase. From X-ray diffraction and DTA experiments it was shown that only for small amounts of Cd^{2+} a stabilization is accomplished, while in all the other cases a mixture

of the component molybdates is formed. Cd^{2+} seems to be better suited for replacing Bi^{3+} in this structure, which can be supported by a nearly identical ionic radius (Bi^{3+} = 0.96 Å, Cd^{2+} = 0.97 Å, and Ca^{2+} = 0.99 Å, while Pb^{2+} = 1.20 Å).

REFERENCES

1. L.Ya. Erman, E.L. Gal'perin, I.K. Kolchin, G.F. Dobrzhanskii, K.S. Chernyshev, Russ. J. Inorg. Chem., 9, 1174 (1964).
2. Ph.A. Batist, A.H.W.M. der Kinderen, I. Leeuwenburg, F.A.M.G. Metz, G.C.A. Schuit, J. Catal., 12, 45 (1968).
3. A.F. van den Elzen, G.D. Rieck, Mat. Res. Bull., 10, 1163 (1975).
4. B. Grzybowska, J. Haber, J. Komorek, J. Catal., 25, 25 (1972).
5. F. Trifirð, H. Hoser, R.D. Scarle, J. Catal., 25, 12 (1972).

CHAPTER 6

MULTICOMPONENT MOLYBDATES

6.1 INTRODUCTION

Since about 1970 an overwhelming amount of patents appeared, all describing catalysts for the selective oxidation of olefins. These catalysts generally have the composition $Me^{II}_{a}Me^{III}_{b}BiMo_{12}O_{n}$ with additions of small amounts of P and K, supported on a silica carrier. Me^{II} is Ni^{2+}, Co^{2+}, Mg^{2+}, Mn^{2+} or a combination of these elements, while Me^{III} is Fe^{3+}, Cr^{3+}, Al^{3+} or a combination.

Outside the patent literature there are only a few reports dealing with this type of catalyst. Wolfs (1) and Wolfs and Batist (2) investigated a lot of metal molybdate combinations for their catalytic activity and selectivity in butene oxidative dehydrogenation. Also structural characteristics were examined.

They concluded that their catalysts consisted of a core of a matrix material, usually cobalt , manganese or magnesium molybdate covered by successive layers of iron(III)molybdate and bismuth molybdates. The surface should then show nearly the same situation as in the pure bismuth molybdates.

Matsuura and Wolfs (3) reported X-ray photo-electron spectroscopy measurements on these catalysts, and could confirm this skin model. Later this model was somewhat adjusted by more accurate measurements (4, 5). The surface was supposed to be enriched in bismuth, whereas there was also a concentration gradient of iron.

The function of Fe is of considerable interest, because it appears to be the only cation that can act as a promotor for bismuth molybdates. It was shown by many workers that all, or the greater part, of the iron(III)molybdate became reduced to Fe(II)molybdate during catalysis.

This indicates that Fe plays a role in the transfer of electrons from hydrocarbons to oxygen. Batist *et al.* (6) were the first to report the presence of molybdates containing both Fe and Bi ("compound X"). Sleight and Jeitschko (7) established the structure of the compound $Bi_3(FeO_4)(MoO_4)_2$ and Lo Jacono *et al.* (8) gave some arguments for the existence of still another compound with a Bi/Fe-ratio of 1.

There is on the other hand the possibility that the $FeMoO_4$ formed by reduction could have a similar structure as the group of compounds almost invariably cited as helpful in making the catalyst operate in optimal manner, *viz.* $MgMoO_4$, $CoMoO_4$, $NiMoO_4$ and $MnMoO_4$. These compounds appear to be able to contain a considerable excess of MoO_3, a feature which is not well understood at this moment.

To illustrate the possible connection between the various catalyst compounds, the following picture may be helpful:

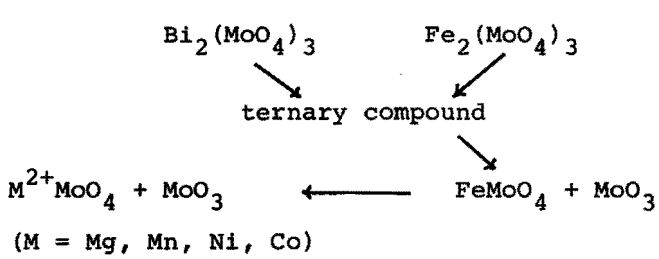

The system $Mg_{11-x}Fe_xBiMo_{12}O_n$ was examined in more detail (1). It was found that for a high activity and selectivity a minimum amount of iron(III) had to be present. The optimum composition for both 1-butene

and propene oxidation was $Mg_{8.5}Fe_{2.5}BiMo_{12}O_n$.

In order to further investigate the role of the different components, we prepared the following samples:

a) $MgMoO_4$
b) $Mg_{11}Mo_{12}O_n$
c) $Mg_{11}BiMo_{12}O_n$
d) $Mg_{8.5}Fe_{2.5}Mo_{12}O_n$
e) $Mg_{8.5}Fe_{2.5}BiMo_{12}O_n$
f) $(Mg_{11}Mo_{12}O_n)Fe_{0.3}Bi_{0.1}$
g) $Mg_{8.5}Fe_{0.3}Bi_{0.1}Mo_{12}O_n$
h) $(MgMoO_4)(Fe_2(MoO_4)_3)(Bi_2MoO_6)$

6.2 PREPARATION OF THE SAMPLES

a. $\underline{MgMoO_4}$
25.64 g $Mg(NO_3)_2.6H_2O$ (Merck p.a.) were dissolved in 100 cm^3 distilled water. 16.41 g powdered molybdic acid (BDH Chemicals Ltd., containing 87,76 w% MoO_3) were added to the hot solution. The pH was adjusted to six by adding aqueous ammonia. Under these conditions, a precipitate is formed. It was evaporated till dryness, dried at 120°C (4 h). Part of the sample obtained was calcined at 550°C (2 h) and another part at 800°C (2 h), respectively designated as sample a1 and sample a2.

b. $\underline{Mg_{11}Mo_{12}O_n}$
A solution of 11.282 g $Mg(NO_3)_2.6H_2O$ in 100 cm^3 water was added to a solution of 8.474 g $(NH_4)_6Mo_7O_{24}.4H_2O$ (Merck p.a.) in 100 cm^3 water. By evaporating the mixture, a white precipitate formed which was subsequently dried (16 h, 120°C) and calcined (16 h, 425°C). This sample was used as matrix material.

c. $\underline{Mg_{11}BiMo_{12}O_n}$
A solution of 11.282 g $Mg(NO_3)_2.6H_2O$ in 100 cm^3 water was added to a solution of 1.940 g $Bi(NO_3)_3.5H_2O$ in

2 cm^3 concentrated nitric acid, afterwards diluted with 20 cm^3 water. A solution of 8.474 g $(NH_4)_6Mo_7O_{24}.4H_2O$ in 100 cm^3 water was added to this mixture. After evaporation, the precipitate was further dried (16 h, 120°C) and calcined (2 h, 500°C).

d. $\underline{Mg}_{8.5}\underline{Fe}_{2.5}\underline{Mo}_{12}\underline{O}_n$
8.718 g $Mg(NO_3)_2.6H_2O$ and 4.04 g $Fe(NO_3)_3.9H_2O$ (Merck p.a.) were dissolved in 100 cm^3 water. 7.812 g powdered molybdic acid were added. After evaporation the resulting precipitate was dried (16 h, 120°C) and calcined (2h, 500°C).

e. $\underline{Mg}_{8.5}\underline{Fe}_{2.5}\underline{BiMo}_{12}\underline{O}_n$
8.718 g $Mg(NO_3)_2.6H_2O$ and 4.04 g $Fe(NO_3)_3.9H_2O$ were dissolved in 100 cm^3 water. 1.940 g $Bi(NO_3)_3.5H_2O$ were dissolved in 2 cm^3 concentrated nitric acid and added to the former solution. The mixture was heated to 80°C. Then 7.812 g powdered molybdic acid was added to the mixture and the pH adjusted at 5. After evaporation, drying (16 h, 120°C) and calcining (2h, 500°C) a light brown sample was obtained.

f. $\underline{(Mg_{11}Mo_{12}O_x)Fe}_{0.3}\underline{Bi}_{0.1}$
2.171 g of the magnesium molybdate matrix (sample b) is impregnated with iron and bismuth ions by slowly adding a solution of 0.121 g $Fe(NO_3)_3.9H_2O$ and 0.0487 g $Bi(NO_3)_3.5H_2O$ in 2 cm^3 diluted nitric acid. After drying and calcining (2h, 500°C) a brown sample was obtained.

g. $\underline{Mg}_{8.5}\underline{Fe}_{0.3}\underline{Bi}_{0.1}\underline{Mo}_{12}\underline{O}_n$
The same preparation method was used as for sample e, but here we used 0.194 g $Bi(NO_3)_3.5H_2O$ and 0.485 g $Fe(NO_3)_3.9H_2O$.

h. A physical mixture of $MgMoO_4$, Bi_2MoO_6 and $Fe_2(MoO_4)_3$ with overall composition $Mg_{8.5}Fe_{2.5}BiMo_{12}O_n$.

6.3 ACTIVITY AND SELECTIVITY

The samples were tested for activity and selectivity in 1-butene oxidative dehydrogenation. Table 6.1 gives the measured activities and selectivities at 425°C. The reaction conditions are those mentioned in chapter 2.

sample	act. (%)	select. (%)
a1	8.8	85
b	20	83
c	20	91
d	23	67
e	82	94
f	32	95
g	21	91
h	20	79

Table 6.1 Activities and selectivities for oxidative dehydrogenation of 1-butene at 425°C

The magnesium molybdate calcined at 500°C (sample a1) has a low activity, but already a good selectivity. By introducing excess MoO_3 (sample b), the activity is increased somewhat, while the selectivity is nearly the same. Incorporation of Bi (sample c) does not change the activity, but considerable increase in selectivity is observed.
On the other hand, incorporation of Fe (sample d) gives a rather low selectivity and nearly the same activity. Simultaneous introduction of Fe and Bi (sample e) leads to the high activity and selectivity catalyst. Impregnation of the magnesium molybdate matrix with bismuth and iron (sample f) gives an increase in activity and selectivity compared to the matrix (sample b). By using the same amounts of bismuth and iron in a precipitation sample (sample g) a lower activity and somewhat lower selectivity compared to sample f are obtained. The physical mixture of the component

α-$MgMoO_4$		β-$MgMoO_4$		$Mg_{11}Mo_{12}O_x$			$Mg_{11}Bi_1Mo_{12}O_x$		
d(Å)	I/Imax	d(Å)	I/Imax	d(Å)	I/Imax		d(Å)	I/Imax	
4.567	44	5.310	14	4.667	17	β	4.657	16	β
4.530	40	4.660	37	4.576	34	α	4.576	17	α
4.498	38	4.345	6	4.444	24	α	4.503	15	α
4.436	36	3.814	78	4.291	6	α	4.444	14	α
4.296	14	3.506	46	3.867	61	α	3.877	33	α
3.863	76	3.373	100	3.811	48	αβ	3.821	32	αβ
3.811	38	3.278	46	3.671	61	α	3.681	35	α
3.665	80	3.246	24	3.595	18	α	3.593	11	α
3.578	22	3.153	30	3.504	19	β	3.506	16	β
3.450	28	3.089	6	3.453	27	α	3.448	10	α
3.363	86	2.794	29	3.363	100	β	3.373	100	αβ
3.324	100	2.720	10	3.314	85	α	3.333	14	α
3.252	50	2.661	27	3.252	75	αβ	3.273	32	β
3.220	34	2.619	5	3.218	27	α	3.224	19	α
3.149	24	2.553	2	3.149	19	αβ	3.186	21	2/3
3.140	24	2.455	12	3.045	14	α	3.151	44	2/1
3.076	12	2.320	15	2.966	17	α	3.056	15	
3.045	18	2.248	11	2.789	7	β	2.974	9	α
2.968	24	2.241	10	2.753	9	α	2.793	13	β
2.753	16	2.174	16	2.670	24	α	2.753	11	α
2.674	28	2.172	6	2.656	24	β	2.674	14	α
2.626	26	2.109	6	2.625	14	β	2.660	14	β

$Mg_{8.5}Fe_{2.5}Mo_{12}O_x$			$Mg_{8.5}Fe_{2.5}BiMo_{12}O_x$			→ idem reduced			$(Mg_{11}Mo_{12}O_x)Fe_{0.3}$		
d(Å)	I/Imax		d(Å)	I/Imax		d(Å)	I/Imax		d(Å)	I/Imax	
4.667	5	β	4.662	19	β	4.652	17	β	4.667	19	β
4.354	15	β	3.880	12	0	3.821	33	β	4.345	2	β
4.227	29		3.822	36	β	3.677	5		3.818	43	β
4.092	8	0	3.648	14		3.587	9		3.515	21	β
3.880	16	0	3.504	28	β	3.504	17	β	3.376	100	β
3.814	47	β	3.363	100	β	3.400	25	$FeMoO_4$	3.276	34	β
3.720	19	0	3.283	35	β	3.368	100	β	3.257	22	β
3.696	19		3.252	26	β	3.273	60	β	3.151	15	β
3.463	46	0	3.182	46	2/3	3.151	22	β	3.083	3	β
3.421	29		3.149	47	β2/1	2.794	10	β	2.794	12	β
3.351	100	β	3.056	16	2/3	2.720	7	β	2.725	5	β
3.257	95	β	2.915	10		2.657	14	β	2.662	14	β
3.150	13	β	2.794	16	β	2.453	10	β	2.457	7	β
3.108	32	β	2.726	6	β	2.361	10		2.322	6	β
2.945	11		2.665	18	β	2.325	7	β	2.248	5	β
2.698	13	β	2.457	6	β	2.268	12	$FeMoO_4$	2.174	6	β
2.653	23	β	2.327	7	β						
2.438	6	β	2.247	7	β						
2.308	15	β			β						

Table 6.1 X-ray diffraction values d(Å) and I/Imax for various catalysts. α =α-$MgMoO_4$, β = β-$MgMoO_4$, 0 = $Fe_2(MoO_4)_3$

molybdates (sample h) showed low activity and selectivity.

6.4 X-RAY DIFFRACTION

Table 6.2 lists the X-ray diffraction lines of these samples.

$MgMoO_4$ was obtained in two different phases. Calcination at 550°C (a1) leads to α-$MgMoO_4$, while at 800°C (a2) β-$MgMoO_4$ was obtained. Introduction of extra MoO_3 (b) leads to a mixture of the α- and β-structure. Bi introduction into this sample (c) gives no influence on the structure; there are only indications for bismuth molybdates ($Bi_2Mo_3O_{12}$: d = 3.186, d = 3.056; Bi_2MoO_6: higher intensity of d = 3.15). The incorporation of Fe (d) into the magnesium molybdate gives a complete reorganization of α- into β-structure. $Fe_2(MoO_4)_3$ is also present (d = 3.88, 4.09, 3.72, 3.46 Å).

The coprecipitated catalyst (e) shows only the β-structure with some lines of $Fe_2(MoO_4)_3$ and bismuth molybdates.

Impregnation of both iron and bismuth into the $MgMoO_4$ matrix results also in a β-structure without indications for iron molybdates or bismuth molybdates.

The X-ray lines for a sample of $Mg_{8.5}Fe_{2.5}BiMo_{12}O_n$ which has been kept in reaction conditions for 2 hours at 475°C are shown also. It shows only the β-structure with some indications for β-$FeMoO_4$ (d = 3.40, 3.27 Å).

6.5 MÖSSBAUER EXPERIMENTS

For some of the samples Mössbauer spectra were recorded (Fig. 6.1).

The Mössbauer spectrum for $Mg_{8.5}Fe_{2.5}BiMo_{12}O_n$ gives a rather complicated pattern. $Fe_2(MoO_4)_3$ is present, but besides this there are iron ions with a different surrounding.

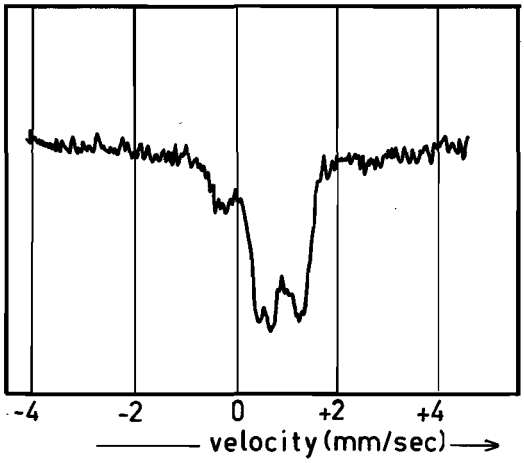

Fig. 6.1a Mössbauer spectrum of fresh catalyst $Mg_{8.5}Fe_{2.5}BiMo_{12}O_n$

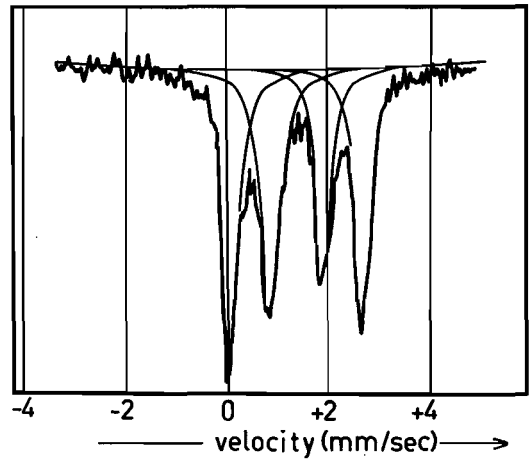

Fig. 6.1b Mössbauer spectrum of used catalyst $Mg_{8.5}Fe_{2.5}BiMo_{12}O_n$

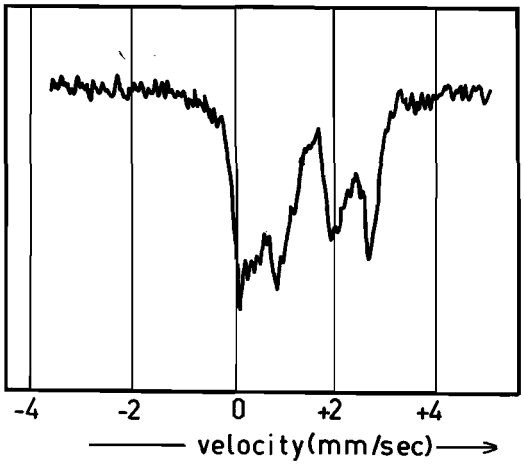

Fig. 6.1c Mössbauer spectrum of $Mg_{8.5}Fe_{2.5}BiMo_{12}O_n$, *after reduction with 1-butene*

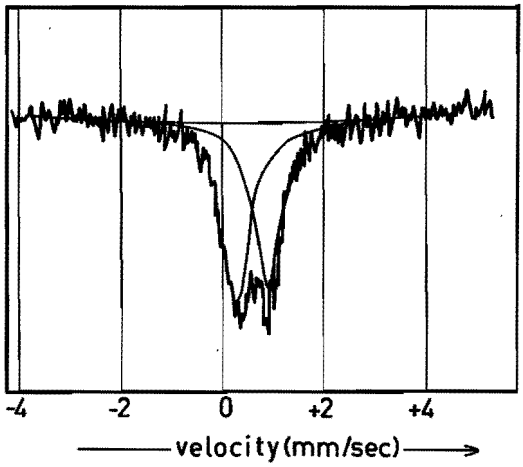

Fig. 6.1d Mössbauer spectrum of the impregnation catalyst, $(Mg_{11}Mo_{12}O_n)Fe_{0.3}Bi_{0.1}$

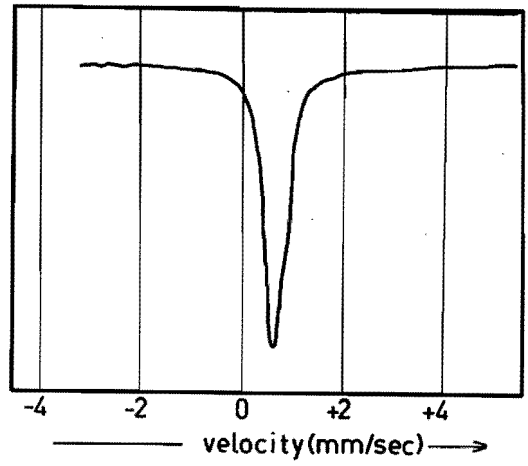

Fig. 6.1e Mössbauer spectrum of $Fe_2(MoO_4)_3$

When we use this catalyst in reaction (usual reaction conditions, 2 h, 475°C) a complete reorganization to β-$FeMoO_4$ is observed. A spectrum with two doublets is present: one doublet with a quadrupole splitting (Q.S.) of 2.63 mm/sec and an isomer shift (I.S.) of 1.42 mm/sec; the other doublet with Q.S. = 1.06 mm/sec and I.S. = 1.43 mm/sec. Because of the non-symmetrical four-line spectrum, there must be still another species present. Reduction with 1-butene during 15 min. at 475°C also results in the formation of $FeMoO_4$. In this case also α-$FeMoO_4$ is present, presumably caused by an inadequate

cooling procedure.

Impregnation of the $MgMoO_4$-matrix leads to a Mössbauer spectrum, composed of a doublet, with parameters Q.S. = 0.63 mm/sec and I.S. = 0.64 mm/sec, which can not be ascribed to $Fe_2(MoO_4)_3$ nor $FeMoO_4$. There is however a possibility that it can be accounted for as α-Fe_2O_3 in small particles (d < 100 Å).

6.6 PULSE AND CONDUCTIVITY MEASUREMENTS

On $Mg_{8.5}Fe_{2.5}BiMo_{12}O_n$ we performed pulse reduction experiments (fig. 6.2). The same conditions were used as with the bismuth molybdates.

After the first pulse of 1-butene, the conversion per pulse decreases strongly. The next pulses result only in a limited decrease of conversion. At 450°C there is even a tendency to arrive at a stationary level.

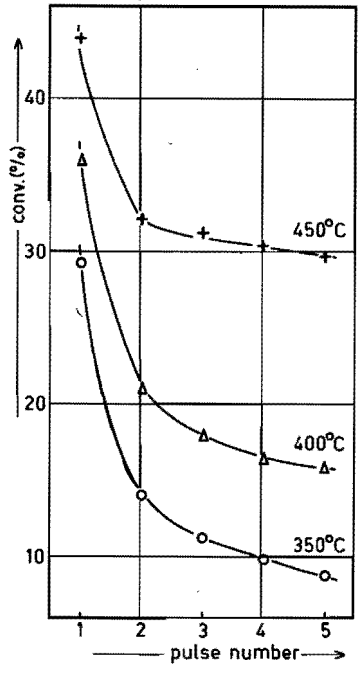

Fig. 6.2 Conversion of 1-butene during pulse reduction of $Mg_{8.5}Fe_{2.5}BiMo_{12}O_n$ at 350, 400 and 450°C

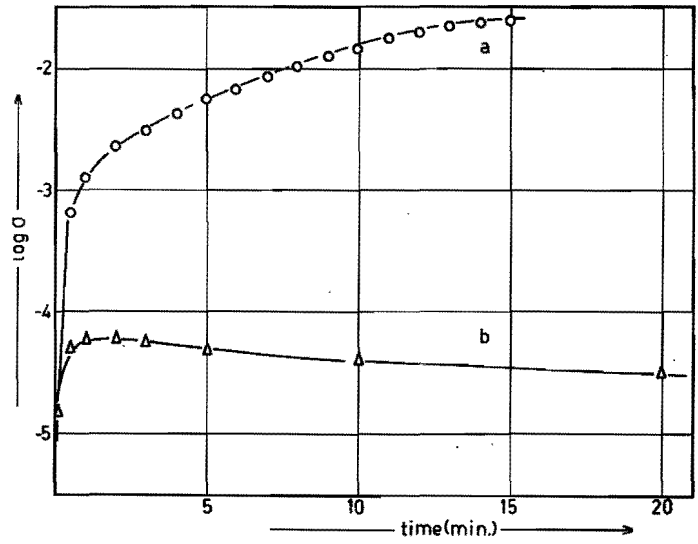

Fig. 6.3 Electrical conductivity as function of the time of reduction at 400°C for (a) Bi_2MoO_6 and (b) $Mg_{8.5}Fe_{2.5}BiMo_{12}O_n$.

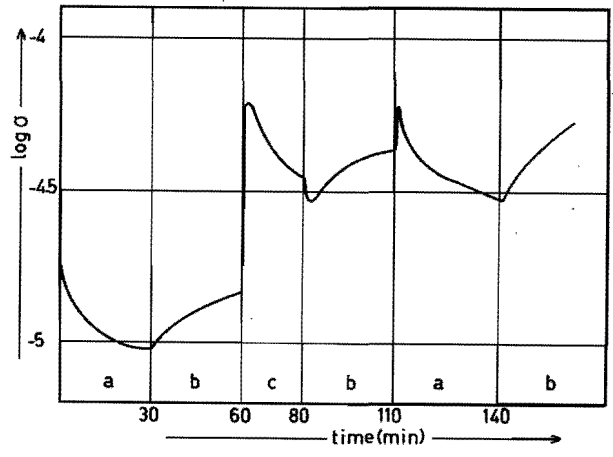

Fig. 6.4 Behaviour of the electrical conductivity of $Mg_{8.5}Fe_{2.5}BiMo_{12}O_n$ under various conditions at 400°C:
a. in a mixture of helium and oxygen
b. in helium,
c. in 1-butene

At 400°C we measured the electrical conductivity of the sample during continuous reduction with 1-butene (flow 100 cm^3/min helium and 10 cm^3/min 1-butene). A sample of Bi_2MoO_6 was used as a comparison (fig. 6.3).

After an initial increase during the first few minutes, the conductivity shows a nearly constant value, with a tendency to decrease again. On the other hand, the sample of Bi_2MoO_6 shows a different behaviour; initially the conductivity increases much more and only in a later stage arrives at a constant level.

The ratio of the conductivities of the compounds Bi_2MoO_6 and $Mg_{8.5}Fe_{2.5}BiMo_{12}O_n$ at their maximal conductivities is ~ 250. This difference might be explained by a lower concentration of Bi in the multi-component sample.

Reduction-reoxidation experiments on this sample show that the conductivity varies only in a small range (fig. 6.4), whereas with bismuth molybdates variations of several orders are measured (see chapter 3).

6.7 DISCUSSION

Magnesium molybdate calcined at low temperatures ($T < 700°C$) has a structure which differs considerably from the product obtained at temperatures higher than 700°C. According to the generally accepted nomenclature we designate the low temperature phase as α-$MgMoO_4$. Only Meullemeestre and Pénigault (9) mention this phase and indicate that it is isotypic with α-$ZnMoO_4$, which has a triclinic structure. The high temperature phase is designated as β-$MgMoO_4$ and is isotypic with β-$FeMoO_4$ and β-$CoMoO_4$ (10).

Because of the broad diffraction lines in the X-ray spectrum of the socalled α-$MgMoO_4$ it is difficult to be sure of its structure. The same situation exists for α-$FeMoO_4$ and β-$FeMoO_4$. Here the low temperature phase

α-$FeMoO_4$ was first also ascribed to the triclinic structure, but later it turned out to be a mixture of α- and β-$FeMoO_4$ (Sleight, 11).

In our case it could also be possible that the complex pattern which we describe as α-$MgMoO_4$, is in fact a mixture of α- and β-$MgMoO_4$. For simplicity reasons we prefer to indicate the low temperature form as α-$MgMoO_4$ and the high temperature form as β-$MgMoO_4$.

When an excess amount of MoO_3 is incorporated into the low temperature form, a mixture of the α- and β-structure is obtained. So this excess MoO_3 has a considerable influence on the structure, but more important it also enhances the activity for oxidation. A similar effect was reported by Oganowski *et al.* (12) for the oxidative dehydrogenation of ethylbenzene to styrene. The excess MoO_3 had an activating effect. Infrared evidence indicated that the MoO_3 occurs with its Mo in octahedral surroundings at the surface, in contrast to the tetrahedral Mo in the bulk material.

Incorporation of Bi into the $MgMoO_4$ has no influence on the structure, but introduction of Fe immediately converts the $MgMoO_4$ into the pure β-structure. Simultaneous use of Bi and Fe into the active catalyst gives the same situation: only a β-structure is observed. In fact only small amounts of Fe^{3+} suffice for this conversion, because the impregnated matrix material, which contained only a limited amount of Fe, was already the pure β-structure.

So it is clear that iron in these catalysts is able to favour the β-structure, *i.e.* a structure in which molybdenum is tetrahedrally surrounded by oxygen. The importance of the β-structure was already pointed out by Wolfs (1). He stated that the stabilization of the β-structure by $Fe_2(MoO_4)_3$ is caused by a better mutual adaptation of these structures. Both $Fe_2(MoO_4)_3$ and the β-structure have corner sharing Mo-O tetrahedra.

A recent patent (13) claims that very active and selective oxidation catalysts can be prepared by

impregnating for instance a matrix material with excess molybdenum ($Mg_{11}Mo_{12}O_n$), with a solution of the nitrates of bismuth and iron. Even with low amounts of bismuth and iron a high conversion and selectivity could be attained.

Our impregnation catalyst (sample f) showed only a low conversion, although with good selectivity.

One important difference between the work mentioned in the patents and our experiments is that in the former much higher contact times were used (6 sec. *vs.* 0.1 sec. in our work). This entirely explains the discrepancy. If for instance at τ = 0.1 sec. a conversion of 0.25 is measured, we can calculate at τ = 6 sec. a conversion which is higher than 0.95.

Another point may be that our surface does not consist of iron(III)molybdate and bismuth molybdate. The Mössbauer spectrum does not present the signals for iron(III)molybdate, but instead shows some evidence for the presence of small particles of α-Fe_2O_3. It seems that the impregnation technique applied is not a guarantee for the formation of the iron molybdate at the surface, even when an excess of MoO_3 is present in the matrix material.

The enhancement in activity, compared to the catalyst with similar composition, but prepared via a precipitation technique, might be ascribed either to the presence of the bismuth molybdates at the surface (which cannot be detected), or the presence of α-Fe_2O_3.

During catalytic reaction (butene-oxygen mixture at 475°C), the iron(III)molybdate in the catalyst gets reduced to a considerable extent. The X-ray diagram of the used catalyst gives some indications for β-$FeMoO_4$. The Mössbauer spectrum clearly indicates that most of the iron(III) is reduced; it shows the typical two-doublet spectrum of β-$FeMoO_4$ (Sleight, 11; Dutta Gupta, 14). Because of the non-symmetrical shape of the spectrum there must be present another kind of iron, this might

be Fe^{3+} in $Fe_2(MoO_4)_3$ because the single Mössbauer peak of iron(III)molybdate falls in the region of the spectrum with the highest intensity, but is not resolved.

However, Rao *et al.* (12) give the Mössbauer data for fresh and used silica supported MCM catalyst and conclude that after use in the ammoxidation of propene the Fe(III)molybdate is completely converted to Fe(II)molybdate. He gives the four-line spectrum and ascribes it to two different iron surroundings.

Reduction of $Mg_{8.5}Fe_{2.5}BiMo_{12}O_n$ with 1-butene gives nearly the same situation. Almost all of the iron(III)-molybdate is converted to iron(II)molybdate.

The role of the iron can be described as follows. Reduction of the catalyst occurs at bismuth ions, because the oxygen of the bismuth is used for the oxidation. Immediately when bismuth gets reduced the iron(III) can act as an oxidator so that bismuth(red.) is again bismuth(III), while Fe(III) is reduced to Fe(II). The reoxidation of the catalyst should then start at the Fe(II), which is oxidized again to Fe(III) and can do the same cycle again.

We could show indeed that $Fe_2(MoO_4)_3$ is able to oxidize Bi metal in an inert atmosphere (helium) to Bi(III)molybdate under formation of Fe(II)molybdate.

An alternative is that the reaction

$$Bi^{n+} + Fe^{3+} \rightleftharpoons Fe^{2+} + Bi^{(n+1)+}$$

is an equilibrium reaction. This would enable the bismuth to perform its usual function (*i.e.* being oxidized by O_2) while preventing a large concentration of Bi^{n+}. If n = 0, we need three Fe^{3+}-cations for the conversion to Bi^{3+}, which is about the value for the Fe/Bi-ratio in $Mg_{8.5}Fe_{2.5}BiMo_{12}O_n$. Bi^0 would tend to form Bi-metal and if oxidized produce Bi_2O_3. Fe^{3+} then acts to prevent the decomposition of the catalyst by acting as an electron trap.

As indicated in the introduction there are reasons

to assume that the interaction between Fe and Bi occurs in a ternary compound. Since we could not find any evidence for such a compound in our experiments, we prefer to leave the question whether formation of a ternary compound is necessary, unanswered.

REFERENCES

1. M.W.J. Wolfs, Ph.D. Thesis, Eindhoven University of Technology, the Netherlands (1974).
2. M.W.J. Wolfs, Ph.A. Batist, J. Catal., 32, 25 (1974).
3. I. Matsuura, M.W.J. Wolfs, J. Catal., 37, 174 (1975).
4. M.W.J. Wolfs, J.H.C. van Hooff, Proc. 1st Int. Symp. on Preparation of Heterogeneous Catalysts, Brussels 1975 (Elsevier, Amsterdam, 1976).
5. G.A. Sawatzky, D.A.G. van Oeffelen, to be published.
6. Ph.A. Batist, C.G.M. van de Moesdijk, I. Matsuura, G.C.A. Schuit, J. Catal., 20, 40 (1971).
7. A.W. Sleight, W. Jeitschko, Mat. Res. Bull., 9, 951 (1974).
8. M. Lo Jacono, T. Notermann, G.W. Keulks, J. Catal., 40, 19 (1975).
9. J. Meullemeestre, E. Pénigault, Bull. Soc. Chim., 1925 (1975).
10. A.W. Sleight, B.L. Chamberland, Inorg. Chem., 7, 1672 (1968).
11. A.W. Sleight, B.L. Chamberland, J.F. Weiher, Inorg. Chem., 7, 1093 (1968).
12. W. Oganowski, J. Hanuza, B. Jezowska-Trzebiatowska, J. Wrzyszcz, J. Catal., 39, 161 (1975).
13. Standard Oil Company of Ohio, Dutch patent application 7,006,454 (1974).
14. M. Dutta-Gupta, A.M. van der Kraan, to be published
15. T.S.R. Prasada Rao, P.G. Menon, J. Catal., 51, 64 (1978).

CHAPTER 7

PULSE EXPERIMENTS AND ELECTRICAL CONDUCTIVITY

7.1 GENERAL

The essence of the redox mechanism as accepted for the catalytic oxidation of olefins over oxide catalysts is the donation of electrons and protons by the hydrocarbon to the solid catalyst. The protons combine with oxygen molecules, thus making up for the anion depletion of the solid. The state of the electrons in the solid is not very well known and one might hope to obtain some information on this subject by studying their mobility in an electric field, *i.e.* measuring the electrical conductivity of the catalyst. A well known difficulty in analyzing the experimental conductivity data is given by the contribution of ion migration to the overall conductivity.

Several reports have appeared in literature covering studies about the electrical conductivity of bismuth molybdates.

Pluta (1, 2) investigated the conductivity of MoO_3, Bi_2O_3 and bismuth molybdate (Bi/Mo = 0.7; SiO_2 carrier) in air, oxygen and propene and at temperatures between 400°C and 500°C.
Already during outgassing of the bismuth molybdate, changes were observed, which were ascribed to desorption of chemisorbed oxygen atoms. Contact with propene raised the conductivity, while air (or oxygen) restored it to its original value. The increase in conductivity during

propene admission was ascribed to a reduction of the oxide, while the decrease after oxygen addition was considered to be caused by the reoxidation.

Peacock *et al.* (3) also investigated the conductivity of pressed discs of Bi_2O_3, MoO_3 and bismuth molybdate (Bi/Mo = 0.7) in propene and air (or oxygen) at 500°C. By admitting propene to bismuth molybdate they observed a considerable increase in conductivity, which could be eliminated by subsequent admission of oxygen. They showed that the increases in conductivity are brought about by extensive reduction of the surface layers of the catalysts. Similarly, the decreases after oxygen admission have to be ascribed to reoxidation of the reduced surfaces. They were able to show that the bismuth molybdate catalyst is about 10% reduced when operating under normal steady state conditions with mixtures of propene and oxygen. Furthermore they were able to determine the temperature dependence of the conductivity of the catalyst in oxidized and in partially reduced states. They showed that the energy gap decreased with increasing reduction. They concluded that the conductivity measurements can produce information about the reduction of the surface and perhaps a few subsurface layers, but do not furnish any information about the oxidation states of the individual ions present in the surface.

Morrison (4) describes the interaction of bismuth molybdates (Bi/Mo = 0.7) with oxygen and propene and the corresponding conductivity changes. At $T < 275^0C$ propene reacts only with what is assumed to be adsorbed oxygen, so that the conductivity after propene admission reaches a maximum. However, at $T > 275^0C$ propene reacts also with "irreversible oxygen", *i.e.* lattice oxygen, so that in this case the conductivity does not reach a maximum and reduction is continuous.

Our conductivity measurements on the bismuth molybdates differ from those mentioned before. Instead of a continuous exposition of the catalyst surface

to reducing or oxidizing conditions, at certain time intervals pulses of butene or oxygen were passed over the catalyst. We also found a raise in conductivity after interaction of the catalyst with butene and a decrease after contact with oxygen. The experiments were designed to simultaneously measure the butene conversion and the change in the electrical conductivity of the catalyst.

We shall now introduce a kinetic model as a formal description for the degree of conversion and the accompanying increase in electrical conductivity, both as a function of the number of pulses and at various temperatures. The model assumes the presence of a surface layer of constant thickness covering the bulk of the catalyst particle. Oxygen anions are removed from the surface and replenished by diffusion from the bulk, that is assumed so large compared to the surface layer that its oxygen concentration does not change appreciably. Only electrons in the surface layer are considered to contribute to the electrical conductivity. Diffusion of O^{2-} from the interior to the outside is accompanied by migration of electrons to the bulk: since these cease to be involved in the electrical conductivity, the conductivity arrives at a level and does not grow anymore with more substantial reduction. The dependency of the maximum level on the temperature is supposed to give us information on the state of the electrons in the surface layers.

The model obviously can lead to a decrease in the degree of conversion of successive pulses since the surface layer becomes depleted in oxygen with increasing reduction. This is approximately true for the doped $PbMoO_4$ and for Bi_2MoO_6, but not for $Bi_2Mo_3O_{12}$ and $Bi_2Mo_2O_9$. The model has to be extended to account for this phenomenon. This will be discussed in the final chapter.

7.2 DESCRIPTION OF THE MODEL

We assume that there is a surface layer on top of the bulk. The surface layer is reduced by C_4H_8 at a rate of

$$\frac{dx}{dt} = k_R(1-x)$$

where k_R = reaction rate constant of the reduction
and x = fraction of all the reducible oxygens in the surface layer that are already reduced.

There is simultaneously a diffusion of oxygens from the bulk to the surface layer: its rate being given by $k_D.x$, where k_D is the diffusion rate constant. This diffusion occurs during the reduction (time of pulse passage is τ_R) and during the intermediate periods between the pulses (τ_D). Generally $\tau_D >> \tau_R$.

The diffusion process on a microscopical scale is assumed to be a simultaneous transport of electrons into the interior and an O^{2-} from the bulk to the surface:

$$(2e)_{s.l.} + O^{2-}_b \longrightarrow (2e)_b + O^{2-}_{s.l.}$$

where s.l. = surface layer and b = bulk.

The entire behaviour of the reduction process can be computed from the change of x during a certain pulse (number p) and the subsequent intermediate period. At the beginning of pulse p, the degree of reduction be $(x_b)_p$ and at the end $(x_e)_p$ with $(x_e)_p > (x_b)_p$ (b = beginning, e = end). At the end of the subsequent intermediate period $x = (x_b)_{p+1}$. At the beginning of pulse 1: $(x_b)_1 = 0$.

From the differential equation

$$\frac{dx}{dt} = k_R(1-x) - k_D.x$$

and the boundary conditions: at $t = 0$, $x = (x_b)_p$ and at $t = \tau_R$, $x = (x_e)_p$, we find:

$$(x_e)_p = \frac{k_R}{k_R + k_D}(1 - C_R) + (x_b)_p C_r \qquad (1)$$

where $C_R = e^{-(k_R + k_D)\tau_R}$

For the intermediate period: $-\frac{dx}{dt} = k_D x$ with boundary condition: $t = 0$, $x = (x_e)_p$.

It follows that

$$(x_b)_{p+1} = (x_e)_p C_D \qquad (2)$$

where $C_D = e^{-k_D \tau_D}$

From (1) and (2) we get:

$$(x_b)_{p+1} = \frac{k_R}{k_R + k_D}(1-C_R)C_D + (X_b)_p C_R C_D \qquad (3)$$

So $$(x_e)_p - (x_b)_p = (1-C_R)\frac{k_R}{k_R + k_D} - (x_b)_p \qquad (4)$$

The general formula for $(x_b)_p$, $(x_e)_p$ and $(x_e)_p - (x_b)_p$ assuming $(x_b)_1 = 0$, become:

$$(x_b)_p = \frac{k_R}{k_R + k_D}(1-C_R)C_D(1 + C_R C_D = \ldots + C_R C_D^{p-2}) \qquad (5)$$

$$(x_e)_p = \frac{k_R}{k_R + k_D}(1-C_R)(1 + C_R C_D + \ldots + C_R C_D^{p-1}) \qquad (6)$$

$$(x_e)_p - (x_b)_p = \frac{k_R}{k_R + k_D}(1-C_R) \cdot$$

$$\cdot \left\{1 - (1-C_R)C_D(1 + \ldots + C_R C_D^{p-2})\right\} \qquad (7)$$

To write this somewhat more concisely, name

$(1-C_R)C_D = \alpha$ and $C_R C_D = \beta$. We now get:

$$(x_b)_p = \frac{k_R}{k_R + k_D} \cdot \alpha \, (1 + \beta + \ldots + \beta^{p-2}) \tag{8}$$

$$(x_e)_p = \frac{k_R}{k_R + k_D} \frac{\alpha}{C_D} \, (1 + \beta + \ldots + \beta^{p-1}) \tag{9}$$

$$(x_e)_p - (x_b)_p = \frac{k_R}{k_R + k_D} \frac{\alpha}{C_D} \left\{ 1 - \alpha(1 + \beta + \ldots + \beta^{p-2}) \right\} \tag{10}$$

It follows that $(\alpha + \beta) = C_D$ and $\frac{\beta}{\alpha + \beta} = C_R$

It may be assumed that in the first pulse the chances are considerable that diffusion is still not operative or only to a negligible extent. Therefore $(x_e)_1 - (x_b)_1$ is a fair measure of surface reduction only. Now, let the number of molecules per pulse be C_o, the number of reducible sites per m^2 be N_s and the surface area of the sample F_s. If the degree of conversion is η, then

$$\eta_1 = \frac{F_s \cdot N_s}{C_o} \quad \frac{k_R}{k_R + k_D} \frac{\alpha}{C_D} \tag{11}$$

because $(x_e)_1 - (x_b)_1 = \frac{k_R}{k_R + k_D} \frac{\alpha}{C_D}$.

We shall now assume that we can write generally:

$$\eta_p = \frac{F_s \cdot N_s}{C_o} \frac{k_R}{k_R + k_D} \frac{\alpha}{C_D} \left\{ 1 - \alpha(1 + \beta + \ldots + \beta^{p-2}) \right\} \tag{12}$$

So $$\frac{\eta_p}{\eta_1} = 1 - \alpha(1 + \beta + \ldots + \beta^{p-2}) \tag{13}$$

which allows a determination of α and β, at least in principle. Actually, the often observed increase in conversion during the first stages of the experiment makes its use somewhat doubtful, not to say impracticable. A certain improvement is obtained by using integral instead of differential conversions. Let $\eta_t = \sum_1^p \eta_p$

Then

$$\eta_t = \frac{F_s N_s}{C_O} \frac{k_R}{k_R + k_D} \frac{\alpha}{C_D} \left(p - \alpha\left\{(p-1) + (p-2)\beta + \ldots + \beta^{p-2}\right\}\right) \qquad (14)$$

$$\text{or } \frac{\eta_t}{p} = \frac{F_s N_s}{C_O} \frac{k_R}{k_R + k_D} \frac{\alpha}{C_D} \left\{1 - \alpha\left(\frac{p-1}{p} + \frac{p-2}{p}\beta + \ldots + \frac{1}{p}.\beta^{p-2}\right)\right\} \qquad (15)$$

$$\text{and } \frac{\eta_t}{p\eta_1} = 1 - \alpha\left(\frac{p-1}{p} + \frac{p-2}{p}\beta + \ldots + \frac{1}{p}.\beta^{p-2}\right) = 1 - \alpha\phi \qquad (16)$$

Fig. 7.1 shows the function ϕ at different β values.

At low temperatures β tends to 1 but α tends to zero. At high temperatures on the other hand β becomes near to zero: consequently $\frac{\eta_t}{p}$ is almost constant.

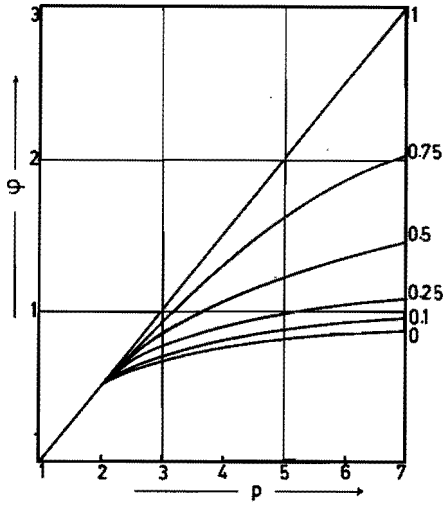

Fig. 7.1 Function $(p, \beta) = \frac{p-1}{p} + \frac{p-2}{p}\beta + \ldots + \frac{1}{p}\beta^{p-2}$ *for different values of* β

The treatment of conductivity is less obvious, because we do not know where the conductivity is located, in the bulk or in the surface layers or both. In any case this conductivity can be written as:

$$\sigma_o = \sigma_o^o . e^{-E/kT}$$

in which σ_o^o represents a frequency constant and E an activation energy. The problem is which process is responsible for the activation energy. We may consider two extreme models:

model 1: The system is composed of separate particles, and conductivity arises by electron transfer from particle to particle through the vacuum or gasphase. This requires an activation energy similar to a work function.

model 2: The interaction between the particles is much more extended and the surface has the nature of a series of defects in the solid. The activation energy is then more similar to the difference in energy between donor levels and the bottom of the conduction band.

Note that the first model allows interaction of the surface with molecules in the gasphase which is not the case for the second model.

The value of $(x_e)_p$ can be related to the conductivity:

$$\sigma_p = \sigma_o F_s (x_e)_p = \sigma_o \frac{k_R}{k_R + k_D} \frac{\alpha}{C_D} F_s (1 + \beta + \ldots + \beta^{p-1}) \qquad (17)$$

The conductivity can be related to the total reduction η_t although some of the charge carriers move into the bulk and therefore excape observation.

So consider

$$\frac{\eta_t}{\sigma_p} = \frac{\frac{F_s . N_s}{C_o} . \frac{k_R}{k_R + k_D} . \frac{\alpha}{C_D} (p - \alpha((p-1) + (p-2)\beta + \ldots + \beta^{p-2}))}{F_s \sigma_o \frac{k_R}{k_R + k_D} . \frac{\alpha}{C_D} (1 + \beta + \beta^2 + \ldots + \beta^{p-1})} \qquad (18)$$

We can write herefore:

$$\frac{\eta_t}{\sigma_p} = \frac{N_s}{\sigma_o \cdot C_o} \; 1 + (1-C_D) \; \frac{(p-1) + (p-2)\beta + \ldots + \beta^{p-2}}{1 + \beta + \beta^2 + \ldots + \beta^{p-1}} \qquad (19)$$

The function $\frac{(p-1) + (p-2)\beta + \ldots + \beta^{p-2}}{1 + \beta + \beta^2 + \ldots + \beta^{p-1}}$ is approximately linear in p for all values of β (fig. 7.2). Because of the $(1-C_D)$ term, its importance is low at low temperatures because C_D 1 but becomes of major importance at high temperatures where C_D 0. If we name the function above $F(p, \beta)$ and extrapolate to p = 1, we find that it is zero for all values of β. In other words, by extrapolating $\frac{\eta_t}{\sigma_p}$ (function of p) to p = 1, we find the specific reciprocal conductivity $\frac{N_s}{\sigma_o \cdot C_o}$. Doing that for different temperatures allows to find E for the temperature dependency of the electrical conductivity.

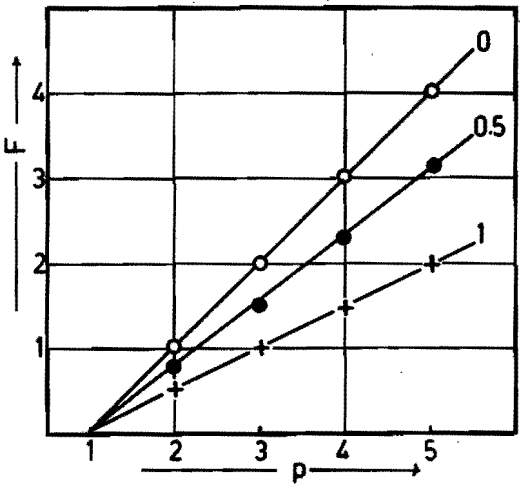

Fig. 7.2 Function $F(p, \beta) = \frac{(p-1) + (p-2) + \ldots + \beta^{p-2}}{1 + \beta + \beta^2 + \ldots + \beta^{p-1}}$ *at different β-values*

7.3 EVALUATION OF THE MODEL FOR OUR CATALYSTS

a) Equation (16) can be used for a comparison of pulse experiments on powder material and pressed tablets. The sample $Bi_2Mo_{1.02}O_{6.06}$ served for this purpose, using the data from the figures 3.4 and 3.12. Fig. 7.3 shows the

results for different temperatures. For most of the temperatures the powder sample shows a linear behaviour of the function $1 - \frac{\eta_t}{p\eta_p}$ (except at T = 350°C). This means that hardly any diffusion is present. The experiments on the pressed tablet however show a significant curvature, which indicates the presence of diffusion ($\beta < 1$). It is however interesting to find that the actual conversions do not differ very much.

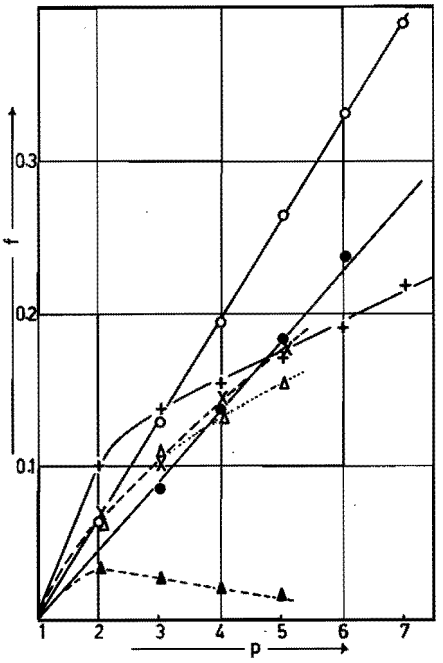

Fig. 7.3 Comparison of powder material and pressed tablets, catalyst $Bi_2Mo_{1.02}O_{6.06}$. $f = 1 - \frac{1}{p}\frac{\eta_t}{\eta_p}$
Powder: + = 350°C, o = 400°C
● = 450°C
Tablet: x = 350°C, Δ = 400°C
▲ = 450°C

b) Equation (19) was used for a comparison of the different catalysts as to the temperature dependence of the conductivity. Use was made of the data from the figures 3.12-3.16 and 4.15-4.17. Fig. 7.4 gives the calculated $\frac{\eta_t}{\sigma}$ -data for two catalysts, *viz.* $Bi_2Mo_{1.02}O_{6.06}$ and $Pb_{0.7}Bi_{0.2}MoO_4$ (precipitated sample). Fig. 7.5 shows the results for the different catalysts. The data in this figure were obtained from extrapolation of the values of $\frac{\eta_t}{\sigma_p}$ to p = 1 for the various temperatures.

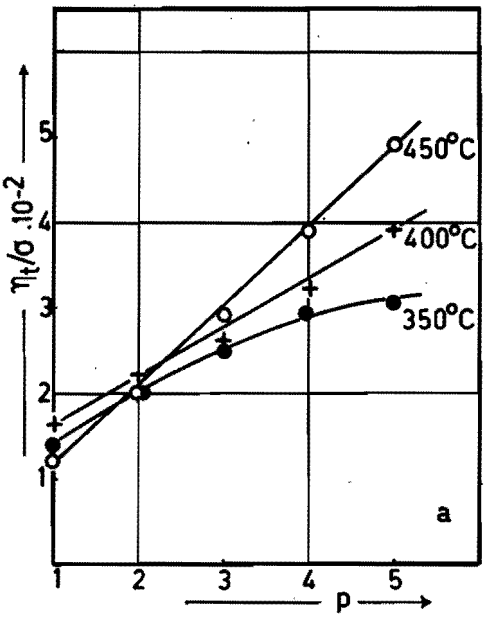

Fig. 7.4a $\frac{\eta_t}{\sigma}$ *-values for* $Bi_2Mo_{1.02}O_{6.06}$ *at different temperatures.*

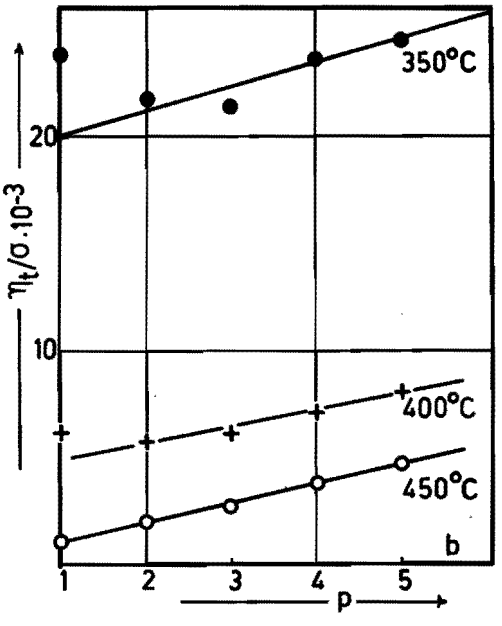

Fig. 7.4b $\frac{\eta_t}{\sigma}$ *-values for* $Pb_{0.7}Bi_{0.2}MoO_4$ *(precipitation sample) at different temperatures*

It is seen immediately that there are two groups of catalysts. The first group includes the lead bismuth molybdates, $PbMoO_4$ and $Bi_2Mo_3O_{12}$ and demonstrates a pronounced activation energy for conduction in the order of 20 kcal/mole. The second group consists of Bi_2MoO_6 and $Bi_2Mo_{1.02}O_{6.06}$ and is connected with a very low (nearly zero) activation energy.

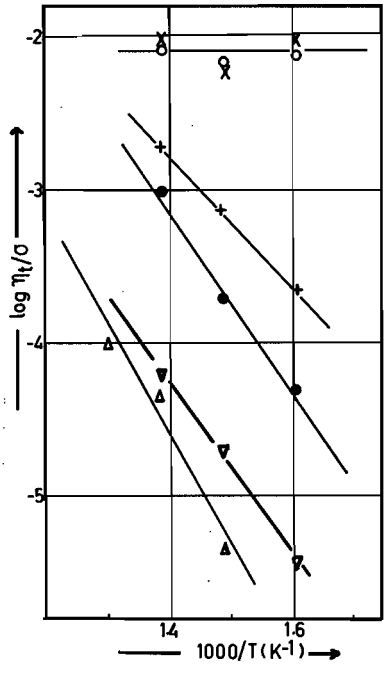

Fig. 7.5 log $\frac{\eta_t}{\sigma}$ vs. $\frac{1}{T}$ for the catalyst Bi_2MoO_6 (X), $Bi_2Mo_{1.02}O_{6.06}$ (o), $Pb_{0.7}Bi_{0.2}MoO_4$ oxidic (+), $Pb_{0.7}Bi_{0.2}MoO_4$ precipitation sample (•), $PbMoO_4$ (Δ) and $Bi_2Mo_3O_{12}$ (∇)

c) The data used for the determination of the specific conductivities should also give information concerning the rate of the diffusion as a function of the temperature since the increase of $\frac{\eta_t}{\sigma_p}$ with p (see equation (19)) contains both β and $(1-C_D)$. It is indeed seen that usually the inclination of the straight line is more pronounced for higher temperatures indicating that C_D is smaller. It is felt however that the data are not extensive enough to make this effort fruitful.

REFERENCES

1. J. Pluta, Z. Anorg. Allgem. Chem., 356, 105 (1967).
2. J. Pluta, Z. Phys. Chem., Neue Folge, 58, 189 (1968).
3. J.M. Peacock, A.J. Parker, P.G. Ashmore, J.A. Hockey, J. Catal., 15, 387 (1969).
4. S.R. Morrison, ACS Preprints, 22 (2), 485 (1977).

CHAPTER 8

A MODEL FOR BISMUTH MOLYBDATE CATALYSTS

Opinions differ as to which bismuth molybdate compound is the real catalyst for the oxidation. It is generally agreed that the active species is located in the range $2/3 \leqslant Bi/Mo \leqslant 2/1$, but which of the three compounds located here is the actual catalyst so far has remained uncertain. Recent experiments such as those of Wragg *et al.* (1) and Matsuura *et al.* (2) leave the impression that at temperatures higher than 400°C activity and selectivity are nearly constant over the whole range to fall off steeply at the limits. Whether pure $Bi_2Mo_3O_{12}$ and Bi_2MoO_6 in themselves are active is still disputed.

In the active range the stable situation is represented by a mixture of α- and γ-bismuth molybdate. Indeed our experiments show that a mixture of two hardly active samples, one with Bi/Mo < 2/3 and another with Bi/Mo > 2 are of similar activity as a single sample in the active range, provided their average Bi/Mo ratio is indeed situated in this range.

This somewhat curious situation could be explained in various manners. One could for instance assume that the two functions in the bifunctional bismuth molybdate, *i.e.* one function to interact with the olefin (Mo) and the other to transport electrons to O_2 (Bi), could also operate when situated on neighbouring particles of two catalysts each containing only one of the functions. Obviously, such a cooperation necessitates the transfer of oxygen anions and electrons from one particle to another. Information as to the relation between catalyst

activity and electrical conductivity might be particularly relevant for this case.

Another explanation favours the existence of a surface layer with a composition different from those of the bulk phases, but uniform over the whole range of constant activity. Matsuura and Hirakawa (3) for instance postulate from spectroscopic evidence that the surface layer is similar in structure to $Bi_2Mo_2O_9$. Instead of a transfer of reaction intermediates between phases it is now necessary to transfer a catalyst component (such as MoO_3) from one phase to another.

Grzybowska *et al.* (4) reported that surface compositions of Bi_2MoO_6 could change considerably if the catalyst was evacuated at high temperature or reduced with H_2 or C_3H_6. However, in the presence of O_2 no such change occurred even when propene was oxidized to acrolein.

Let us now consider the pulse experiments with the bismuth molybdates (fig. 3.4-3.7) together with the XPS results for the same catalysts. During the initial pulses there is an increase in conversion of butene for most of the catalysts. We compared the different bismuth molybdates as to their XPS surface composition and the rise in conversion (table 8.1)

		η_1			max.
	XPS Mo/Bi	350°C	400°C	450°C	450°C
$Bi_2Mo_3O_{12}$	1.44	0.125	0.195	0.295	0.505 pulse 5
$Bi_2Mo_2O_9$	1.08	0.175	0.290	0.485	0.610 pulse 5
$Bi_2Mo_{1.02}O_{6.06}$	0.60	0.245	0.445	0.455	0.495 pulse 2
$Bi_{2.04}MoO_{6.06}$	0.44				

Table 8.1 Comparison of the different bismuth molybdates as to their XPS surface composition, the rise in conversion during pulse experiments (first pulse) and the maximum conversion at 450°C

For all first pulses the conversion rises with decreasing Mo/Bi-ratio to suddenly become zero at 0.44. At 350°C there is the usual picture of decreasing conversion with increasing number of pulses but at 450°C the conversion of α- and β-bismuth molybdate rise with the pulse number to come to a maximum before decreasing again. Something else than reduction appears to occur at the surface.

This change is obviously connected with the reduction as also found by Grzybowska *et al.* (4), since all these catalysts were already calcined earlier at 500°C in air. However, reaction is not intrinsically connected with reduction because the $Bi_2Mo_{1.02}O_{6.06}$ catalyst is almost at maximum activity at the first pulse.

We therefore propose that the activation is connected with a migration of MoO_3 from the surface, a migration that is activated by the reduction. For instance one could imagine a reaction such as

$$Bi_2Mo_3O_{12} \longrightarrow 2\ x\ Bi + x\ MoO_2 + (1-x)Bi_2MoO_6 + 2MoO_3$$

If now Bi_2MoO_6 is the active system and if $(1-x) > x$, than the catalyst becomes more active. Actually, the most active catalyst probably has a somewhat higher Mo/Bi ratio than 0.5 since the highest conversion is found not for $Bi_2Mo_{1.02}O_{6.06}$ but (0.610) for a surface layer formed from $Bi_2Mo_2O_9$ after having had its first pulse conversion at 0.485 (Mo/Bi = 1.08).

What happens to the MoO_3? It might be forming crystals in the catalyst mass, but it may also evaporate out of the reactor. At any rate its migration is probably the reason why a mixture of two inactive catalysts, one with a high and the other with a very low Mo/Bi ratio indeed combine to act as a reasonable catalyst. The Mo-rich catalyst loses Mo to the Mo-poor catalyst and both become activated. Parenthetically, this means that surfaces not only lose MoO_3 but also can "adsorb" it which indeed

follows already from the fact that the surface layer of $Bi_2Mo_{1.02}O_{6.06}$ has a Mo/Bi ratio of 0.60.

Our conclusion is therefore that there is good reason for the assumption of a special surface layer with an optimal activity at a Mo/Bi ratio between 1 and 0.5.

If a catalyst only loses MoO_3 from its surface, catalysts with a high Mo/Bi ratio should first increase in activity until they arrive at some point comparable to that on fresh $Bi_2Mo_{1.02}O_{6.06}$ after which a precipitous decrease occurs. Actually, for $Bi_2Mo_2O_9$ we find only a slow decrease which might indicate that MoO_3 diffuses from the bulk to the surface. In other words, it might be of advantage to use catalysts with an excess of MoO_3 to compensate the loss in MoO_3 by evaporation that will always occur. This explains why the original commercial bismuth molybdate catalyst - now replaced by other more sophisticated catalysts - had a Mo/Bi composition of about 1.3. This is an important detail to which we will return later.

The $Bi_2Mo_{1.02}O_{6.06}$ catalyst declined very rapidly in the absence of O_2. If used in actual catalysis no decline is observed in periods of hours. This is probably due to the fact that rapid reoxidation leads to a restoration of the surface without appreciable loss of MoO_3, agreeing with Grzybowska's observations.
However, although to a much lesser degree, loss of MoO_3 will occur at operation times in the order of months necessitating the presence of a considerable amount of more or less tightly bonded MoO_3 as a reserve (as in $Bi_2Mo_3O_{12}$).

Parenthetically, the sharp increase in conversion with increasing pulse number as exemplified by $Bi_2Mo_{1.02}O_{6.06}$ may be a combination of two processes, reduction and MoO_3 loss and therefore somewhat anomalous as indicated before.

Before leaving the subject of changes in surface layer composition the $Bi_{2.04}$ $MoO_{6.06}$ catalyst should be discussed. It shows the anomalous picture of a catalyst

that is initially inactive because of its low Mo/Bi surface ratio. Surprisingly enough it begins to become active after some pulses have passed without any observable reaction. The presence of oxygen appears to inhibit this reaction. We might have to do here with the inverse of the MoO_3 loss, *i.e.* a loss of Bi as a vapour. It is known that bismuth containing catalysts become reduced in a vacuum or also by the action of reducing agents and then tend to lose Bi metal by evaporation. This would then tend to increase the Mo/Bi ratio and therefore bring the catalyst back into the active region.

The greater part of our work has been concerned with the electrical conductivity measurements of pressed samples of bismuth molybdate and lead bismuth molybdates either as such or after reduction.

The fact that we have to do with a pressed powder presents considerable difficulties. For measurement of electrical properties of the bulk we need single-crystals. However, catalyst materials always are in the form of powders and the only way to investigate some properties concerning electrical conductivity of catalytic materials is the use of pressed powders.

The assumption that the measured conductivity is entirely located at the surface can be supported by several facts:

a. The conduction immediately starts when the catalyst is brought in contact with butene, *i.e.* at the first reduction.
b. The conduction immediately decreases very fast after contact with O_2.
c. A comparison of low and high surface areas of lead bismuth molybdates (*i.e.* the samples prepared respectively by oxide mixing and precipitation) shows that the amount of butene needed to attain maximal conductivity is proportional to the surface area of the sample.

The electrons formed during reduction are located either in a localized orbital of one of the metal atoms,

Mo or Bi, or occur in a delocalized band system of overlapping Mo 4d states and Bi 6p states, as suggested by Sleight (5).

We propose, as suggested by Grzybowska *et al.* (4), that the electrons are first located at Mo, but can be transported very quickly to Bi, thus forming a reduced Bi ion, a Bi atom or even bismuth metal. This charge transfer from Mo to Bi forms one of the intermediate steps in the reoxidation of the system to the highest oxidation state. Peacock *et al.* (6) already stated that Mo^{5+} is formed in first instance, but it is removed by a reoxidation process to Bi; at high temperatures this process is very fast.

The comparison of the activation energies for conduction (chapter 7) furnishes a useful means of comparison of the different types of catalysts.

If model 1 (p. 105) is accepted, then the conductivity is a measure of the work function. This work function is also connected with the transfer of electrons to an approaching oxygen molecule. A low work function (corresponding with low activation energy) is equivalent to an easy transfer from the reduced surface to oxygen, implying that the reaction is fast, and not rate determining so that a zero order dependency on the oxygen partial pressure of the catalytic reaction results. On the other hand, a high work function means a difficult reaction with oxygen that can become rate determining so that the rate of the overall reaction is that of the reoxidation, which is first order in the oxygen partial pressure.

It is more difficult to rationalize the activation energies from model 2 and in particular to connect them with the kinetic data. If we assume that the differences in energy between the donor levels and the bottom of the conduction band (this being the activation energy measured) can be related to the vacuum reference level, we can imagine that this activation energy is also connected with the transfer of electrons to an approaching oxygen molecule. As earlier proposed (above) the energy levels

(donor levels) may be a Mo-level (Mo^{4+}) and a Bi-level (Bi^{0}). These can be formed during reduction by applying the following reactions:

$$Mo^{6+} + 2e \longrightarrow Mo^{4+}$$
$$3Mo^{4+} + 2Bi^{3+} \longrightarrow 2Bi^{0} + 3Mo^{6+}.$$

Both models then are in qualitative agreement with kinetic observations .

The bismuth molybdates are supposed to be rapidly reoxidized as evidenced by the zero order dependence on the oxygen partial pressure (7). On the other hand, the activation energy of the electrical conductivity is very low. Contrary hereto, the lead bismuth molybdates show a definite dependence on the partial pressure of oxygen (5), while their electrical conductivity is connected with a considerable activation energy.

Let us finally turn to the case for the multicomponent catalyst systems with its use of relatively large amounts of molybdates of bivalent metals of such a diversity as Mg, Mn, Co, Ni on the one hand and $Fe_2(MoO_4)_3$ on the other hand.

The only elements that the bivalent molybdates seem to share are:

a. the possibility to occur in a similar crystal structure, the β-$CoMoO_4$ structure. This appears a fundamental principle since some of those can also adopt another related structure and it is known (see Wolfs and Batist (8)) that in this second form they are not acting as an acceptable catalyst component. $MgMoO_4$ is commonly present in the latter form, but in the presence of $Fe_2(MoO_4)_3$ it adopts the requested crystal structure as shown before (chapter 6).
b. the property to contain a certain excess of MoO_3 in the particular crystal structure. The nature of this incorporated MoO_3 is not clear.

When the catalyst is in operation, $Fe_2(MoO_4)_3$ is known to be rapidly reduced under formation of $FeMoO_4$ of the

same structure as requested above. During this reduction it forms MoO_3. We have shown that the inclusion of $Fe_2(MoO_4)_3$ strongly decreases the electrical conductivity of the catalyst (chapter 6). We postulated above that the strong electrical conductivity of the bismuth molybdates has such a low activation energy that it may be due to the presence of metallic Bi. But metallic Bi after reoxidation will form Bi_2O_3, which means that the molybdate can become decomposed. Therefore this formation of the metal should be inhibited.

We have shown also that Bi metal can be oxidized by $Fe_2(MoO_4)_3$ under formation of $FeMoO_4$ and bismuth molybdate. So the Fe^{3+} cation appears to act as an electron trap:

$$Bi^0 + 3Fe^{3+} \longrightarrow Bi^{3+} + 3Fe^{2+}$$

which is in agreement with the ratios applied in the catalyst.

The other default in the bismuth molybdate structure is its tendency to lose MoO_3. This has been met in the earlier catalyst by applying molybdates with a higher molybdate content which was not in accordance with the demands for maximal activity. $Fe_2(MoO_4)_3$ can act as a source of MoO_3 after reduction but the amount of MoO_3 released is so large that it needs a considerable excess of the divalent molybdates to house it. We now propose that the function of the $Me^{II}MoO_4$ components is the storage of MoO_3 thereby replacing the need for large amounts of bismuth molybdates such as $Bi_2Mo_3O_{12}$.

At the end of this chapter we want to give an overview of the catalyst textures dealt with in this thesis (fig. 8.1). Starting from the bismuth doped lead molybdate, which has a random orientation of active sites, we get the surface layer model of the bismuth molybdates characterized by a special active Bi/Mo-ratio at the surface. The multicomponent molybdates offer a system which is composed of bismuth molybdates, which deliver the active sites,

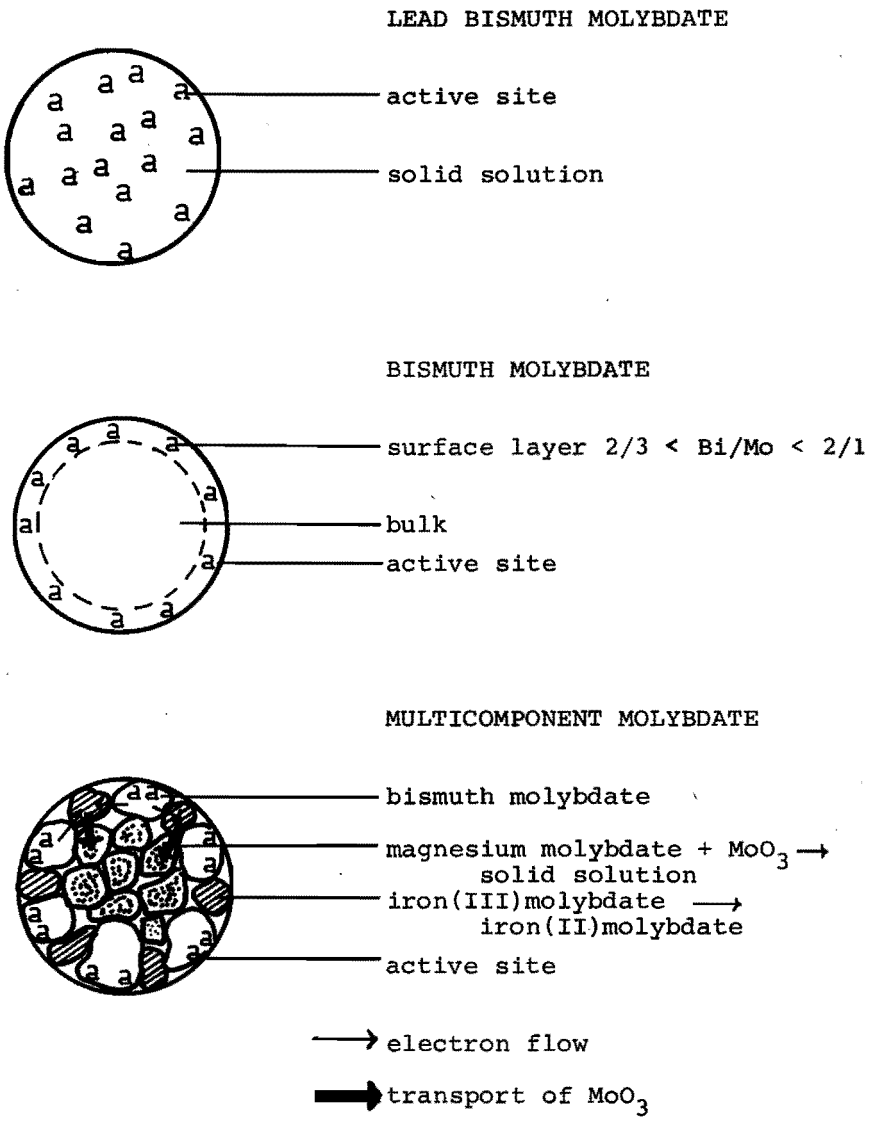

Fig. 8.1 Scheme of catalyst textures

iron molybdate, which is helping to reoxidize reduced bismuth (thereby forming β-$FeMoO_4$) and magnesium molybdate which can take up large excess of the MoO_3, which has come free during the formation of β-$FeMoO_4$.

REFERENCES

1. R.D. Wragg, P.G. Ashmore, J.A. Hockey, J. Catal., 31, 293 (1973).
2. I. Matsuura, K. Hirakawa, R. Schut, submitted to J. Catal.
3. I. Matsuura, K. Hirakawa, submitted to J. Catal.
4. B. Grzybowska, J. Haber, W. Marczewski, L. Ungier, J. Catal., 42, 327 (1976).
5. A.W. Sleight in "Advanced Materials in Catalysis" (J.J. Burton, R.L. Garten, eds.) Ac. Press, N.Y., 1976.
6. J.M. Peacock, A.J. Parker, P.G. Ashmore, J.A. Hockey, J. Catal., 15, 398 (1969).
7. Ph.A. Batist, H.J. Prette, G.C.A. Schuit, J. Catal., 15, 267 (1969).
8. M.W.J. Wolfs, Ph.A. Batist, J. Catal., 32, 25 (1974).

SUMMARY

This thesis deals with the selective catalytic oxidation of olefins over oxide catalysts, the oxides or combination of oxides all containing Bi^{3+} and Mo^{6+} together with other cations such as Pb^{2+}, Fe^{3+} and Mg^{2+}. The model reaction used was the conversion of 1-butene to butadiene at temperatures between 350°C and 500°C. The catalysts were characterized by the rate of conversion (activity) and the ratio of oxidation to butadiene to complete combustion (selectivity). Catalyst properties were determined in continuous flow and also in experiments in which pulses of 1-butene in the absence of O_2 and oxygen in the absence of hydrocarbon were passed over the catalyst in a stream of helium.

The catalysts were studied by X-ray diffraction to determine bulk structures and by XPS to find surface compositions. Mössbauer spectroscopy was used to determine the valency and surrounding of Fe admixtures. A considerable amount of work was devoted to the study of electrical conductivities of the catalysts when in operation. Tablets pressed of powdered catalysts were exposed to pulses of butene (increasing the conductivity) and to oxygen in the reduced state (decreasing the conductivity) with simultaneous determination of butene or oxygen consumed.

A kinetic model was developed to account for the results. It was based on the assumption that the electrical conductivity is entirely determined by the concentration of charge carriers in the surface layer. From the dependency of the conductivity on the temperature it was attempted to characterize the nature of the charge carriers.

Bismuth doped $PbMoO_4$ samples (with the scheelite structure), as introduced by Sleight, were prepared by precipitation to give surface areas comparable to those of bismuth molybdates. They were found to be highly active but thermally unstable as a consequence of solid demixing. Reduction by 1-butene leads to formation of a surface state with the electrons in a relatively stable state (Mo^{4+}) so that the activation energy for electrical conductivity is considerable. This is probably connected with observations by others that find reoxidation of a partly reduced catalyst to be relatively slow as demonstrated by a dependency of the overall reaction on the oxygen partial pressure.

Several bismuth molybdates such as $Bi_2(MoO_4)_3$, $Bi_2Mo_2O_9$ and Bi_2MoO_6 were prepared in pure form. XPS measurements and pulse experiments show that their activity is determined by the Bi/Mo ratio at the surface, maximal activity being observed between 2 and 1, but nearer to 2. Rapid migration of Mo (evaporation) causes the surfaces of different bismuth molybdates to become similar in composition and different from that of the bulk so that the overall activity of different compounds can become similar after a short time. Reduction leads to an electrical conductivity that for all bismuth molybdates is almost temperature independent and ascribed to the presence of Bi^0 (bismuth metal particles) on the surface. Since electron donation from this state can be assumed to be fast, also reoxidation of a partly reduced catalyst is fast and the rate of the overall reaction is not determined any more by the oxygen partial pressure. However, reduction and subsequent reoxidation may form Bi_2O_3 and thus lead to decomposition of the catalyst with consequent loss of activity.

Modern commercial catalysts are believed to be combinations of small amounts of bismuth molybdates with larger amounts of $Fe_2(MoO_4)_3$ and molybdates of bivalent metals such as Mg^{2+}. Mössbauer studies on our catalysts

containing Fe confirm earlier results that this cation during operation becomes reduced to Fe^{2+}. We find that this is accompanied by a considerable lower electrical conductivity which is explained by the reaction $3Fe^{3+} + Bi^{0} \longrightarrow 3Fe^{2+} + Bi^{3+}$. Reduction cannot occur without a formation of MoO_3.

We found that $MgMoO_4$ occurs in a special structure (with Mo^{6+} tetrahedrally surrounded) if in the presence of $Fe_2(MoO_4)_3$, the structure being the same as that of β-$FeMoO_4$. It is known that also $CoMoO_4$ and $NiMoO_4$ can occur in this structure and that it is necessary for an active catalyst to have its $Me(MoO_4)$ compound with the Mo^{6+} in tetrahedral surrounding, while an otherwise similar structure with the molybdenum in octahedral surrounding has no promotor action. The "active" structure is able to contain MoO_3 in considerable excess over the stoichiometric amount which might serve to facilitate the reduction of the iron molybdate. Moreover it represents a reservoir of bulk MoO_3, presumably necessary to counteract a loss of MoO_3 by evaporation during commercial operation.

SAMENVATTING

Dit proefschrift beschrijft enige aspekten van de selektieve katalytische oxidatie van olefinen over oxidische katalysatoren. De oxiden, of combinaties van oxiden, bevatten allen Bi^{3+} en Mo^{6+}, samen met andere kationen zoals Pb^{2+}, Fe^{3+} en Mg^{2+}.

De gebruikte modelreaktie was de omzetting van 1-buteen in butadieen bij temperaturen tussen 350°C en 500°C. De katalysatoren werden gekarakteriseerd door de omzettingssnelheid (aktiviteit) en de verhouding van de oxidatie tot butadieen en volledige verbranding (selektiviteit). Katalysatoreigenschappen werden bepaald in continue stromingsexperimenten en in experimenten, waarbij pulsen 1-buteen in afwezigheid van O_2 en zuurstof in afwezigheid van koolwaterstof in een stroom helium over de katalysator werden geleid.

De katalysatoren werden bestudeerd m.b.v. röntgendiffractie om de bulkstruktuur te bepalen en met XPS voor het bepalen van oppervlakte samenstellingen. Mössbauer spectroscopie werd gebruikt om de valentie en de omringing van Fe-toevoegingen te bepalen. Een belangrijk deel van het werk werd besteed aan het bestuderen van de elektrische geleidingen van de katalysatoren in reaktiekondities. Geperste tabletten van poedervormige katalysatoren werden blootgesteld aan pulsen 1-buteen (waardoor de geleiding stijgt) en aan zuurstof in de gereduceerde toestand (waardoor de geleiding daalt). Tegelijkertijd kon het buteen- of zuurstofverbruik worden bepaald.

Een kinetisch model werd ontwikkeld om de resultaten te kunnen interpreteren. Het werd gebaseerd op de veronderstelling dat de elektrische geleiding volledig be-

paald wordt door de concentratie aan ladingsdragers in de oppervlaktelaag.

Uit de afhankelijkheid van de geleiding van de temperatuur werd getracht de aard van de ladingsdragers te karakteriseren.

Bismut-gedoopte loodmolybdaat preparaten (met de scheelietstruktuur), zoals door Sleight werden geïntroduceerd, werden bereid door middel van precipitatie waardoor specifieke oppervlakken werden verkregen vergelijkbaar met de bismutmolybdaten. Gevonden werd dat deze een hoge aktiviteit vertoonden, maar thermisch niet stabiel waren als gevolg van ontmenging. Reduktie met 1-buteen leidt tot vorming van een oppervlaktetoestand waarbij de elektronen in een relatief stabiele toestand (Mo^{4+}) zijn zodat de aktiveringsenergie voor elektrische geleiding aanzienlijk is. Dit heeft waarschijnlijk te maken met waarnemingen van anderen, die vinden dat reoxidatie van een gedeeltelijk gereduceerde katalysator relatief langzaam is, zoals ook wordt aangetoond door een afhankelijkheid van de totaalreaktie van de zuurstofpartiaalspanning.

Verschillende bismutmolybdaten zoals $Bi_2(MoO_4)_3$, $Bi_2Mo_2O_9$ en Bi_2MoO_6 werden in zuivere vorm bereid. XPS-metingen en pulse-experimenten tonen aan, dat hun aktiviteit bepaald wordt door de Bi/Mo-verhouding aan het oppervlak. De maximale aktiviteit wordt waargenomen tussen 2 en 1, maar ligt dichter bij 2. Snelle migratie van Mo (verdamping) is er de oorzaak van dat oppervlakken van verschillende bismutmolybdaten gelijk in samenstelling worden en verschillend van de bulk zodat de totale aktiviteit van verschillende verbindingen na een korte tijd gelijk kan worden. Reduktie leidt tot een elektrische geleiding die voor alle bismutmolybdaten bijna temperatuuronafhankelijk is en toegeschreven wordt aan de aanwezigheid van Bi^0 (bismut metaal deeltjes) aan het oppervlak. Omdat elektronenafgifte vanaf deze toestand verondersteld wordt snel te zijn, zal ook de reoxidatie van een gedeeltelijk gereduceerde katalysator snel zijn en de

snelheid van de totaalreaktie wordt niet meer bepaald door de zuurstofpartiaalspanning. Echter, reduktie en daaropvolgende reoxidatie kan Bi_2O_3 vormen en kan zo leiden tot ontleding van de katalysator met als gevolg een daling van de aktiviteit.

Moderne commerciële katalysatoren bestaan uit combinaties van kleine hoeveelheden bismutmolybdaten met grote hoeveelheden $Fe_2(MoO_4)_3$ en molybdaten van tweewaardige metalen, zoals Mg^{2+}. Mössbauer metingen aan onze katalysatoren, die Fe bevatten, bevestigen vroegere resultaten, dat dit kation tijdens de reaktie gereduceerd wordt tot Fe^{2+}. We vinden dat dit samengaat met een aanzienlijk lagere elektrische geleiding, hetgeen verklaard kan worden door de reaktie: $3Fe^{3+} + Bi^0 \rightarrow 3Fe^{2+} + Bi^{3+}$. Reduktie kan niet optreden zonder vorming van MoO_3.

We vonden dat $MgMoO_4$ voorkomt in een speciale struktuur (met Mo^{6+} tetraëdrisch omringd) in de aanwezigheid van $Fe_2(MoO_4)_3$. Deze struktuur is dezelfde als die van β-$FeMoO_4$. Het is bekend dat ook $CoMoO_4$ en $NiMoO_4$ in deze struktuur kunnen voorkomen en dat bij een aktieve katalysator de $Me(MoO_4)$-verbinding Mo^{6+} in tetraedrische omringing heeft, terwijl een anderszins zelfde struktuur met Mo in oktaëdrische omringing geen promotorwerking heeft. De "aktieve" struktuur kan MoO_3 in aanzienlijke overmaat bevatten, welke de reduktie van het ijzermolybdaat kan doen vergemakkelijken. Bovendien vormt het een reservoir van bulk MoO_3, dat nodig is als compensatie voor verlies aan MoO_3 door verdamping tijdens commercieel gebruik.

DANKWOORD

Op deze plaats wil ik alle leden van de vakgroep Anorganische Chemie bedanken voor de prettige samenwerking, die ik tijdens mijn verblijf aan de T.H.E. heb mogen ondervinden. Een speciaal woord van dank is nodig voor Ph.A. Batist en dr. I. Matsuura, de eerste voor de hulp bij de bereiding van de gebruikte katalysatoren en beiden voor de stimulerende diskussies over de oxidatiekatalyse.

De studenten C.H.M. Suykerbuyk, M.W.A.M. Aarts en J.J.G.S.A. Willems dank ik voor de medewerking aan dit onderzoek tijdens hun S8-praktikum.

De XPS-metingen werden uitgevoerd in het Laboratorium voor Fysische Chemie van de R.U. Groningen op apparatuur gesubsidieerd door ZWO. Dr. G.A. Sawatzky en ir. A. Heeres dank ik voor hun belangrijke bijdrage in de interpretatie resp. de uitvoering van de metingen.

Dr. A.M. van der Kraan van het Interuniversitair Reactor Instituut te Delft ben ik dankbaar voor de uitvoering en de bijdrage aan de interpretatie van de Mössbauermetingen.

Verder dank ik mevr. M. Duran voor de vele röntgendiffractieopnamen, mej. M.A. van Straten voor de DTA/TGA-opnamen, W. van Herpen voor de voortdurende technische assistentie en voor hulp en advies bij het maken van de tekeningen.

Tenslotte ben ik Ine van 't Blik-Quax zeer veel dank verschuldigd voor het omzetten van een nauwelijks leesbaar handschrift in accuraat typewerk.

LEVENSBERICHT

De schrijver van dit proefschrift werd geboren op 14 januari 1950 te Wintelre (gem. Vessem c.a.)

Hij behaalde in 1967 het diploma HBS-B aan het Rythovius College te Eersel. Van 1967-1971 volgde hij de HTS-chemie te Eindhoven. In september 1971 begon hij aan de studie voor scheikundig ingenieur aan de Technische Hogeschool te Eindhoven. In juni 1973 behaalde hij het kandidaatsexamen. Zijn afstudeeronderzoek werd uitgevoerd onder leiding van prof. dr. G.C.A. Schuit in de vakgroep Anorganische Chemie. Op 8 januari 1975 behaalde hij het ingenieursdiploma.

Van 1 februari 1975 tot 1 september 1978 was hij in tijdelijke dienst van de Nederlandse organisatie voor Zuiver-Wetenschappelijk Onderzoek werkzaam in de vakgroep Anorganische Chemie van de Technische Hogeschool te Eindhoven, waar hij het in dit proefschrift beschreven onderzoek uitvoerde.

STELLINGEN

1. Bij de techniek die Kumar *et al.* toepassen voor het maken van dunne films van bismutmolybdaat wordt ten onrechte geen rekening gehouden met fouten, voortkomende uit die techniek.

   J. Kumar, E. Ruckenstein, J. Catal., 45, 198 (1976).

2. De conclusie van Otsubo *et al.* dat bij de oxidatie van waterstof over bismutmolybdaten de zuurstof van het bismut gebruikt wordt, is gebaseerd op moeilijk te rechtvaardigen aannamen.

   T. Otsubo, H. Miura, Y. Morikawa, T. Shirasaki, J. Catal., 36, 240 (1975).

3. De toepassing van Raman-spectroscopie op bijv. molybdaatkatalysatoren zal, afgezien van het feit dat het een goede "fingerprint"-methode is, niet aan de verwachtingen voldoen zolang er geen kwantitatieve theorie bestaat voor het berekenen van de struktuur uit de spectra.

4. De manier waarop vele leerboeken in de anorganische chemie de opvulling van de elektronenschillen bij de overgangsmetalen verklaren (nl. door aan te nemen dat bijv. het 3d-niveau hoger in energie is dan het 4s-niveau) is niet in overeenstemming met de experimentele gegevens.

5. Zowel overheid als bedrijfsleven zouden meer mogelijkheden moeten scheppen voor part-time arbeid, met name voor hoger opgeleiden.

6. De bezoldiging van leraren in het middelbaar onderwijs dient niet langer gebaseerd te zijn op een gradenstelsel, maar eerder op de zwaarte van de te geven lessen.

7. Het huidige systeem van keuzepakketten op de middelbare scholen leidt vaak tot ernstige moeilijkheden bij de overgang naar vervolgonderwijs. Een terugkeer naar de vroegere bredere opleiding dient overwogen te worden.

8. De feitelijke samenhang tussen de vakken natuurkunde, scheikunde en biologie dient benadrukt te worden door invoering van een vak "natuuroriëntatie" in de lagere klassen van het middelbaar onderwijs.

9. Het doen van zgn. spectaculaire proefjes (met stank, knallen e.d.) in de scheikundeles op de middelbare scholen is niet bevorderlijk voor de verbetering van het negatieve beeld van de chemie.

10. De in de Engelse taal voorkomende uitdrukkingen met "dutch" (zoals dutch comfort, dutch courage, dutch concert, dutch defense) met veelal een ongunstige betekenis, zijn ontstaan in de zeventiende eeuw toen Hollanders en Engelsen niet zo vredelievend tegenover elkaar stonden. Het feit dat sindsdien geen nieuwe uitdrukkingen meer zijn toegevoegd aan deze reeks, doet ten onrechte vermoeden dat de Hollanders populairder geworden zijn.

Eindhoven, 17 oktober 1978 D.A.G. van Oeffelen